AD NUMBER

AD596342

CLASSIFICATION CHANGES

TO: unclassified

FROM: confidential

LIMITATION CHANGES

TO:

Approved for public release, distribution unlimited

FROM:

Distribution: Controlled: all requests to Chief, Office of Naval Research, Attn: Code 102-OS. Arlington, Va. 22217.

AUTHORITY

1978 per document markings; ONR ltr., Ser 93/160, 10 Mar 1999

MC REPORT 006

Volume 2

PARKA II-A

THE OCEANOGRAPHIC MEASUREMENTS

PARKA II-A • THE OCEANOGRAPHIC MEASUREMENTS

February 1972

Omit From General Bibliographic Listings.

OCEAN SCIENCE PROGRAM

MAURY CENTER FOR OCEAN SCIENCE

Department of the Navy

Washington, D.C.

CONFIDENTIAL

"NATIONAL SECURITY INFORMATION"

"Unauthorized Disclosure Subject to Criminal Sanctions"

MC Report 006
Volume 2

LONG RANGE ACOUSTIC PROPAGATION PROJECT

THE PARKA II-A EXPERIMENT [U]

PACIFIC ACOUSTIC RESEARCH KANEOHE-ALASKA

FEBRUARY 1972

OCEAN SCIENCE PROGRAM
MAURY CENTER FOR OCEAN SCIENCE
Department of the Navy
Washington, D.C.

CONFIDENTIAL

CONTENTS

CONTENTS

FOREWORD

The PARKA II-A Report consists of three parts, of which the present volume is Volume 2, *The Oceanographic Measurements*. Volumes 1 and 3, which will be bound separately, will describe *The Acoustic Measurements* and *The Propagation Modeling*, respectively.

The Report was generated by a cooperative effort which was an extension of the teamwork of the experiment itself. The individual writings of a number of scientists from the participating organizations were edited and interwoven to form each Volume. The principal contributors to Volume 2 were K. W. Lackie, L. C. Breaker and J. K. Duncan of the Naval Oceanographic Office, and K. W. Nelson of the Naval Undersea Research and Development Center. Contributors to the writing of the other two volumes will be listed therein.

Special acknowledgment is also gratefully given to the many individuals who made the achievement of the experiment possible by their dedicated efforts in the face of great difficulties at sea.

R. H. Nichols

R. H. NICHOLS
Chief Scientist, PARKA

ACKNOWLEDGMENTS

On behalf of the Navy Managers responsible for the PARKA experiments, the contributions of senior officers of the Navy, members of the scientific community who participated in PARKA II-A, and seafaring men, both naval and civilian, who contributed in various ways are gratefully acknowledged.

Dr. R. H. Nichols, Bell Telephone Laboratories, served as Chief Scientist, and in that role was responsible for the scientific planning and execution of the PARKA series. Mr. R. W. Hasse, Navy Underwater Sound Laboratory, was the Deputy Chief Scientist. Mr. A. J. Hiller and Capt. A. E. White, USN (Ret.) served consecutively as Project Coordinator. Mr. K. W. Lackie, Naval Oceanographic Office, acted as the Scientist-in-Charge of Oceanographic Operations. Capt. R. H. Smith, USN, and Lt. Cdr. E. E. Flesher, USN, ASWFORPAC, directed naval aspects of the operations.

The assistance of those providing broad scientific planning, as well as facilities and support in conducting the entire PARKA II-A Experiment has been acknowledged in Volume I of this report. A few others should be listed, however, as having made a significant contribution to the success of the environmental effort in the experiment.

From the Navy Underwater Sound Laboratory: T. A. Bender, J. F. Crotty, Lt. Cdr. J. M. Heiges, L. C. Maples, W. H. Thorp, R. H. Smith, H. B. Williams, R. F. LaPlante, F. C. Walsh, and R. K. Dullea.

From the Naval Undersea Research and Development Center: P. A. Hanson, C. T. Smallenberger, and F. K. Adams.

From the Naval Oceanographic Office: B. A. Watrous, C. L. Davis, and N. V. Lombard.

From Fleet Numerical Weather Central: Lt. N. L. Perkins and Lt. Cdr. K. G. Hinman.

From Fleet Weather Central, Pearl Harbor: Lt. C. H. West, Lt. j.g. D. R. McConathy, Jr., and Lt. j.g. H. L. Peterson.

From the Hawaii Institute of Geophysics: R. C. Latham, Antares Parvulescu, Edward Houlton, N. J. Thompson, Romondt Budd, R. G. Zachariadis, B. E. Gottensburen, and J. R. Ryan.

From the Lamont-Doherty Geological Observatory: J. I. Ewing, C. C. Windisch, Peter Buhl, and Sydney Griffin.

Obviously, many other individuals and organizations have contributed to the planning and execution of the experiment. Although it is not practical to list them all here, their contributions are most gratefully acknowledged.

J. B. Hersey

J. B. HERSEY
Director, Maury Center
for Ocean Science

I. THE EXPERIMENT

INTRODUCTION

The PARKA II-A Experiment was performed in the North Pacific Ocean in November and December of 1969 as a cooperative venture of fourteen Navy and civilian laboratories and other organizations under the sponsorship of the Office of Naval Research (ONR). It followed PARKA I as the second of a series of three experiments designed to acquire a comprehensive bank of detailed acoustic and oceanographic data to be employed in the development and test of acoustic prediction models.

PARKA II-A was a combined oceanographic-acoustic experiment, in which the oceanographic effort was designed to provide a better understanding of the acoustic results. A description of PARKA II-A acoustic programs and a discussion of the results is contained in Volume I of this report.

With each individual acoustic event, a series of concurrent oceanographic observations was taken in order to describe the environmental conditions along the acoustic path which caused the observed propagation characteristics. Wherever possible, environmental data were collected at the acoustic source, the receiver, and at one to three points between them. This is similar to the environmental program carried out in PARKA I (Maury Center for Ocean Science, 1969b, and Lackie, 1971). A complete description of ship and aircraft schedules is contained in the PARKA II Scientific Plan (Maury Center for Ocean Science, 1969a).

The oceanographic effort was divided into several distinct phases to coincide with the acoustic experiments. These experiments, or Events, which are outlined below, are described in detail in the PARKA II Scientific Plan (Maury Center for Ocean Science, 1969a), and are summarized in Volume I of this report. In this volume the oceanographic observations and results will be associated with the corresponding acoustic measurements.

PARKA II-A was a modification of the originally-planned PARKA II program which envisioned SEA SPIDER as the receiver platform. When the SEA SPIDER installation proved unsuccessful, R/V FLIP was substituted and the program revised to accommodate the change. The new program comprised two parts, PARKA II-A and PARKA II-B. The latter, which included a seasonal repeat of part of PARKA II-A, was performed in March of 1970; it will be reported separately.

FLIP was stationed during PARKA II-A at approximately the same position as during PARKA I, 330 nautical miles north of Oahu in water 18000 feet deep, and was securely moored to keep her closely on station. Various acoustic runs utilizing both ship and aircraft were made in the area, either orginating or terminating at the FLIP site.

The ship runs (Fig. 1) were made on three bearings from FLIP, 000°T, 180°T, and 247°T to ranges of 300 to 500 nautical miles, over a variety of bottom topographies. The aircraft runs (Fig. 2) were made between FLIP and Adak, between FLIP and the Alaskan coast due north (the PARKA I track), and between FLIP and San Diego.

PRE-EXPERIMENT OPERATIONS

Long Range Transits

All PARKA ships collected bathymetric profiles and limited oceanographic data on their transits to the Hawaiian area for PARKA operations. These transits were designed to cover the same tracks that Navy aircraft would

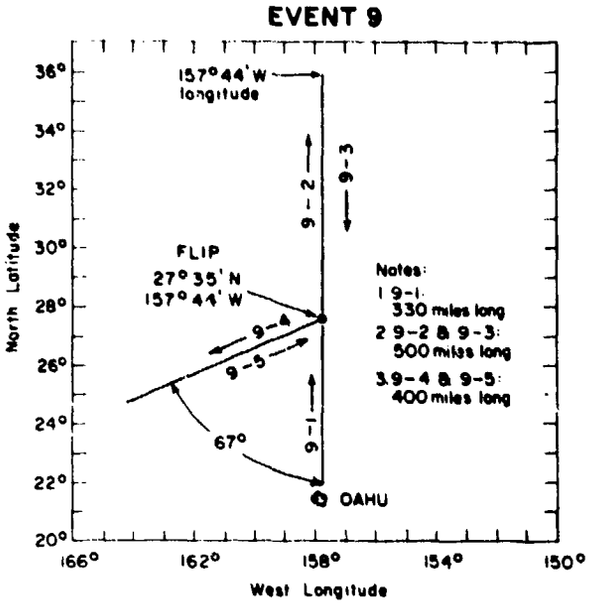

Fig. 1 — Track Chart of Event 9 (Propagation Loss and Arrival Structure)

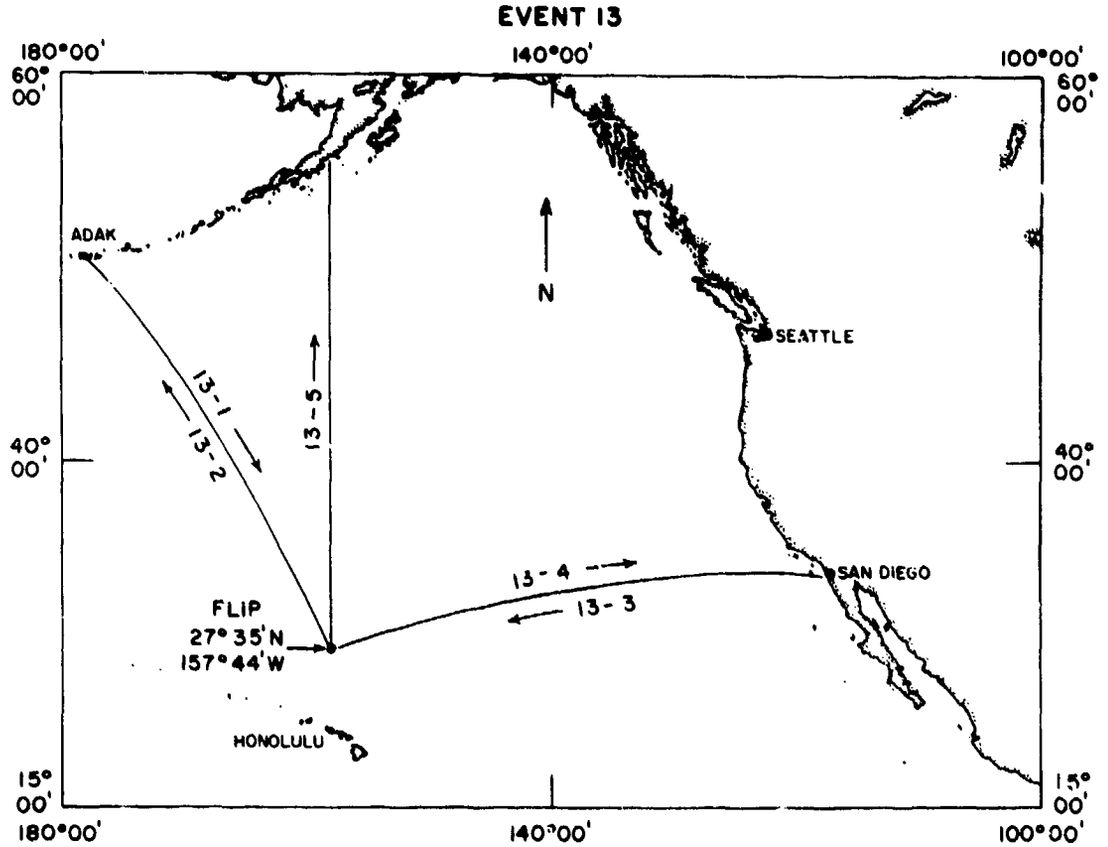

Fig. 2 — Track Chart of Event 13 (Long Range Propagation Loss, Aircraft)

traverse later in the experiment during the propagation loss studies of Event 13 (Fig. 2).

1. R/V CONRAD – Lamont-Doherty Geological Observatory (LDGO): Adak to the site where FLIP was to be anchored (nominally, 27°35'N, 157°44'W). This run corresponded to Events 13-1 and 13-2.
2. USNS SANDS – Navy Underwater Sound Laboratory (NUSL): San Diego to FLIP site, corresponding to Events 13-3 and 13-4.
3. USS MARYSVILLE – Hawaii Institute of Geophysics (HIG): Seattle to FLIP site (Latham and others, 1969) corresponding to Events 13-7 and 13-8, which were cancelled after FLIP was damaged by high seas. (See Rudnick and Hasse, 1971.)
4. USS REXBURG – Naval Undersea Research and Development Center (NURDC): San Diego to FLIP site.

The track due north to the Alaska Peninsula, corresponding to Events 13-5 and 13-6 (the latter was cancelled when FLIP was damaged), had been adequately surveyed during PARKA I in 1968. In addition, USC&GSS MCARTHUR collected bathymetric data on her transit between Hawaii and Seattle in May. Profiles of these bathymetric data are plotted versus range and are included as Figs. 36 through 39. Superimposed on these bathymetric profiles are the sound velocity profiles that were predicted by Fleet Numerical Weather Central (FNWC).

Operations During SEA SPIDER Implantment Attempts

During various periods in August, September, and October 1969, SANDS, CONRAD, and MARYSVILLE collected limited quantities of oceanographic data in the PARKA area. These observations were made during the two unsuccessful attempts to implant SEA SPIDER, as well as during other local operations in the area. In addition, HIG made current measurements from R/V TOWNSEND CROMWELL and R/V MAHI. These data, which were collected prior to the commencement of PARKA II-A experimental operations in November, were intended partly to support the SEA SPIDER implantment, and partly to provide data on temporal variability of sound velocity structure; they are not presented here. However, they are included in the PARKA archival data file. The PARKA II-A data are available to qualified agencies upon application to the Director, Maury Center for Ocean Science, Code 102-OS, Office of Naval Research, Arlington, Virginia 22217.

ACOUSTIC PROPAGATION LOSS AND ARRIVAL STRUCTURE, SHIP RUNS (EVENT 9)

General

During Event 9, which was the first propagation experiment, CONRAD was the source ship and FLIP and SANDS were located at the receiver position, approximately 27°35'N, 157°44'W. CONRAD dropped explosive charges on five radial runs from FLIP (Fig. 1).

1. Event 9-1: from 22°N (335 nautical miles south of FLIP) north to FLIP.
2. Event 9-2: from FLIP due north to a range of about 500 nautical miles (36°N).
3. Event 9-3: from the end point of Event 9-2 due south back to FLIP.
4. Event 9-4: from FLIP to a range of about 400 nautical miles on a great circle having a bearing of 247°T at FLIP.
5. Event 9-5: from the end point of Event 9-4 back on the same great circle to FLIP.

Sound velocity profiles collected on each of the above events are plotted against range in Figs. 22, 23, 24, 28, and 29. Contoured cross sections

of the same data are shown in Figs. 25, 26, 27, 30, and 31. These are presented with the discussion of sound velocity structure in Section IV.

As the source ship CONRAD advanced along each run at a speed of about 9.5 knots, MARYSVILLE and REXBURG took a series of positions between CONRAD and FLIP, collecting environmental data along the acoustic path. In this manner, concurrent oceanographic data were collected over as much of the path as possible.

CONRAD

On each run CONRAD collected a 2500-foot expendable bathythermograph (XBT) record every six hours (approximately 55 nautical miles), or more frequency if a significant change in surface temperature was noted. Sea surface temperatures were taken every two hours. In addition, a deep salinity-temperature-depth (STD) station was occupied at the beginning and end of most runs.

SANDS

SANDS took two XBT's each day during the entire experimental period. In addition, deep velocimeter measurements (temperature and sound velocity versus depth) were made on four occasions during the experiment when acoustic operations permitted. A time series plot of these deep velocimeter measurements is shown in Fig. 41. Profiles of SANDS's XBT data, converted to sound velocity and plotted versus time, are displayed in Fig. 42.

MARYSVILLE

MARYSVILLE was the primary oceanographic ship of PARKA II-A. During most of the experiment MARYSVILLE took a series of positions approximately halfway between SANDS and CONRAD. Deep velocimeter stations were taken every 20 to 30 miles to a range of 180 nautical miles on Events 9-1, 9-2 and 9-3, and to a range of 250 nautical miles on Events 9-4 and 9-5. XBT's were taken about midway between stations, except between 19 and 23 November, when MARYSVILLE's XBT recorder was inoperative. Shallow velocimeter stations were taken at close intervals during that period. A summary of MARYSVILLE operations during PARKA II-A is given in Latham (1970).

REXBURG

The NURDC thermistor chain was mounted on REXBURG for PARKA II-A. This chain measures temperature continuously in time at 47 points between the surface and a depth of 220 meters (Hansen, 1969, LaFond and LaFond, 1971, Smith, 1969). REXBURG followed a plan similar to that of MARYSVILLE, taking a series of positions between source and receiver. However, REXBURG remained closer to the source ship CONRAD in order to monitor more effectively the small scale temperature variations at shallow depth near the acoustic source. Chain data were collected to a maximum range of 330 nautical miles on Event 9-1, 265 nautical miles on Events 9-2 and 9-3, and 400 nautical miles on Events 9-4 and 9-5. REXBURG also carried out a 48-hour drift station at maximum range (265 nautical miles) between Events 9-2 and 9-3 to investigate time series effects. Whenever possible XBT data were collected for comparison with the thermistor chain results. Selected results from the chain were coded and transmitted as BT's. These are included in Figs. 11 through 15. Because of the unique nature of the thermistor chain data, Section III, Part B, of this volume deals exclusively with results of chain operations in PARKA II-A.

Aircraft

Aircraft expendable bathythermograph (AXBT) flights were scheduled once on each

radial run, usually when CONRAD was close to maximum range from FLIP. These are called Short AirCraft (SAC) flights. Drops were to be made every 24 miles out to a range of about 330 nautical miles on Event 9-1 and 500 nautical miles on Events 9-3 and 9-5. The flights occurred on 18, 23, and 28 November, and were numbered SAC-1, SAC-2, and SAC-3, respectively. Because of operational problems aboard the aircraft, only 11 out of 14 drops were good on SAC-1, 20 out of 21 on SAC-2, and none out of 21 on SAC-3. The AXBT's extended to a depth of 1000 feet and gave an almost instantaneous "snapshot" of the near-surface environment over long stretches of ocean. Converted to sound velocity, these data are included in Figs. 22 and 24.

LONG RANGE PROPAGATION LOSS, AIRCRAFT RUNS (EVENT 13)

Event 13 was scheduled to consist of four round trip Long AirCraft (LAC) flights from FLIP to Adak, to San Diego, due north to Alaska, and to Seattle. Explosive charges were to be dropped on both runs on each track, with AXBT measurements every 24 miles on the flights inbound to FLIP only.

FLIP was damaged by heavy seas on 1 December (Rudnick and Hasse, 1971) which ended its participation in PARKA II-A. At this time, five of the eight flights had taken place (Fig. 2):

1. LAC-1 from Adak to FLIP
2. LAC-2 from FLIP to Adak
3. LAC-3 from San Diego to FLIP
4. LAC-4 from FLIP to San Diego
5. LAC-5 from FLIP due north to 55°N

Flights LAC-1 and LAC-3 yielded AXBT data; 15 of 66 AXBT's dropped were good on LAC-1 from Adak to FLIP (17 November), and 69 of 88 were good on LAC-3 from San Diego to FLIP (23 November). The temperature profiles resulting from these AXBT's were converted to sound velocity using archival salinities and Wilson's equation (Wilson, 1960), and are plotted against range from FLIP in Figs. 34 and 35.

PROPAGATION LOSS AND TEMPORAL FLUCTUATION OF CONTINUOUS WAVE (CW) SIGNALS (EVENT 11)

General

Event 11 was scheduled to take place along the same track as Events 9-2 and 9-3 north of FLIP, and was to consist of a projector tow by CONRAD out to a range of 500 nautical miles (11-1) and back to FLIP (11-2). However, the damage to FLIP prior to the commencement of the exercise on 1 December precluded the execution of the event as planned. MARYSVILLE and REXBURG, who had already started north on Event 11-1, returned to FLIP. Their participation in PARKA II-A ended a few days later. A shortened version of the event was eventually carried out with CONRAD as source ship and MAHI as receiving ship. The revised Event 11-1 was run due northward from MAHI's position at 26°09'N, 157°41'W to about 33°20'N, a distance of 430 nautical miles (Fig. 3). Profiles and contoured cross sections of sound velocity data taken during Event 11 are shown in Figs. 32 and 33, respectively.

CONRAD

CONRAD continued to take XBT's every six hours as during Event 9, and occupied a deep STD station at the beginning and end of Event 11-1.

SANDS

SANDS continued to collect XBT's every 12 hours at her position near the FLIP site and occupied one deep velocimeter station.

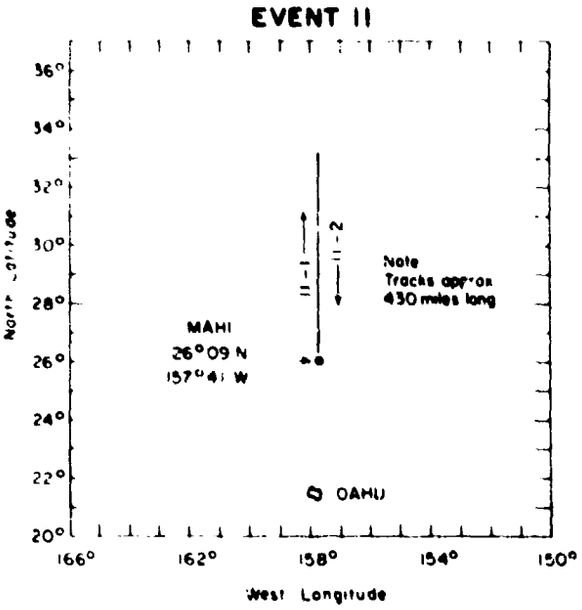

Fig. 3 -- Track Chart of Event 11 (Propagation Loss and Temporal Fluctuation of CW Signals)

MARYSVILLE

MARYSVILLE had already left the area when the acoustic phase of Event 11-1 started on 8 December. However, the XBT's and velocimeter stations she collected along the Event 11 track during the period 1 through 4 December are included in the Event 11 data file because they are considered close enough in time to be pertinent to the experiment.

REXBURG

Thermistor chain and XBT data collected on the Event 11 track by REXBURG from 1 to 4 December are considered to be a part of the Event 11 data for the reasons cited above for MARYSVILLE. Thermistor chain results are discussed in Section III, Part B.

DATA TRANSMISSION

All XBT, STD, and sound velocimeter data were coded at sea using standard National Oceanographic Data Center (NODC) procedures and standard NODC logs. The data were transmitted by voice radio to Naval Oceanographic Office (NAVOCEANO) personnel located at the PARKA Operation Control Center (OCC) at Pearl Harbor, Hawaii. After preliminary checking, the data were punched on cards, recorded on magnetic tape, computer plotted for additional checking, corrected, and transmitted by direct wire from Fleet Weather Central (FWC), Pearl Harbor to FNWC, Monterey, California by FNWC and FWC personnel. As part of the archives, they were available to update the PARKA propagation loss predictions made by FNWC, and for Fleet use.

Thermistor chain data were handled in a similar manner, except that not all the data were transmitted in real time. Hourly averages of temperatures at each measured depth were calculated at sea, and selected averages were coded and transmitted as BT's. The remainder of the data were analyzed later by computer and form the basis for the discussion in Section III, Part B.

AXBT data were hand-carried from Barbers Point Naval Air Station to HIG and FWC Pearl for analysis. After checking by PARKA personnel, they were sent to FNWC in the same manner as the other oceanographic data.

The velocimeters on MARYSVILLE and SANDS measured sound velocity directly. The STD system on CONRAD measured both temperature and salinity as a function of depth, from which sound velocity was computed by Wilson's equation (Wilson, 1960). XBT's, AXBT's, and the thermistor chain measure only temperature as a function of depth. FNWC calculated most of the sound velocity data cited in this report by combining XBT, AXBT, and thermistor chain temperatures with assumed salinities based on archival Nansen cast data. A comparison of directly-measured sound velocities and sound velocities computed from temperature and salinity data is presented in Section IV of this report.

II. REGIONAL OCEANOGRAPHY

THE NORTHEASTERN NORTH PACIFIC OCEAN

The geographic boundaries for PARKA II extend northwestward from Hawaii to Adak and from Hawaii eastward to San Diego, and together with the coast of North America and the Aleutian chain enclose a large portion of the northeastern North Pacific Ocean. This ocean area can be subdivided into a subarctic region to the north and a subtropical region to the south. The boundary between these regions lies approximately on a great circle path from Tokyo to Los Angeles, and in mid-ocean is located in the vicinity of latitude 45°N (Subarctic Convergence).

Several major currents and current systems (gyres, loosely), are located in the northeastern North Pacific Ocean. The paths of the major currents form a geographical framework witnin which various near-surface water masses are located (see Fig. 4). These prevailing currents help to replenish and thus preserve the characteristic properties of the existing near-surface water masses in this region. Two major currents flow eastward along the subarctic boundary: the Subarctic Current to the north, and the North Pacific Current to the south, this second current being an extension of the Kuroshio Current. The North Pacific Current carries water that is warm and saline in comparison to the Subarctic Current. The Subarctic Current divides before reaching the North American

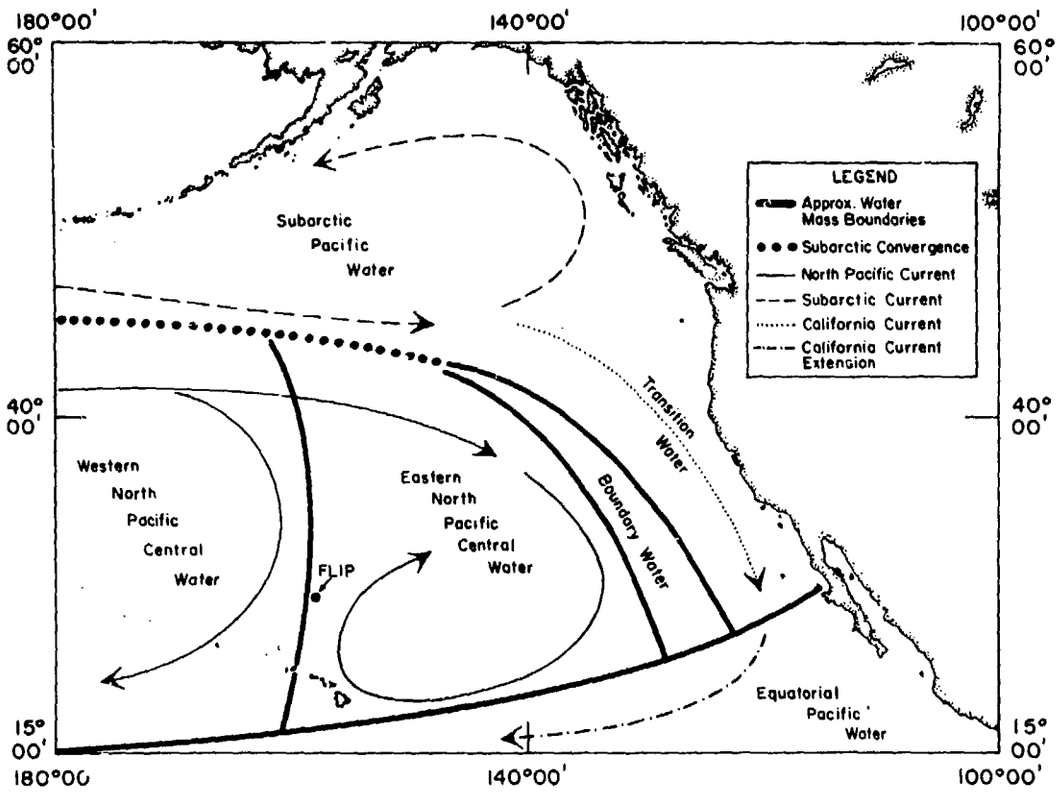

Fig. 4 -- Major Water Masses and Current Systems in the Northeast Pacific

coast, part being diverted to the north, and part to the south. The northern extension forms a loop in the Gulf of Alaska (the Alaskan Gyral) and the southern extension becomes the California Current. An extension of the California Current eventually flows southwestward toward the equator passing just south of the Hawaiian Islands. The North Pacific Current also turns southward. Its flow pattern in the area is not clearly defined, but it appears to form a complete loop or gyre, at least during the summer and has been named the Eastern North Pacific Gyral with its center located northeast of Hawaii (Seckel, 1962).

The Northeast Pacific contains a number of large water masses, each of which possesses characteristic properties. Water masses can be identified through their respective temperature-salinity relationships or "signatures". Some typical ones are presented in the following Section in Fig. 5a. Starting just north of Hawaii and looking northwest toward Adak, the following major water masses are encountered between the mixed layer and the bottom: North Pacific Central Water, North Pacific Intermediate Water, Pacific Deep Water. North Pacific Central Water is characterized by decreasing temperature and salinity with depth, a temperature range of 18°C to 11°C, and a salinity range of 35.00°/$_{oo}$ to 34.00°/$_{oo}$ (Sverdrup and others, 1942). North Pacific Intermediate Water is located below the North Pacific Central Water and is found over most of the North Pacific (Reid, 1965). It is characterized by a core of low salinity water and has a minimum value of about 34.00°/$_{oo}$ which occurs at 600 meters at the FLIP location. Pacific Deep Water occurs below 1000 meters and has a temperature range of 4°C to 1.5°C and a salinity range of 35.50°/$_{oo}$ to 35.70°/$_{oo}$. This deep water mass is quite uniform and originates in high southern latitudes. North of the Subarctic Convergence, Subarctic Pacific Water spans the entire Northeast Pacific. Subarctic Pacific Waters are cold and of low salinity.

The same subarctic water mass extends south between the eastern boundary of North Pacific Central Water and the west coast of North America, mixing with Equatorial Pacific Water as it penetrates this subcoastal region. This mixture of subarctic and equatorial waters, located south of 45°N and off the coast of California, has been given the name Transition Water. Between the North Pacific Central Water Masses and the Pacific Subarctic/Transition Water Masses, a boundary region follows approximately the subarctic-subtropical divide along the western side of the California Current. This boundary region constitutes what is called the Boundary Water Mass. It is typified by pronounced variations of temperature and salinity across it, and attributes of neighboring water masses are often found here (Christensen and Lee, 1965).

THE FLIP AREA

Due to the fact that most oceanographic measurements made during PARKA II-A were concentrated in a relatively small area north of Oahu, Hawaii, the oceanographic features of this area deserve a more detailed discussion. The area is roughly circular, with its center located at the FLIP site, and has a radius of approximately 500 nautical miles. It is an oceanographically complex transition region containing varying proportions of several adjacent water masses. In addition, the distributions of temperature and salinity in the area are not constant from one year to the next (Seckel, 1969). Eddies and turbulence arising from current flow around the Hawaiian Islands may be present, and there is a zone of convergence between the North Pacific Current and the California Current Extension in the southern part of the region (McGary and Stroup, 1956).

In the vicinity of FLIP at least three major water masses are consistently found: North Pacific Central Water, North Pacific Intermediate Water, and Pacific Deep Water. In the upper layers, the relative proportions of the various water masses appear to vary significantly with time and with slight changes in location. From just below the mixed layer down to 200 to 300 meters, a mixture of Eastern and Western North Pacific Central Water appears to be present. Eastern North Pacific Central Water can be distinguished from Western North Pacific Central Water by its lower values of salinity with increasing depth. From about 275 meters down to almost 1000 meters, North Pacific Intermediate Water exists, with Pacific Deep Water found below 1000 meters. Roden (1970) defines the zone of transition between subarctic water and subtropical water occurring at the northern end of the FLIP area as lying between 32°N and 42°N latitude. Thus, subarctic waters may at times intrude into the northern extremity of the FLIP area. On rare occasions, intermediate and shallow equatorial waters may be found at the southern edge of the area.

During November and December, the mixed surface layer in the FLIP area is well defined. It ranges in depth from a little less than 45 meters to a little more than 90 meters. The average layer depth is slightly greater in December. At the FLIP site, surface temperatures are generally in the range of 21°C to 24°C, and the surface salinity ordinarily is about 35.00°/$_{oo}$.

Large-scale current flow past the Hawaiian Islands causes the formation of eddies which have been found on both sides of the island chain and identified through geographic plots of certain isotherms. Wyrtki (1967) found eddies in this area with dimensions on the order of 110 nautical miles, and a life span of a few months. He also found large-scale ocean turbulence to be associated with these eddies.

Recent deep ocean temperature measurements through the FLIP area have revealed a definite temperature inversion toward the bottom (Latham and others, 1970). A temperature minimum was found to occur at about 3800 meters. Temperature increases with depth beyond this level to the bottom, as the result of adiabatic heating (Roden, 1970).

III. OCEANOGRAPHIC RESULTS

Part A. Analysis of PARKA II-A Data

GENERAL

The foregoing discussion of the ocean environment in the PARKA II-A area was based on existing literature. The following discussion of the ocean environment in the general vicinity of the FLIP/SANDS location (27°35'N, 157°44'W) is based on data collected during the experimental period, November and December 1969. Oceanographic and acoustic data were collected only along several tracks terminating at the FLIP site, and the discussion will be limited to the area of these observations. Vertical profiles of certain oceanographic parameters and the variability of the environment near the FLIP site will be discussed.

The vertical distribution of the relevant variables near the FLIP site has been emphasized because the density of measured data is highest at this location. The high concentration of data near the receiver site was intended to provide ample oceanographic data for acoustic modeling purposes. A similar program was conducted during PARKA I (Maury Center for Ocean Science, 1969b, and Whalen and others, 1971).

As was indicated in Section I, only CONRAD carried an STD system capable of measuring the variation of both temperature and salinity with depth. The velocimeters aboard SANDS and MARYSVILLE sampled temperature and sound velocity; the thermistor chain aboard REXBURG and the XBT's on all ships measured temperature only. Therefore, the discussion of oceanographic variables such as salinity, density, and stability will be largely limited to CONRAD data; the salinity structure is necessary for the computation of density and stability. Although CONRAD occupied several STD stations during PARKA II-A (normally at the beginning and end of each acoustic run), no attempt has been made here to contour the measured data spatially because of the great horizontal separation between observations. However, CONRAD STD data are included in the vertical cross sections of sound velocity presented in Section IV.

TEMPERATURE-SALINITY (T-S) DIAGRAMS

Between 17 November and 10 December, CONRAD occupied nine STD stations. All but one of the stations were located along the north-south track through the FLIP site between 36°N and 22°N latitude. T-S diagrams, constructed from these data, identify the various water masses and help to explain certain variations found in the sound velocity structure. An example of such a T-S construction is shown in Fig. 5a. A close relationship usually exists between the T-S field and the sound velocity structure in the region between the mixed layer and the sound channel axis. For example, inflection points indicated by T-S diagrams are often reflected in corresponding sound velocity profiles at equivalent depths. Figure 5 compares T-S and sound velocity profiles for a CONRAD station; both curves show inflection points between 100 and 200 meters. This relationship is not valid at depths below the sound channel axis, because pressure is the only variable that normally undergoes significant change in this depth interval.

Initially, the PARKA T-S diagrams were compared with historical T-S plots for the area in order to identify the water masses (Fig. 5a). Comparisons were not made for the surface layer because temperature and salinity there are affected by external sources (i.e., temperature and salinity are not conservative properties in this region). At the northern end of the track the intrusion of cold, low-salinity water (apparently of subarctic origin) is evident centered at about

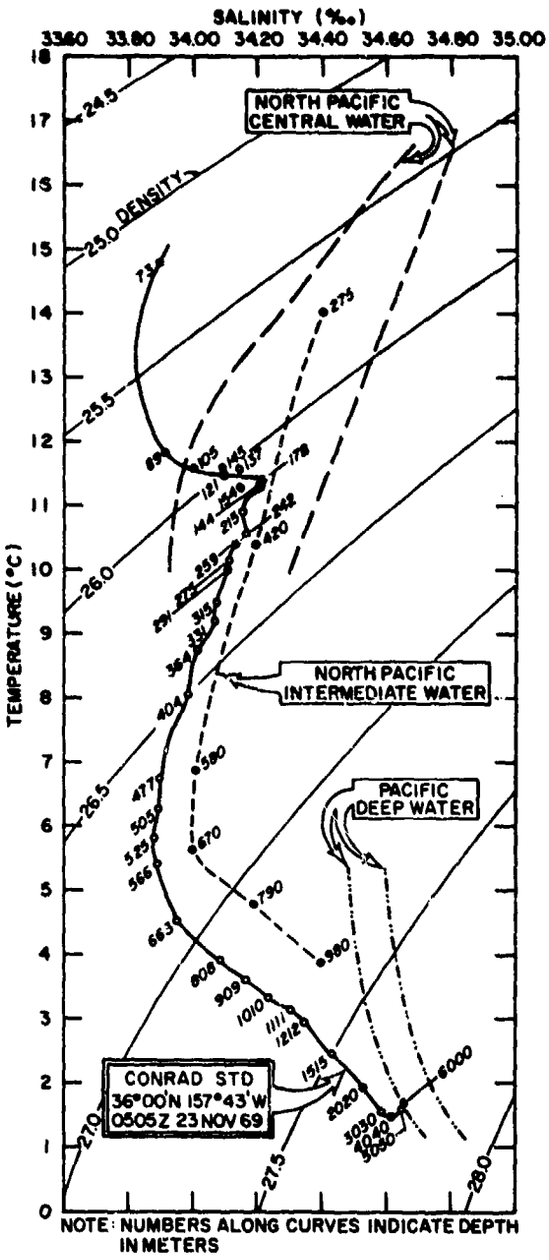

Fig. 5a — Temperature-Salinity Plot for a CONRAD STD Station

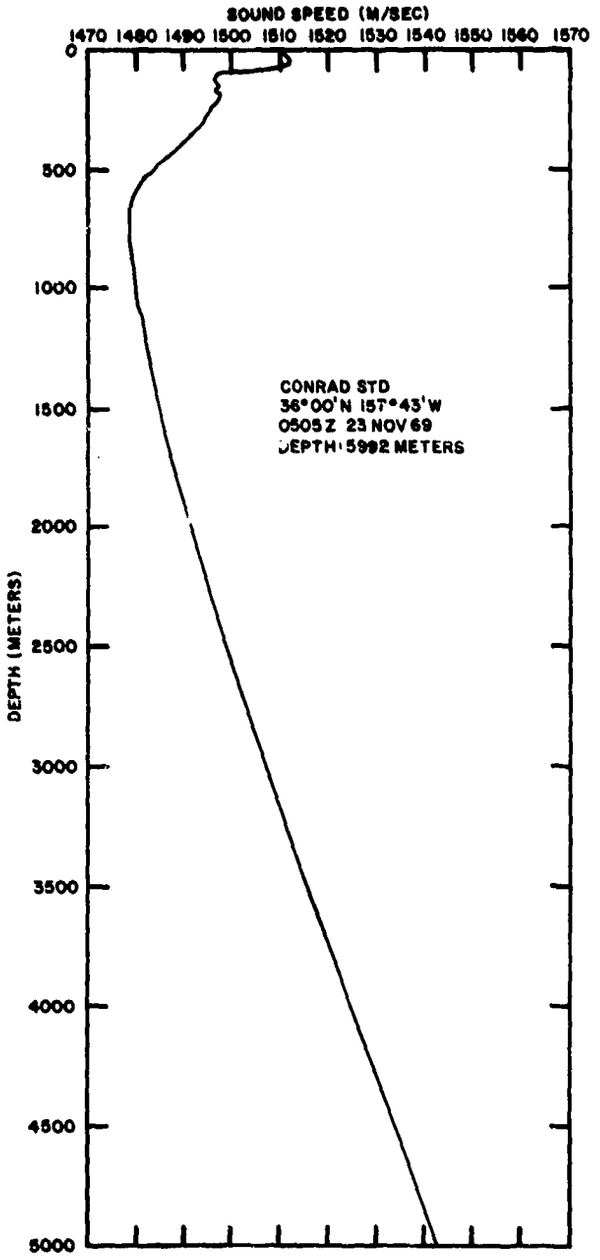

Fig. 5b — Sound Velocity Profile for a CONRAD STD Station

80 meters depth, just below the mixed layer. Farther south, this feature disappears. From 33°N to 22°N, North Pacific Central Water can be identified below the mixed layer. Pickard (1963) states that it may not be advisable to distinguish between the Eastern and Western North Pacific Central Water Masses (Fig. 4), since their T-S properties are quite similar. Consequently, this distinction has not been made in this report. The most obvious feature common to all T-S profiles along the north-south track is the North Pacific Intermediate Water Mass. PARKA II-A T-S diagrams indicate its presence from a depth of several hundred meters down to almost 1000 meters. The occurrence of the low salinity core between 500 and 600 meters at the FLIP site (Fig. 5a) agrees closely with Reid (1965). South of the northernmost station, a slight increase in salinity of about 0.10°/$_{oo}$ occurs in the low salinity core. Reid attributes this to vertical exchange with the waters immediately above and below the core. All T-S profiles indicate a gradual transition to Pacific Deep Water below 1000 meters, approaching values of about 1.5°C and 34.70°/$_{oo}$.

TEMPERATURE STRUCTURE

A typical vertical temperature distribution in the FLIP area during PARKA II-A is shown in Fig. 6. The surface temperature is slightly more than 23°C, and essentially isothermal conditions exist down to the bottom of the mixed layer, which occurs at 80 meters*. The surface and near-surface conditions are based on data collected during the final portion of the experiment, and closely resemble the representative autumn environment in this region. The isothermal layer apparent at the FLIP site during

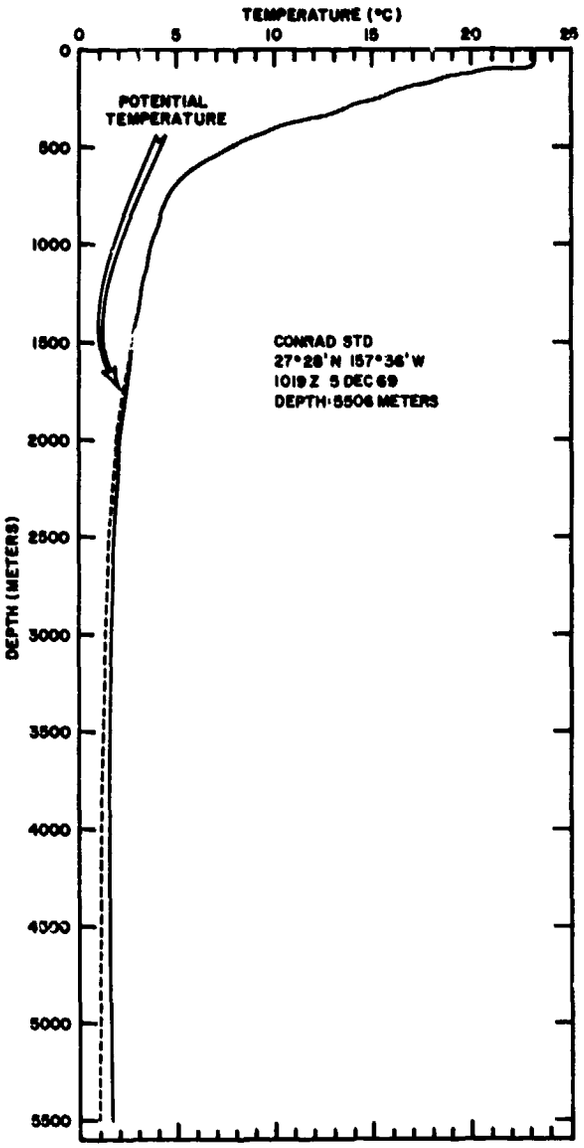

Fig. 6 — Temperature Structure and Potential Temperature at the FLIP/SANDS Site

PARKA I (Maury Center for Ocean Science, 1969b, and Smith, 1971b) was thinner, about 40 or 45 meters, and was not as well defined as in the PARKA II-A measurements. This difference is to be expected, because PARKA I was conducted in the summer (August and September). The maximum temperature gradient occurs

*The mixed layer is defined as that layer above the depth at which the temperature is 1°C less than the surface temperature.

below the mixed layer in the region of the thermocline, below which temperature decreases fairly uniformly with increasing depth. However, the thermocline is quite variable, and the apparent smoothness indicated in Fig. 6 results from the number of data points selected when coding the original trace. The maximum depth of the thermocline region is somewhat arbitrarily placed at about 800 meters, below which the temperature profile continues to decrease with increasing depth, but much more slowly, to about 4000 meters. The temperature increases between 4000 meters and the bottom (not clearly shown in Fig. 6). This results from pressure effects causing adiabatic heating. A plot of potential temperature (the temperature if the effect of adiabatic heating were removed) in water below 1000 meters in depth is included on Fig. 6. Adiabatic heating causes an increase in water temperature of almost 0.5°C at a depth of 5000 meters, which agrees well with a report by Latham and others (1969). The temperature inversion can thus have a significant effect on the sound velocity structure at depth.

SEA SURFACE TEMPERATURE

The sea surface temperature at the FLIP/SANDS site decreased from 24.2°C to 22.6°C during the 24-day period that SANDS collected XBT's during PARKA II-A. During most of this period, the mixed layer was approximately isothermal. The depth of the mixed layer was almost always less than 100 meters, and averaged about 70 to 75 meters.

SALINITY STRUCTURE

The surface salinity in the FLIP area averaged slightly more than 35.20°/$_{oo}$. The relatively high salinity results from an excess of evaporation over precipitation, and according to Jacobs (1951), is distributed in a broad band by the prevailing surface currents in the area. A salinity profile constructed from a CONRAD STD station taken near FLIP (Fig. 7) shows that an isohaline mixed layer extending from

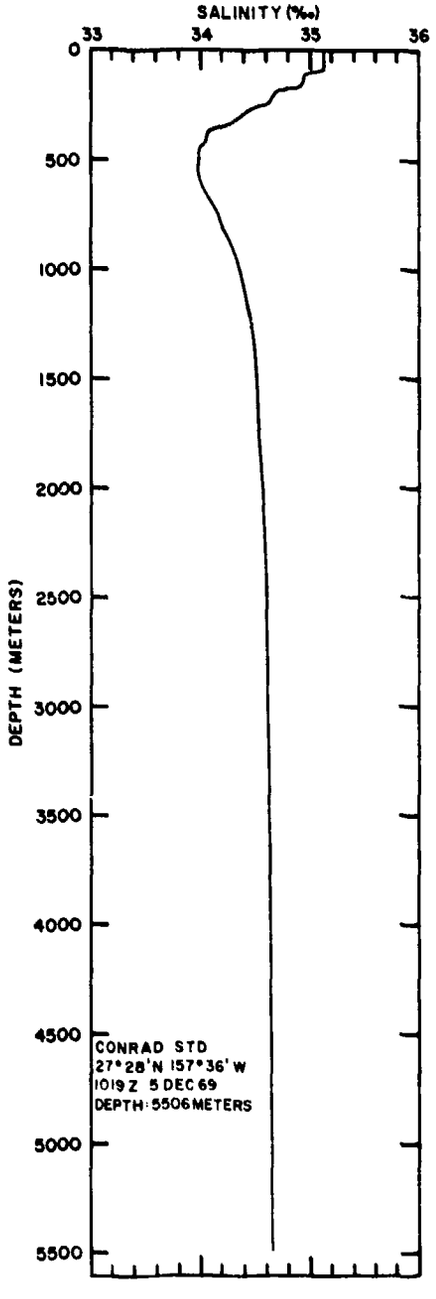

Fig. 7 — Salinity Profile at the FLIP/SANDS Site

the surface to almost 100 meters is succeeded by an irregular halocline down to the salinity minimum which occurs around 500 meters. Between 100 and 500 meters the average salinity gradient approaches a maximum negative value of 3×10^{-3} °/₀₀ per meter. The salinity minimum represents North Pacific Intermediate Water, which has been investigated in great detail by Reid (1965). The salinity of the bottom water in this area approaches a constant value of about 34.70°/₀₀.

At the northern end of the track around 36°N, the salinity structure is somewhat more complex. The influx of less saline subarctic water causes a pronounced salinity minimum to occur between 50 and 150 meters in depth. This anomaly is indicated by the bulge to the left above 178 meters in the T-S curve shown in Fig. 5a. The second minimum around 525 meters agrees well with the station taken near FLIP, presented in Fig. 7.

SIGMA-T PROFILES

Figure 8 shows the vertical distribution of sigma-t, a quantity closely related to the density of sea water. For comparative purposes, these quantities are often used interchangeably. Sigma-t is defined as:

$$\sigma_t = (\text{specific gravity-1}) \times 10^3$$

where the pressure has been reduced to atmospheric pressure, but the temperature and salinity are in situ values. The relationship between sigma-t, salinity, and temperature is rather complicated, and it is normally obtained from tables. A comparison of Fig. 8 with historical data shows the vertical distribution of sigma-t near FLIP to be typical of middle latitudes. Below the isopycnal (constant density) surface layer is a strongly stratified pycnocline, which approaches a constant value of 27.80 to great

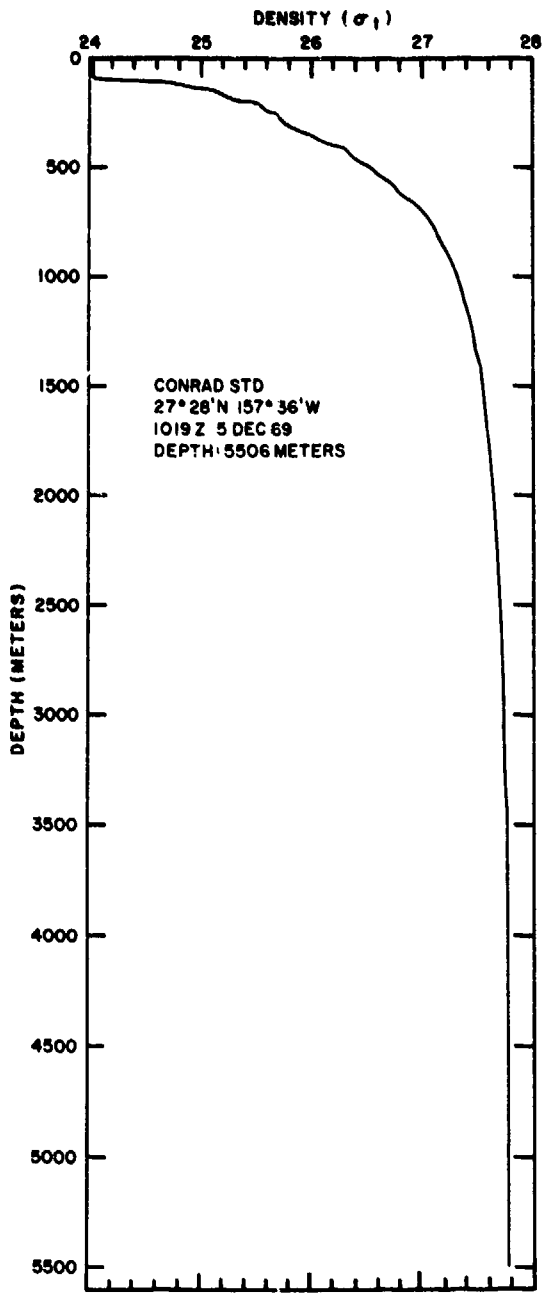

Fig. 8 — Sigma-t Profile at the FLIP/SANDS Site

depths. This strongly stratified pycnocline indicates the high vertical stability (resistance to vertical motion) of water masses in this area. A complementary profile of the stability parameter,

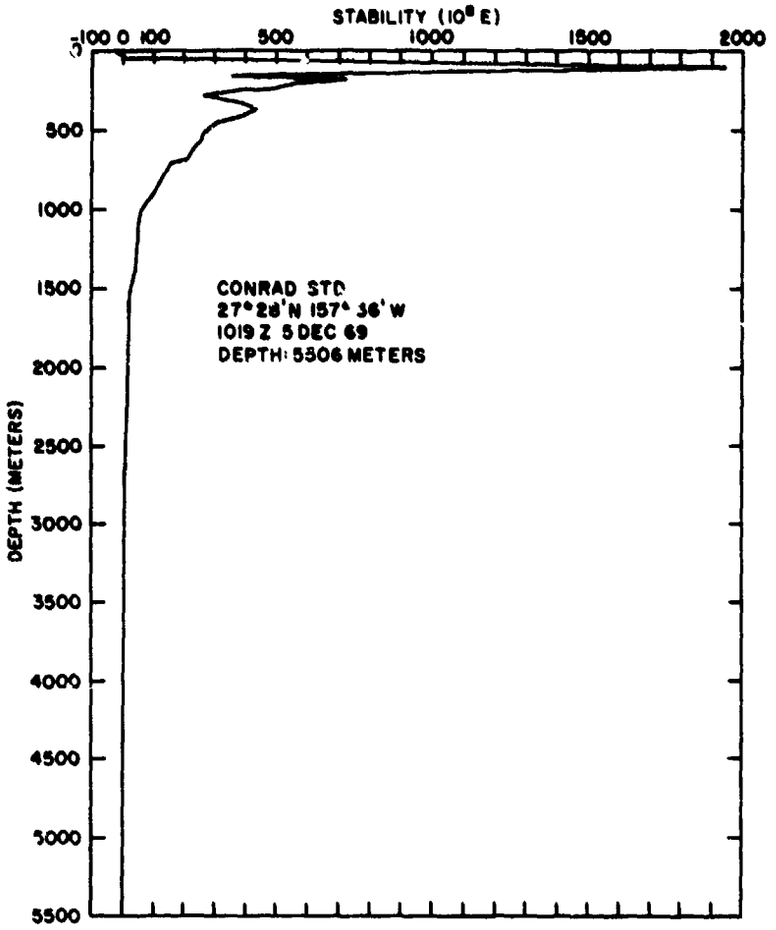

Fig. 9 — Stability Profile at the FLIP/SANDS Site

E(Z) plotted against depth Z, is shown in Fig. 9, using a relationship for E given by Hesselberg and Sverdrup (1915). Negative values of E represent unstable conditions, positive values represent stable conditions and zero represents neutral conditions. Maximum and minimum stability values may indicate transition zones between water masses separated vertically. Extreme values may indicate levels where internal oscillations are most likely to occur. Negative stabilities are frequently found in surface layers, and often indicate unstable conditions, which cannot persist for long periods. A readjustment toward more stable stratification generally occurs, with consequent change to the sound velocity structure.

Figure 9 shows that unstable conditions occur in at least the upper 25 meters at the FLIP site, and that vertical overturn may occur. Three closely-spaced maxima occur between 100 and 400 meters, which coincide with the most stable portion of the water column. The stability maximum at about 370 meters may correspond to the transition zone between the North Pacific Central and the North Pacific Intermediate Water Masses. Below 2500 meters, stabilities approach zero but are slightly positive, indicating a trend toward neutral conditions.

ENVIRONMENTAL VARIABILITY

The extensive oceanographic program in PARKA II-A acquired as much environmental data as possible spread out along the track of the acoustic experiments. One consequence was that the oceanographic data collected during the experiment varied considerably in space and time. Only on infrequent occasions were two or more PARKA ships close enough to each other to collect simultaneous data that could be compared for quality control. Although all PARKA ships passed the FLIP/SANDS site several times during the course of the experiment, they departed the site as soon as possible in order to minimize ship-generated noise at the hydrophones. Thus, one of the few data records that can be examined for evidence of temporal environmental variability is the series of XBT's that were collected by SANDS twice daily during PARKA II-A.

The data collected during this 16-day period at essentially the same location were examined to determine the depth of the mixed layer. Figure 10 shows the layer depths plotted in the form of a time series; these were obtained from the temperature data used to compute the sound velocity profiles included in Fig. 42, which will be discussed in Section IV below. The points have not been connected because a significantly higher sampling rate would have been required for true resolution of the curve. However, the data plot shows that layer depths ranged at least from 56 meters to 88 meters. This variability could affect sound transmission in the surface duct.

The data plotted in Fig. 10 show that more than two observations should have been taken each day in order to resolve the period and amplitude of the layer depth fluctuations. Nevertheless, it is apparent from the stability profile in Fig. 9 that internal oscillations are likely to occur in this shallow depth region. It is also likely that the high wind speeds and large wave heights which were observed during PARKA II-A could have generated internal waves sufficient to cause the fluctuations in observed layer depth. Estimates of internal wave frequency based on the density profile of Fig. 8 yield a maximum value of eight cycles per hour (at a depth of 90 meters), and a minimum value of 0.92 cycles per day. At this time, the existence of internal waves significant to the PARKA II-A acoustic program is conjectural.

Part B. Thermistor Chain Observations

THERMISTOR CHAIN AND ANCILLARY EQUIPMENT

Capability

The NURDC thermistor chain measures short-period temporal and small-scale spatial variations in temperature between the sea surface and a maximum depth of approximately 220 meters, while operating at its normal tow speed of six knots. Vertical thermal structure is recorded as a function of geographic position and time. Forty-seven temperature sensors on the chain are scanned sequentially (from the surface to the deepest sensor) once every ten seconds. Each scan includes outputs from two calibrating resistors and a depth sensor. At a six-knot tow speed the chain data are equivalent to a bathythermograph drop every 31 meters along the ship's track. Each ten-second scan is recorded in digital form on an incremental magnetic tape recorder, and a UNIVAC 1218 computer and peripheral equipment are interfaced with the digital system to accomplish real-time data analysis. The real-time program computes the average (equal weight) output from each chain sensor over time intervals that may be preset from 3.0 to 94.5 minutes. Hansen (1969) has described the computer installation and programming in detail.

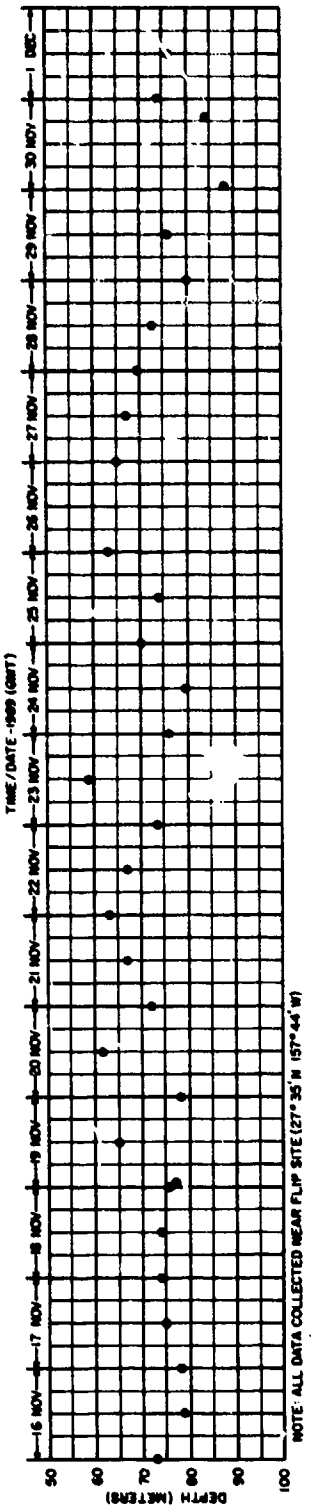

Fig. 10 — Temporal Variations in Mixed Layer Depth from SANDS XBT Data

Sensors

The 47 thermistors on the chain are spaced at 5.1 meter intervals. Temperatures are recorded to the nearest 0.05°C, although the accuracy of the measured temperatures is approximately ±0.1°C. The sensors are thermally lagged and have a response time of 20 seconds. The two calibrating resistors show any electronic drift in the system, and the temperature data are corrected with a slope-intercept formula computed from the calibration readings.

CONFIGURATION

The chain assumes the configuration of a modified catenary when under tow. Smith (1969), in an intensive examination of the chain's towing characteristics, empirically derived the towed configuration. He obtained equations for the depth of each thermistor as a function of the maximum depth of the chain. Computed sensor depths are accurate to ±0.5 meter.

OPERATIONS

NURDC operational procedures were identical throughout the PARKA II-A Experiment. The thermistor chain was operated continuously whenever underway or drifting on the PARKA II-A tracks. Temperature data were smoothed by averaging over intervals of one hour. Each average was assigned the time and geographic position of the midpoint of the time interval over which the average was made. Mean sensor depths were computed for each interval, and temperatures were logged for each hourly average in the standard BATHY format. When the chain was not in operation, XBT drops were made at 0000, 0600, 1200, and 1800Z daily. A few XBT's were taken while the chain was operating, but were discontinued when the XBT wire fouled the chain. Chain and XBT messages were transmitted to the PARKA II-A Operation Control Center. Sea surface temperatures were recorded every other hour on the odd hour. OMEGA, LORAN A, and celestial observations were used for navigation.

During PARKA II-A, REXBURG towed the chain along five tracks or runs radiating from the FLIP site at 27°35'N, 157°44'W as shown in Fig. 1. These are the same tracks used by the source ship during the acoustic experiments. The tracks and lengths of tow are tabulated in Table 1.

TABLE 1
Thermistor Chain Tracks in PARKA II-A

Event	Chain Tow Track	Track Length
9-1	From 22°N to FLIP site along 157°44'W	330 nmi
9-2	From FLIP site to 31°45'N along 157°44'W	265 nmi
9-3	From 31°45'N to FLIP site along 157°44'W	265 nmi
9-4	From FLIP site out on a great circle track bearing 247°T from FLIP	400 nmi
9-5	Return to FLIP site following the same great circle route traveled for Event 9-4	400 nmi

The thermistor chain was also operated continuously during the time period between the end of Event 9-2 and the beginning of Event 9-3, when REXBURG drifted to conserve fuel, except for a two-hour system maintenance interval. Operations while drifting were identical to those conducted while underway.

The thermistor chain thus furnished many details of the thermal structure in the upper layers of the water column, supplementing the XBT and STD data which were received from discrete geographical locations. Salient features of the thermistor chain data are described in the following discussion.

DISCUSSION

Isotherm Contour Plots

Isotherm-depth contours were plotted from the hourly averaged temperature data for each run and are presented in Figs. 11 through 15. Whole-degree isotherm depths were obtained by linear interpolation between adjacent temperature sensors on the chain. The vertical axes in the plots represent depth in meters, and the horizontal axes are labeled according to time and geographic position. The vertical exaggeration of the plots is 1850:1.

Event 9-1 (From 22°N to FLIP)

Temperature structure recorded during Event 9-1 is shown in Fig. 11. Vertical thermal gradients observed on this run are strongest in the depth interval from 60 to 90 meters. These gradients range in magnitude from about 0.1 to 0.2°C/m. At depths greater than 90 meters, vertical gradients decrease to approximately 0.02 to 0.05°C/m. Mixed layer depth averages slightly more than 50 meters, with an approximate range of between 25 and 70 meters. The temperature of the entire water column sampled by the chain decreases by nearly 1.0°C from south to north along the run.

A ridge-like structure centered at 25°N latitude appears in the isotherm contours in the deeper levels. Such a structure could represent sections through thermal domes associated with cyclonic eddies of dimensions comparable to those given by Wyrtki (1967). The deeper isotherms change depth by as much as 50 meters in less than 30 nautical miles horizontal distance, and horizontal temperature gradients as strong as 5.0×10^{-3}°C/m occur. The "ridge" is asymmetric, with steeper isotherm slopes accompanied by stronger horizontal gradients occurring on its northern side. Vertical displacement of isotherms decreases with decreasing depth as a result of increased vertical mixing toward the surface. Smith (1971a) reports a similar, though more extensive structure at nearly the same location in PARKA I. Vertical sections of temperature along 158°W longitude prepared from bathythermograph data recorded during the NORPAC expeditions in 1955 (NORPAC Committee, 1960) also show a ridge near 25°N. The presence of these structures in data from PARKA I, PARKA II-A, and NORPAC indicates that they may be a semi-permanent characteristic of the thermal structure north of the Hawaiian Islands.

Events 9-2 and 9-3 (Runs North of FLIP)

Temperature data from Events 9-2 and 9-3 (Figs. 12 and 13) will be considered simultaneously since these runs were made on the same track. Strong horizontal gradients are present in the thermal structure in this region. These occur between about 28°N and 30°N latitude at depths of 80 meters and deeper, and range up to approximately 2.5×10^{-3}°C/m. Similar horizontal gradients were observed in PARKA I (Smith, 1971a), and also are indicated in isotherm contours from NORPAC (NORPAC Committee, 1960). The NORPAC data show these gradients to extend to a depth of at least 700 meters. In the present data, temperature throughout the

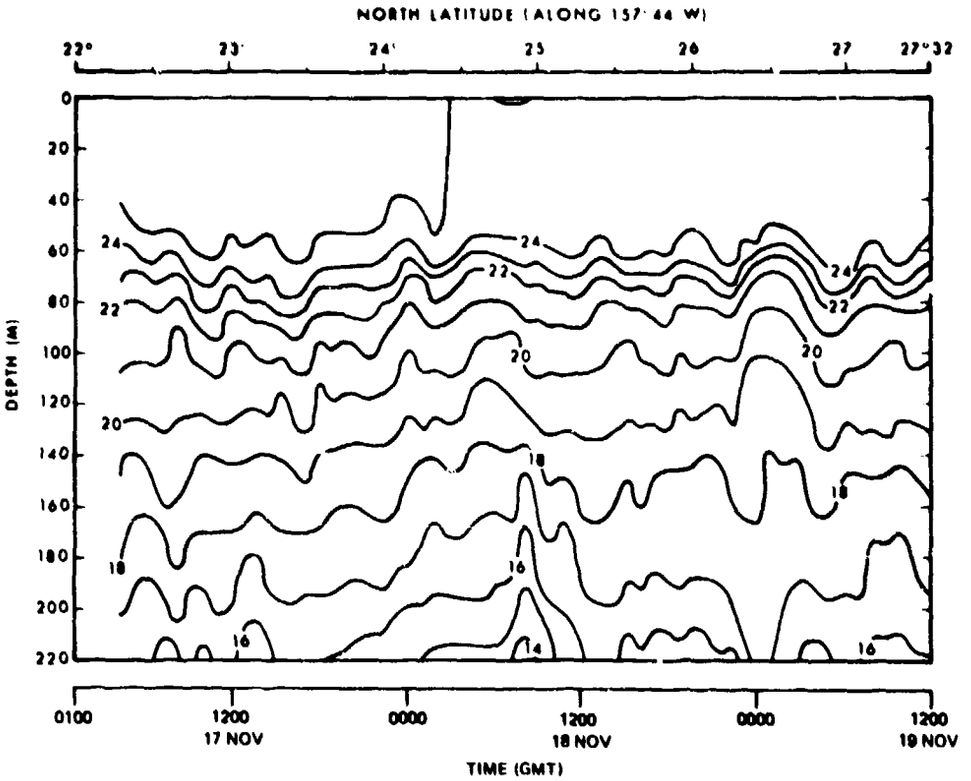

Fig. 11 — Temperature Structure (°C), REXBURG Event 9-1 (22°N to FLIP)

water column between the surface and 220 meters depth decreases by slightly more than 2°C from the southern to the northern end of the runs.

Vertical temperature gradients are greatest at depths from 50 to 90 meters. Gradients in this depth interval range in magnitude from approximately 0.1 to 0.2°C/m. At depths greater than 90 meters, vertical gradients decrease to magnitudes of from 0.025 to 0.05°C/m. Mixed layer depth varies from slightly more than 40 meters to almost 70 meters, with the deeper values generally occurring toward the southern end of the track. There is always a great deal of microstructure within the mixed layer, although it is sometimes masked by experimental error. At several locations along the PARKA track, the mixed layer is isothermal only to a depth of about 20 meters, then shows a slight decrease in temperature over the next 20 or 30 meters. Depending on how persistent this temperature change is and how gradually it occurs, it can change the sign of a sound velocity gradient within the layer from slightly positive to slightly negative, thus reducing the effectiveness of acoustic propagation via the surface duct.

Such a situation was observed around 29°40′N on Event 9-2 and 29°10′N on Event 9-3. Although isotherm contour plots like those in Figs. 12 and 13 do not clearly show such a phenomenon, a clue to its existence can be seen in the way the isotherms approach the surface. In these two instances, the isotherms approach the surface at an angle, rather than vertically. The mixed layer thus cannot be truly isothermal in such a region.

An apparent southward translation of the thermal structure of about 20 nautical miles from Event 9-2 to Event 9-3 is evident when the contours are compared. It is important to note, however, that the measured acoustic propagation loss versus range reported in Volume 1 was identical for Events 9-2 and 9-3 within experimental error. This indicates that this degree of difference in the contours did not observably affect propagation.

Events 9-4 and 9-5 (Southwest Runs)

Vertical temperature gradients recorded on Events 9-4 and 9-5 (Figs. 14 and 15) are strongest at depths from 60 to approximately 110 meters and range from nearly 0.1 to nearly 0.2°C/m. At depths greater than 110 meters, vertical gradients remain within the limits of 0.03 to 0.1°C/m. Mixed layer depth varies from less than 40 meters to slightly more than 80 meters over the length of the runs. The mixed layer is generally isothermal, although a small area of negative gradients appears at a range of about 325 miles from FLIP on Events 9-4 and 9-5. In this region, isothermal water extends only to a depth of about 15 or 20 meters, and in some places may disappear completely. Below this isothermal layer, the water cools slowly with depth. In several isolated cases, the temperature at the bottom of the mixed layer (about 80 meters) was nearly 1°C colder than the near-surface isothermal layer. Acoustic transmission via the surface duct would be impossible through any region where this negative gradient extended all the way to the surface.

There is no appreciable net change in temperature throughout the water column along the track, except in the near-surface layer where temperature increases by a little more than 1.0°C from FLIP to the end of the track 400 nautical miles away. As a consequence, the vertical temperature gradient increases slightly with increasing distance from FLIP.

Two ridges dominate the profiles from this track. These structures are centered at ranges from the FLIP site of 100 and 225 nautical miles. As mentioned above, they may represent cross sections through thermal domes associated with cyclonic eddies; eddy-associated domes of this size are not unusual in the Hawaiian Islands

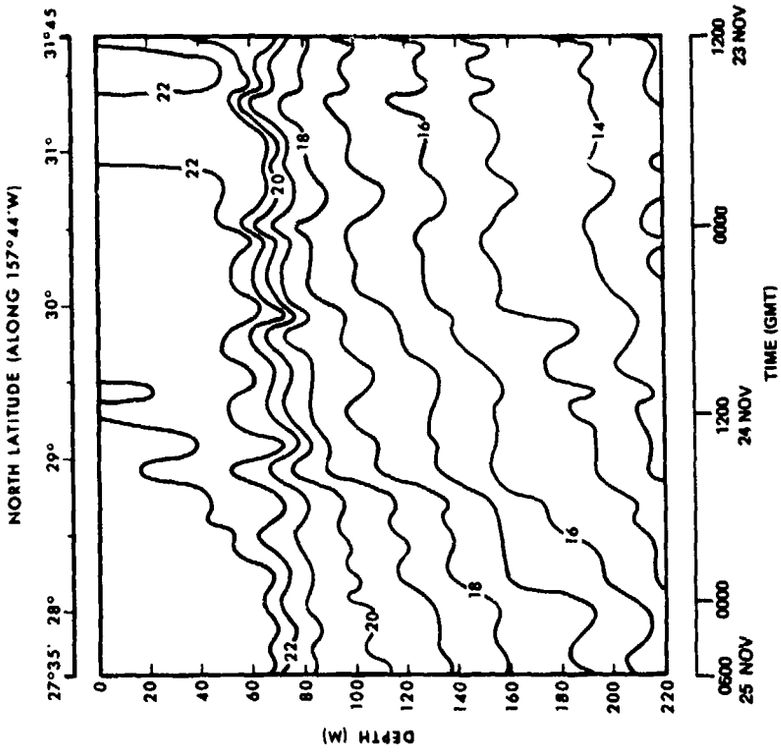

Fig. 13 — Temperature Structure (°C), REXBURG Event 9-3 (31°45'N to FLIP)

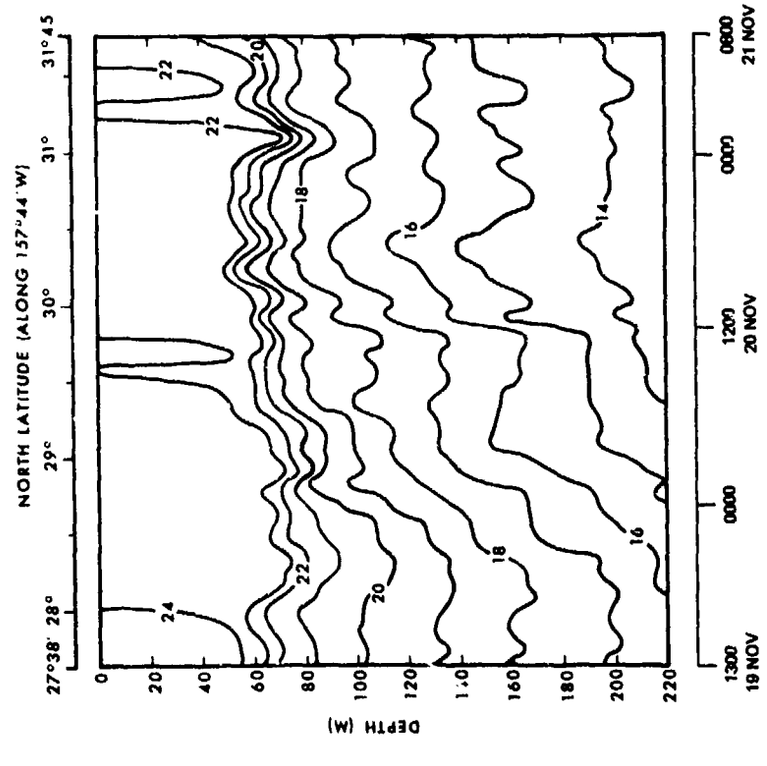

Fig. 12 — Temperature Structure (°C), REXBURG Event 9-2 (FLIP to 31°45'N)

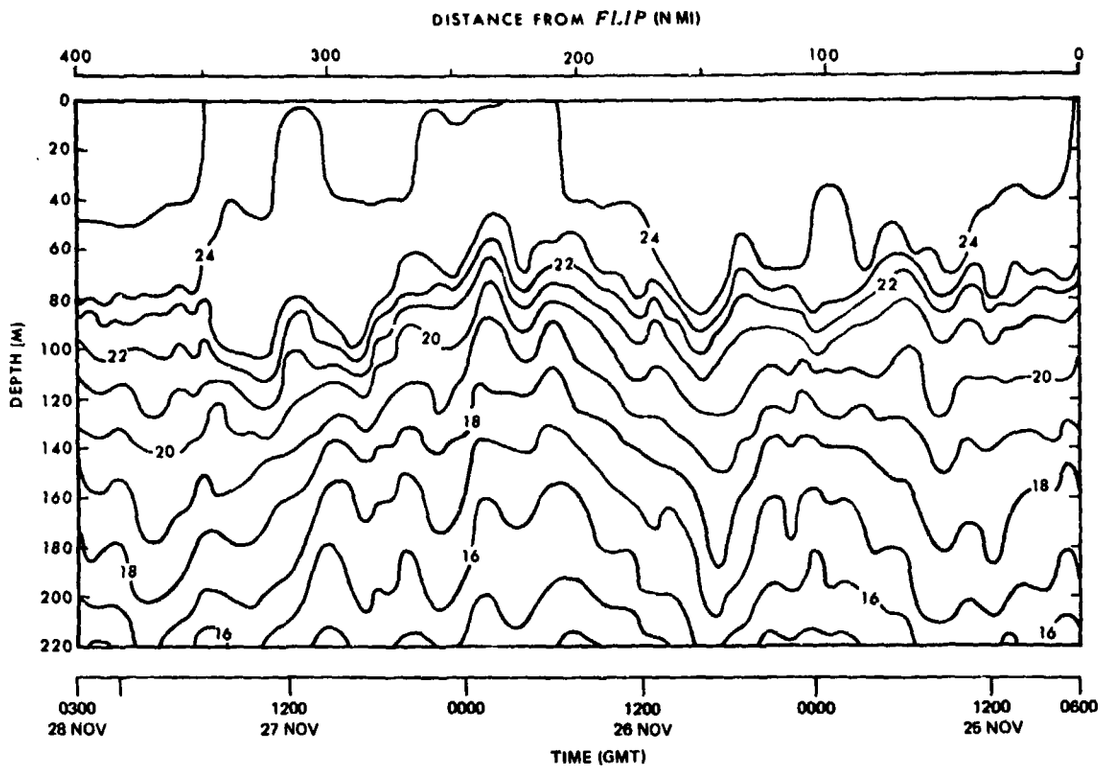

Fig. 14 — Temperature Structure (°C), REXBURG Event 9-4 (247°T from FLIP)

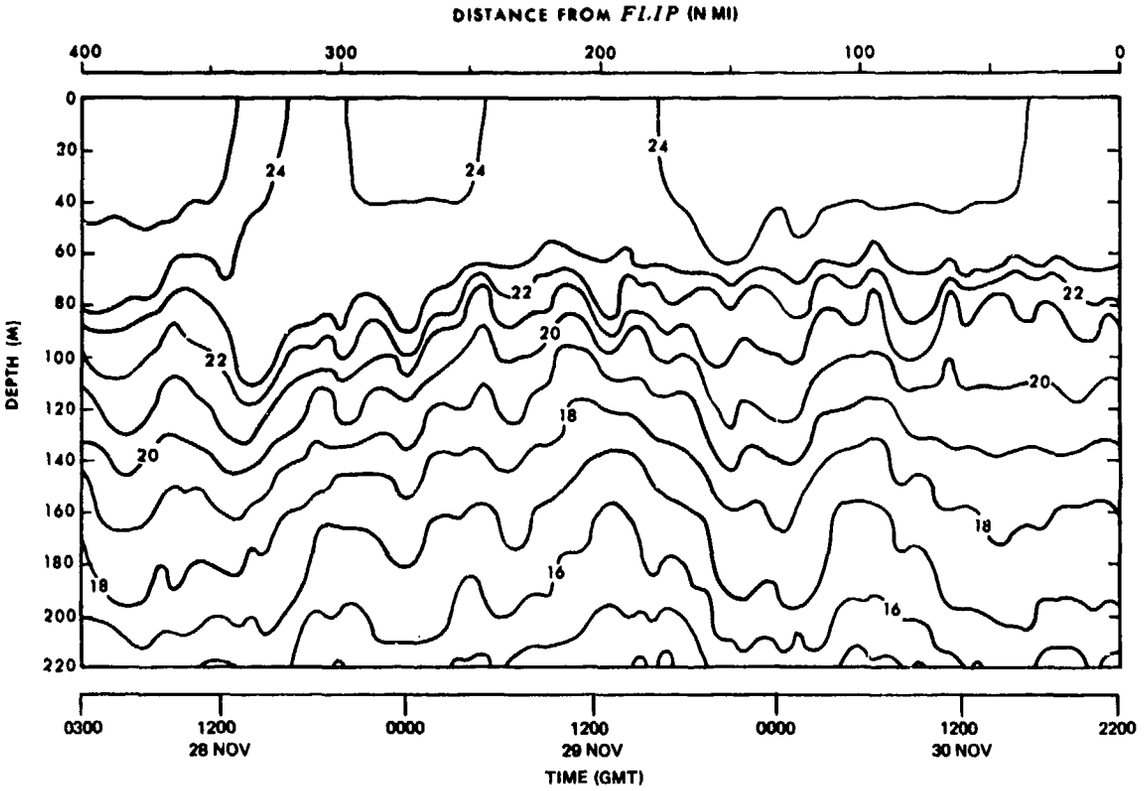

Fig. 15 — Temperature Structure (°C), REXBURG Event 9-5 (067°T to FLIP)

region (Smith, 1967, and Patzert, 1969). Because no data were recorded transversely to the track of Events 9-4 and 9-5, no determination can be made of the true cause or geographical extent of the ridges. Vertical excursions of isotherms in the larger ridge (centered 225 nautical miles from FLIP) occur throughout the depth range sampled by the chain. Isotherm depth changes in the smaller ridge (centered 100 nautical miles from FLIP) occur only in the lower half of the chain records. In both structures, depth changes of isotherms decreased with decreasing depth. Vertical excursions of isotherms of up to 80 meters in horizontal distances as short as 60 nautical miles accompany the larger ridge. In the smaller ridge, isotherms undergo depth changes of as much as 50 meters in horizontal distances of 25 nautical miles. Horizontal gradients within the ridges are as great as 5.0×10^{-5}°C/m. The larger ridge is asymmetric, with stronger horizontal gradients on the side closer to FLIP than on the side away from FLIP.

GENERAL

No temperature inversions were encountered in the chain data with the smoothing scale exployed; however, the incidence of inversions in temperature records is largely a function of sampling method and scale (Roden, 1964). At the chain's normal towing speed of six knots the hourly averaging process filters out depth oscillations of isotherms which have wavelengths less than six nautical miles. This averaging method also eliminates, partially or totally, the non-oscillatory thermal features of small horizontal extent. Isothermal conditions prevailed in the mixed layer throughout the runs. However, as pointed out above, there were several regions along the PARKA II-A tracks to the north and southwest of FLIP where the mixed layer showed a mild negative gradient below a shallow isothermal layer. Unfortunately, the configuration, inherent accuracy, and processing scheme of the chain system as employed in PARKA II-A tended to mask much of this thermal microstructure.

Gross features of the thermal structure were stationary over the intervals between chain tows over the same tracks, but high variability was present in the small scale features having wavelengths less than approximately 25 nautical miles and vertical amplitudes less than about ten meters (compare Events 9-2 and 9-3, Figs. 12 and 13, with Events 9-4 and 9-5, Figs. 14 and 15). These oscillations are superimposed on the larger scale features and show no correlation from run to run over the same track.

The depth of strongest vertical gradient and the mixed layer depth vary more in the profiles from Events 9-4 and 9-5 than on the other tracks, and the strongest vertical gradient and the mixed layer depth average about 10 to 20 meters deeper on these runs than on any of the other runs. Even at the maximum depth (220 meters) sampled by the chain, there is still an appreciable vertical temperature gradient which indicates that the chain is not long enough to penetrate the permanent thermocline.

IV. SOUND VELOCITY STRUCTURE

GENERAL

Sound velocity in the ocean is usually expressed as a function of three variables: temperature, salinity, and pressure. Between the surface and the depth of the deep sound channel axis (about 750 meters near FLIP), temperature is the most important variable influencing sound velocity. Below the depth of the sound channel axis, the cumulative effect of pressure controls the structure of the sound velocity profile since temperature and salinity usually vary little at these depths.

Two aspects of the vertical sound velocity structure are of major importance in sound propagation, the sound velocity and its gradient. The sign of the gradient is a most important feature which is often ignored when the gradient itself is small. The sign, of course, determines whether the sound is bent upwards or downwards and thus is of critical importance in such regions as the mixed layer and for sonar systems designed to exploit that layer as a sound channel. The strength of the gradient and the sound velocity itself determine the severity of bending and determine travel times.

Two different presentations will be used to describe these two characteristics of the sound velocity structure. The first is a series of shallow and deep profiles of sound velocity as a function of depth that indicate the strength and sign of the gradient at various locations along the PARKA track. Each profile is plotted at the range from FLIP at which the observation was made, and carries a ship indicator letter at the bottom of the trace. Because of space limitations, no absolute values are indicated on the profiles. The second presentation is the standard cross section, showing contours of sound velocity. From these the velocity of sound at any range and depth along the track can be determined. The methods used in constructing these plots are discussed below.

As discussed in Section II above, the PARKA II-A area falls largely within the North Pacific Central Water Mass. Therefore, the properties of the near-surface water do not change greatly out to a range of about 900 nautical miles from FLIP (shorter ranges to the south). All of the tracks covered by the various ships in Events 9 and 11 (Figs. 1 and 3) fall within the region, as do the first 900 nautical miles of the aircraft runs in Event 13 (Fig. 2).

The sound velocity structure within this area is characterized by a deep, well-formed sound channel, with an average axial velocity of 1480 m/sec, and an axial depth of 750 meters. The bottom of the sound channel in November and December is at a depth of about 4500 meters; bottom topography penetrates into the channel on the runs to the east, south, and southwest of FLIP (Events 9-1, 9-4, 9-5, 13-3, and 13-4). The mixed layer averages between 70 and 80 meters in depth, though it can display considerable variability. (See Section III, Parts A and B above.) The mixed layer is generally isothermal, and in most cases shows a slight positive sound velocity gradient, caused by increasing pressure. However, in several locations along the PARKA II-A tracks, isothermal water extends only to a depth of 15 to 20 meters, followed by a weak negative gradient to the bottom of the mixed layer. In areas where this negative gradient extended all the way to the surface, it would effectively block sound transmission by the surface duct.

To the north, both the axis and the bottom of the sound channel shoal rapidly in the vicinity of the water mass boundary between 42°N and 45°N, and the thickness of the mixed layer decreases also.

To the east the axis of the sound channel remains deep almost until landfall at San Diego, although there is substantial bathymetric inter-

ference. In addition, a boundary region near the edge of the California Current could change acoustic conditions in that region (about 1300 nautical miles from FLIP).

A comparison of directly-measured and computed sound velocities shows the computed values to be consistently about 0.5 m/sec greater, below the axis of the deep sound channel. This discrepancy is attributed to minor inaccuracies in Wilson's equation, and is probably of little importance in predicting acoustic propagation.

PROPAGATION LOSS AND ARRIVAL STRUCTURE, SHIP RUNS (EVENTS 9 AND 11)

Summary

Throughout the region covered by ship runs during PARKA II-A, a well-formed sound channel prevails, with an average axial depth of about 750 meters and an average axial velocity of about 1480 m/sec (±1 m/sec). The mixed layer averages between 70 and 80 meters in depth, producing a weak surface duct in this area during the autumn season. Occasionally, the usual weakly-positive gradients in the surface layer are interspersed with profiles displaying slightly negative gradients. These would have the effect of interrupting propagation via the surface duct. The greatest variations in sound velocity in each profile occur in the interval between the bottom of the mixed layer and the sound channel axis.

Figures 16, 17, 19, and 20 display all the deep velocimeter and STD data collected along the PARKA II-A ship tracks (Figs. 1 and 3), regardless of the time during the experiment when the observation was made. Data shallower than 1000 meters were eliminated from these illustrations to avoid overplotting near the surface. Figures 16 and 17 cover the north-south track from 22°N to 36°N, and include all deep data from Events 9-1, 9-2, 9-3, 11-1, and 11-2. Figures 19 and 20 are based on the data collected along the southwest track during Events 9-4 and 9-5. The techniques used in constructing these figures will be discussed under Figure Construction below.

The deep sound velocity structure along the PARKA north-sound track from 22°N, through the FLIP site (27°35'N), to 36°N is shown by the velocity profiles plotted in Fig. 16. The depth of the sound channel axis averages between 740 and 750 meters, which is in close agreement with PARKA I data (Maury Center for Ocean Science, 1969b). In PARKA I the axis remained around 750 meters between 22°N and 31°N, then shoaled to 700 meters at 36°N. Because of a paucity of data north of 32°N, this latter feature cannot clearly be identified during PARKA II-A, although several CONRAD profiles seem to indicate such behavior.

The maximum sound velocity above the axis is generally located in the mixed layer. The bottom of the sound channel, that depth at which the surface (or near-surface) sound velocity maximum recurs below the axis (also called critical depth), occurs around 4500 meters. Where the water depth is 5500 meters, this results in a "depth excess" of about 1000 meters, which provides for reliable convergence zone propagation. As shown in the bathymetric profile of the north-south track from 22°N to 36°N (Fig. 18), such a depth excess prevails on the track north of FLIP. The track to the south toward Oahu is severely bottom limited, however, by shoaling of the average depth to about 4500 meters, and by several seamounts rising above the critical depth. These intrude into the bottom third of the sound channel, and can be expected to degrade acoustic propagation severely on this leg.

The sound velocity gradient is normally quite stable in the deep ocean below the axis of the sound channel. From Fig. 16, the gradient is determined to be 0.0176 sec^{-1}. This agrees

closely with 0.0178 sec^{-1}, the gradient predicted by Wilson's equation (Wilson, 1960) when only the effect of pressure is considered. The negative gradient above the sound channel axis is considerably steeper than the deep gradient, and is much more variable.

Figure 17 displays in contoured form the velocity profile data of Fig. 16. The sound velocity contours (isotachs) were drawn for a contour interval of 5 m/sec. The axial velocity of slightly more than 1480 m/sec over the length of the track is not specifically contoured. Surface velocity decreases from 1534 m/sec at 22°N (−330 nautical miles) to 1511 m/sec at 36°N (510 nautical miles), with most of the decrease occurring in the transition zone north of 32°N (265 nautical miles). This decrease in sound velocity is caused by the influence of cooler northern water. Because of the vertical scale employed here, little detailed structure is evident, particularly near the surface, but the uniformity of the deep ocean environment is clearly indicated.

The sound velocity structure along the 400 nautical mile track southwest of FLIP (Events 9-4 and 9-5) is shown in Figs. 19 and 20. The deep axial sound velocity, depth of axis, and the gradients above and below the axis are similar to those north and south of FLIP discussed above (Figs. 16 and 17). The bathymetric profile for this track is displayed in Fig. 21. Starting at a range of about 150 nautical miles from FLIP, this track encounters very rough terrain, with a seamount rising over 2000 meters from the ocean floor at a range of 225 nautical miles from FLIP. Other seamounts on both sides of the track also intrude into the sound channel, interfering with acoustic propagation throughout the area.

Figure Construction

The prominent characteristics of the sound velocity structure are shown in profiles (such as Figs. 16 and 19) and contoured cross sections (as in Figs. 17 and 20). These illustrations are based only on the somewhat sparse deep observations, and nearly all the available data were plotted. When confronted with high data density (as in the figures for shallow depths discussed below) the method used in plotting the data becomes important, since some data must arbitrarily be eliminated to insure the legibility of what remains.

The following discussion describes the techniques used in plotting the profiles and contoured cross sections shown in this volume.

1. Sound Velocity Profiles

The shallow sound velocity structure in the PARKA area from the surface to a depth of 750 meters is shown by six shallow sound velocity profile plots (Fig. 22, 23, 24, 28, 29, and 32), one for each acoustic event (Events 9-1, 9-2, 9-3, 9-4, 9-5, and one for both 11-1 and 11-2). Each profile includes oceanographic data collected only during the time the particular acoustic experiment was being conducted. The shallow profiles extend to a depth of only 750 meters, because not enough deeper data were collected during the two and one-half to three day duration of each run to justify extending the scale any deeper. Most of the shallow profiles are constructed from XBT's, which terminate at this depth. These plots permit a detailed analysis of the near-surface environment, where the sound velocity structure is most variable. Nearly all of the profiles were computed by FNWC using measured temperature data from XBT's, AXBT's, and the thermistor chain, combined with archival salinity data. A few MARYSVILLE profiles are based on shallow measurements of sound velocity obtained with a velocimeter.

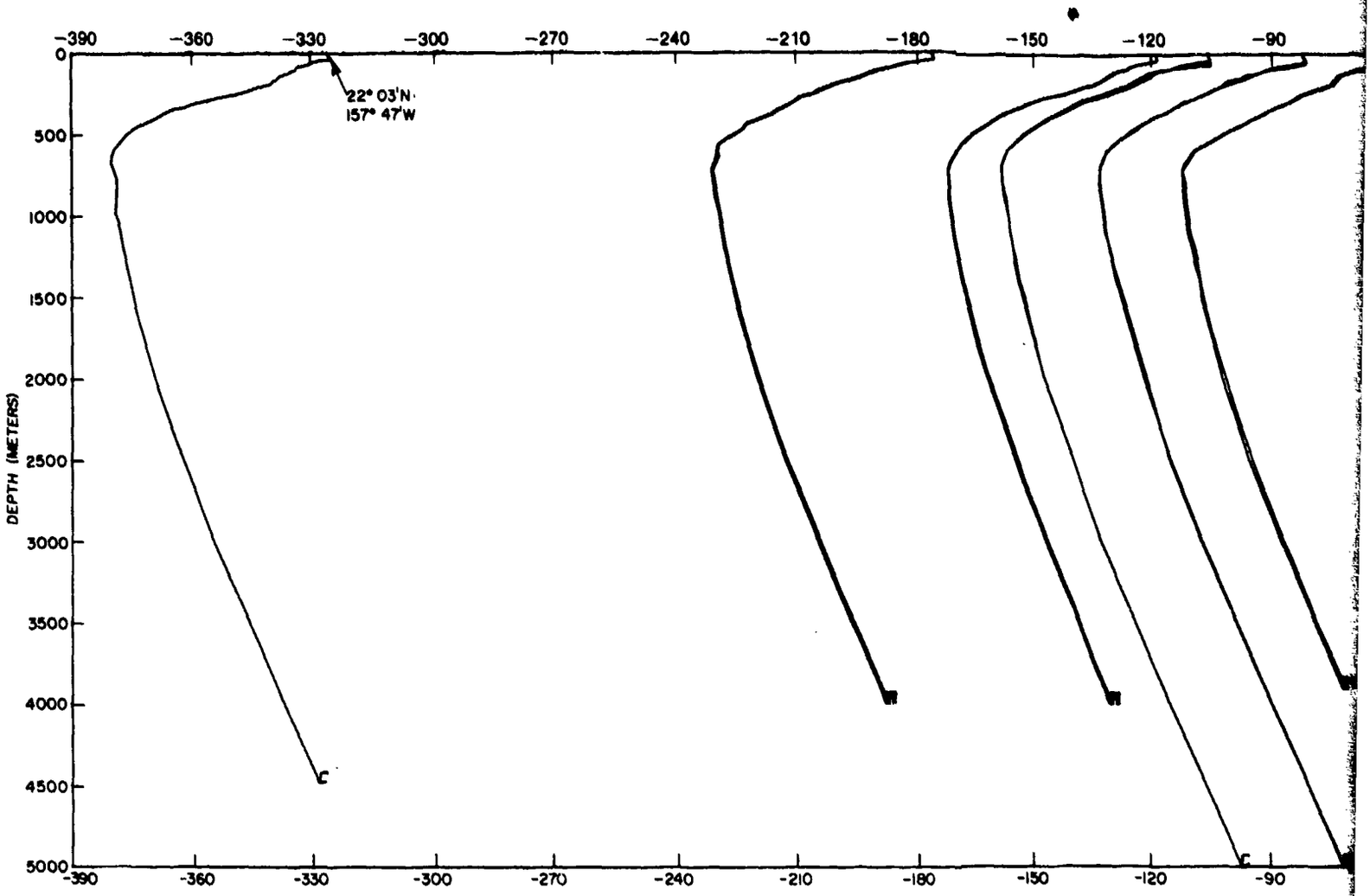
-390
-360
-330
-300
-270
-240
-210
-180
-150
-120
-90
0
500
1000
1500
2000
2500
3000
3500
4000
4500
5000
DEPTH (METERS)
22° 03'N
157° 47'W
C
C

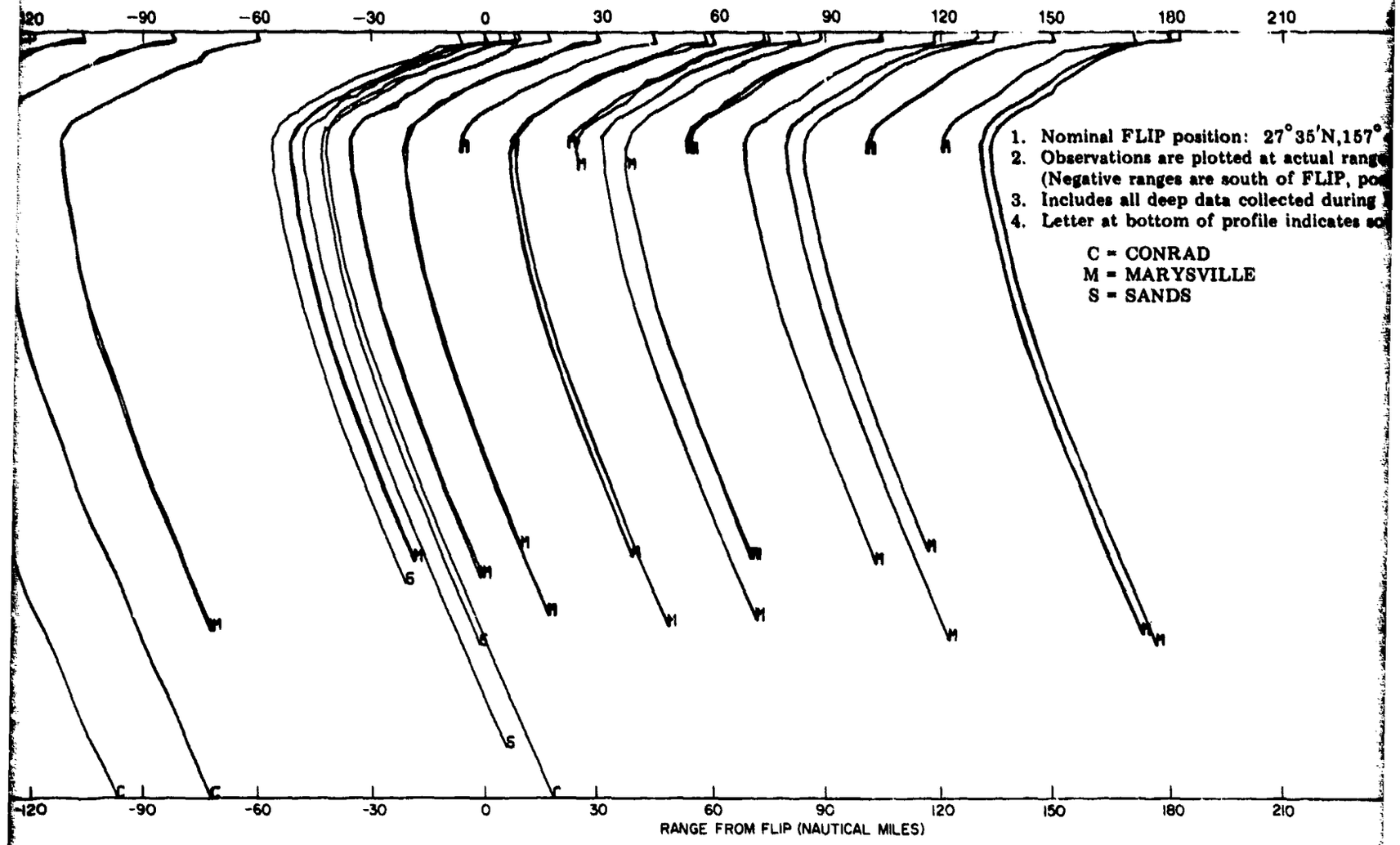

Fig. 16 — Deep Sound Velocity Profiles Along PARKA II-A North-South Track (157°44'W)

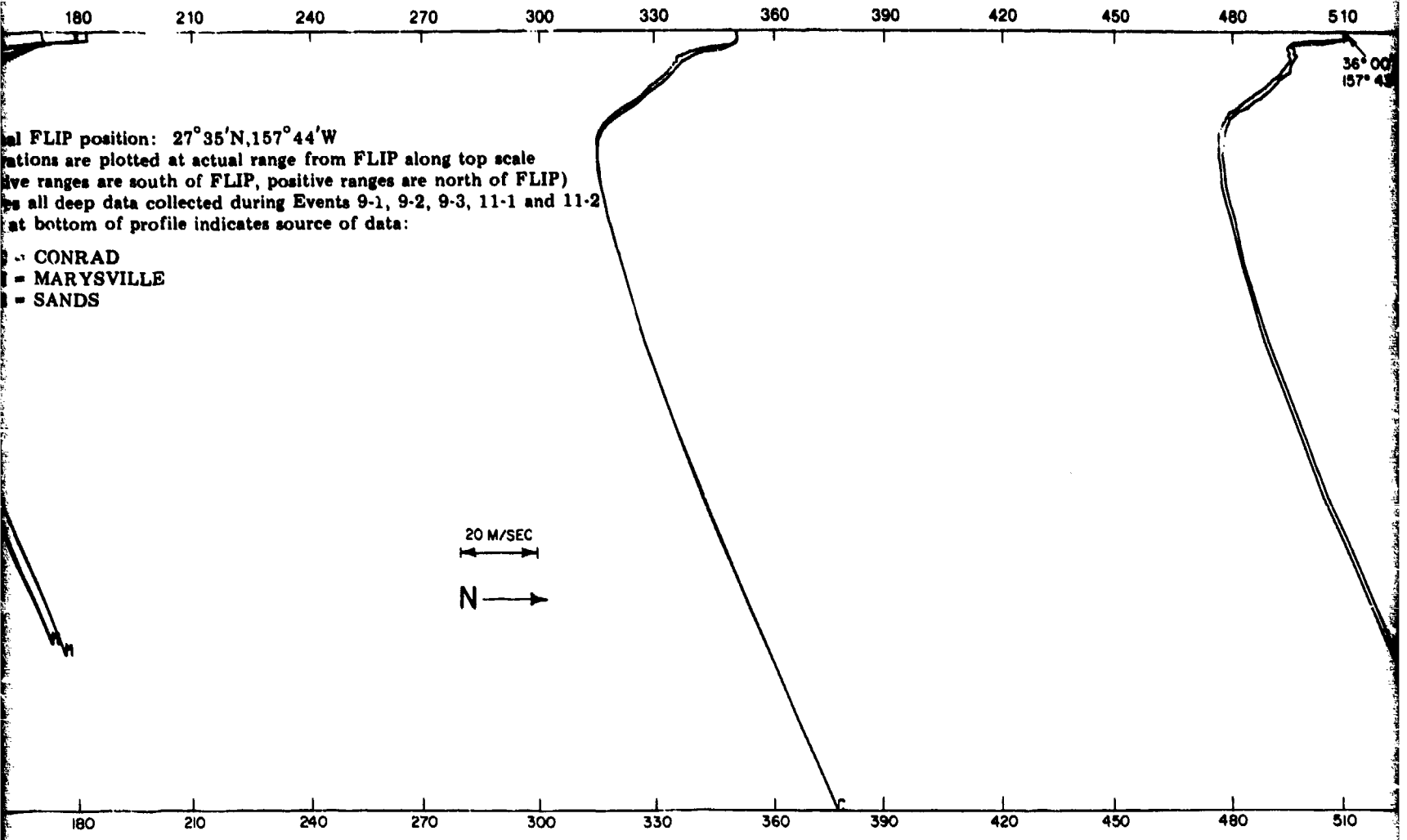

al FLIP position: 27°35'N,157°44'W
ations are plotted at actual range from FLIP along top scale
ive ranges are south of FLIP, positive ranges are north of FLIP)
s all deep data collected during Events 9-1, 9-2, 9-3, 11-1 and 11-2
at bottom of profile indicates source of data:

- CONRAD
- MARYSVILLE
- SANDS

(157°44'W)

3

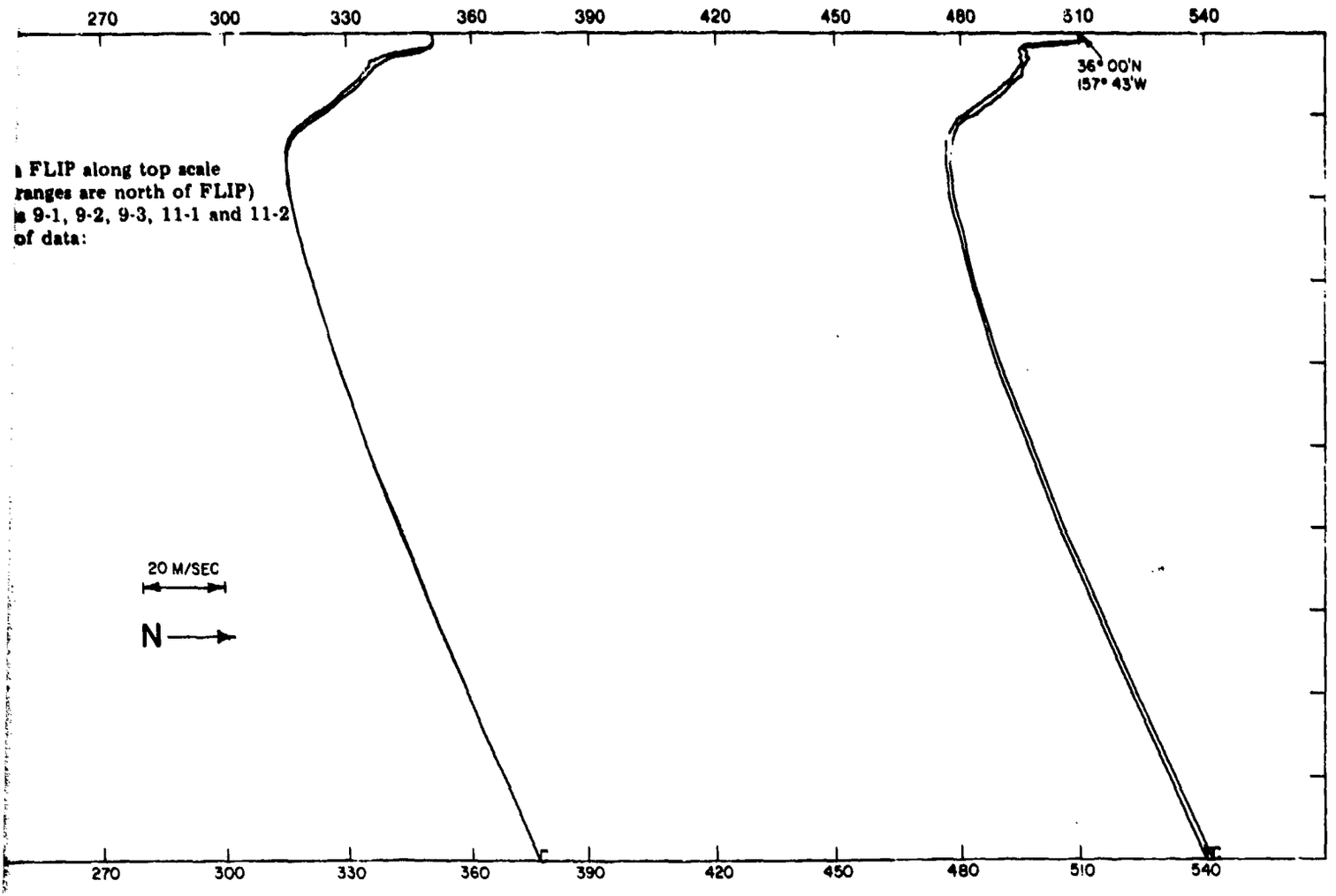

FLIP along top scale
ranges are north of FLIP)
9-1, 9-2, 9-3, 11-1 and 11-2
of data:

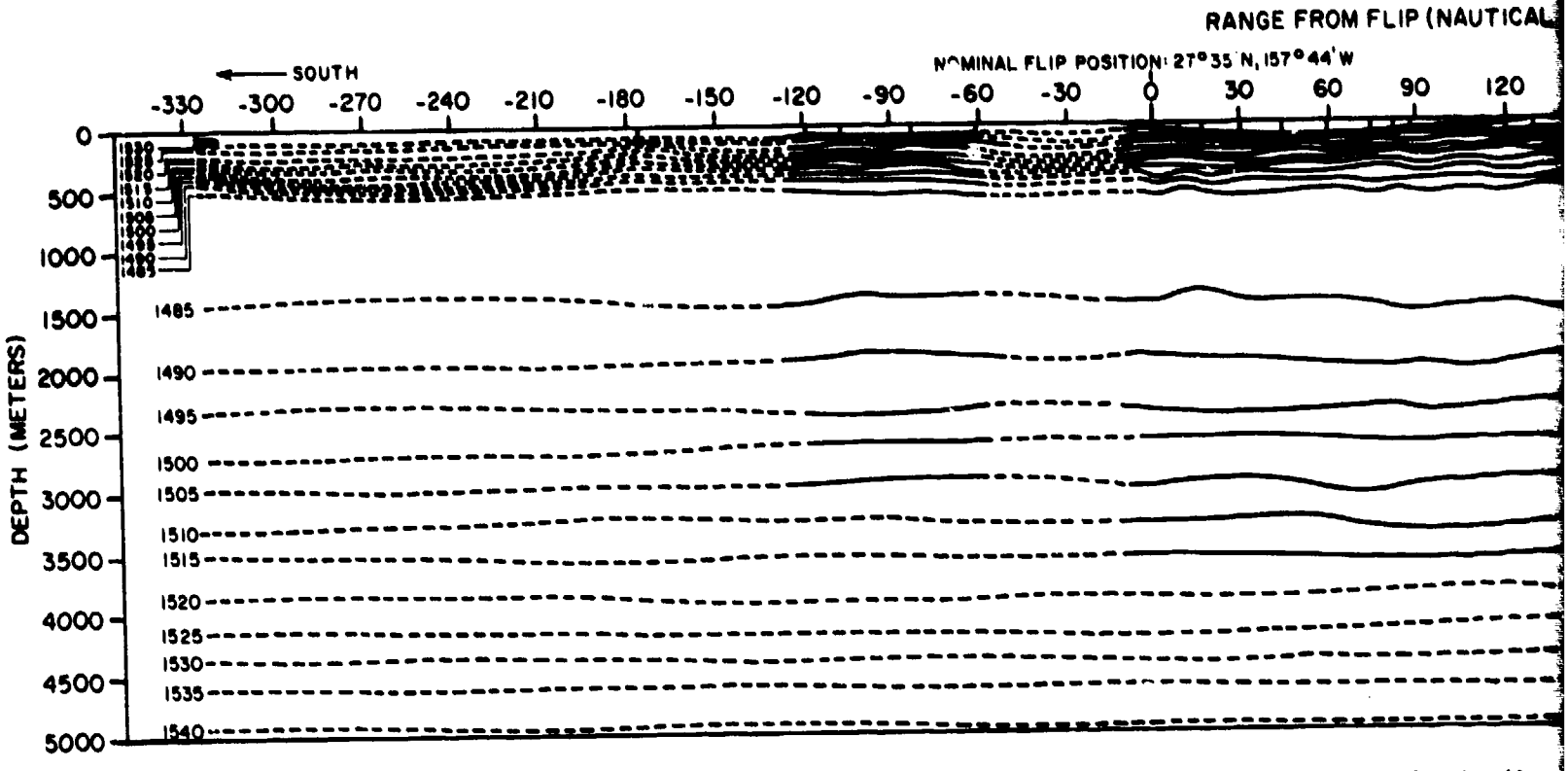

Fig. 17 — Contoured Deep Cross Section of Sound Velocity Along

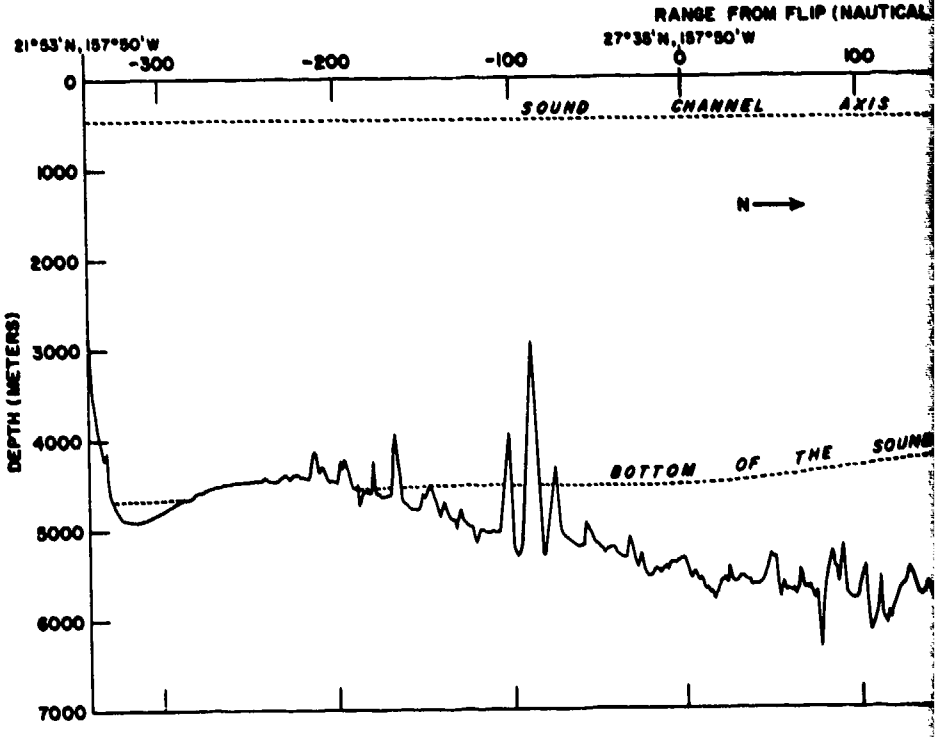

Fig. 18 — Bathymetric Profile, PARK

(Page 32 Blank)

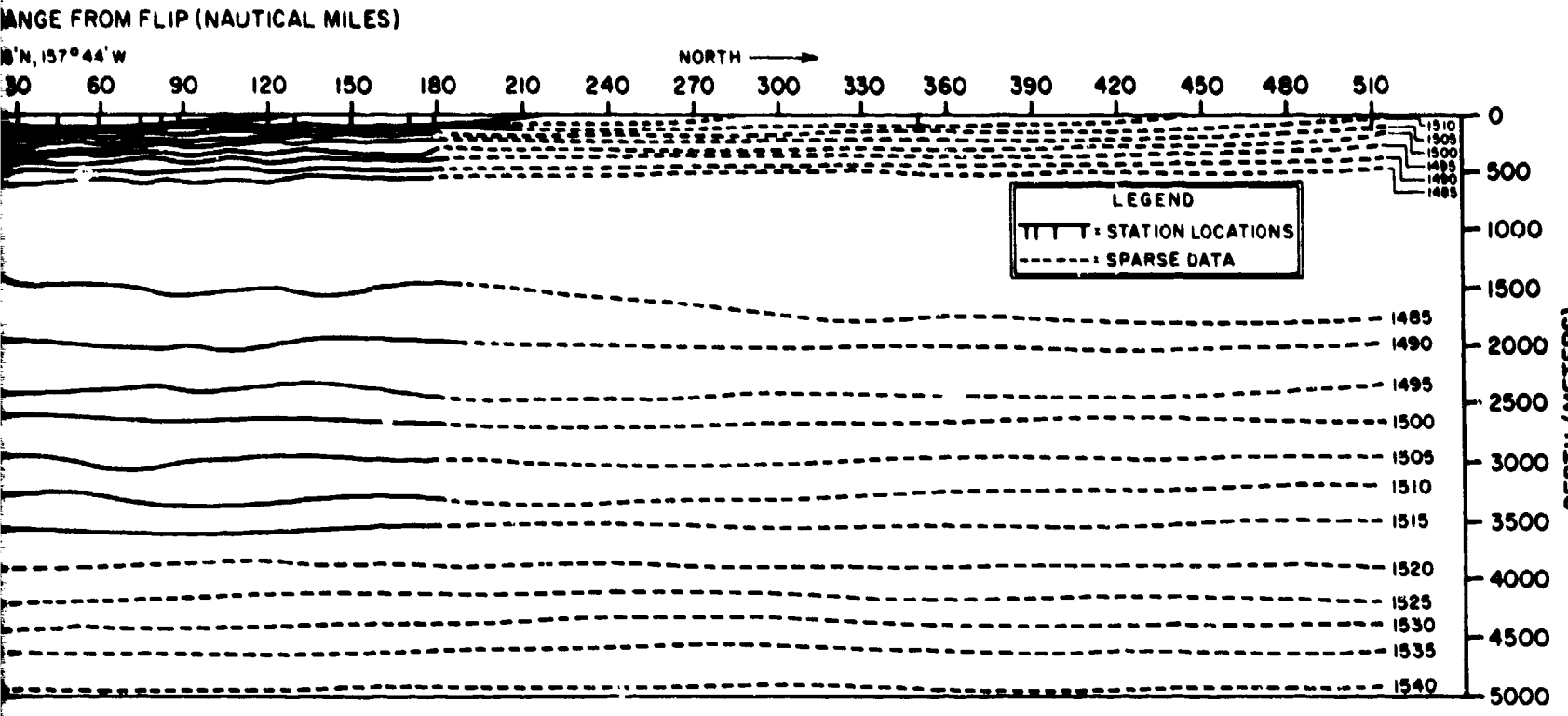

tion of Sound Velocity Along PARKA II-A North-South Track (157°44'W)

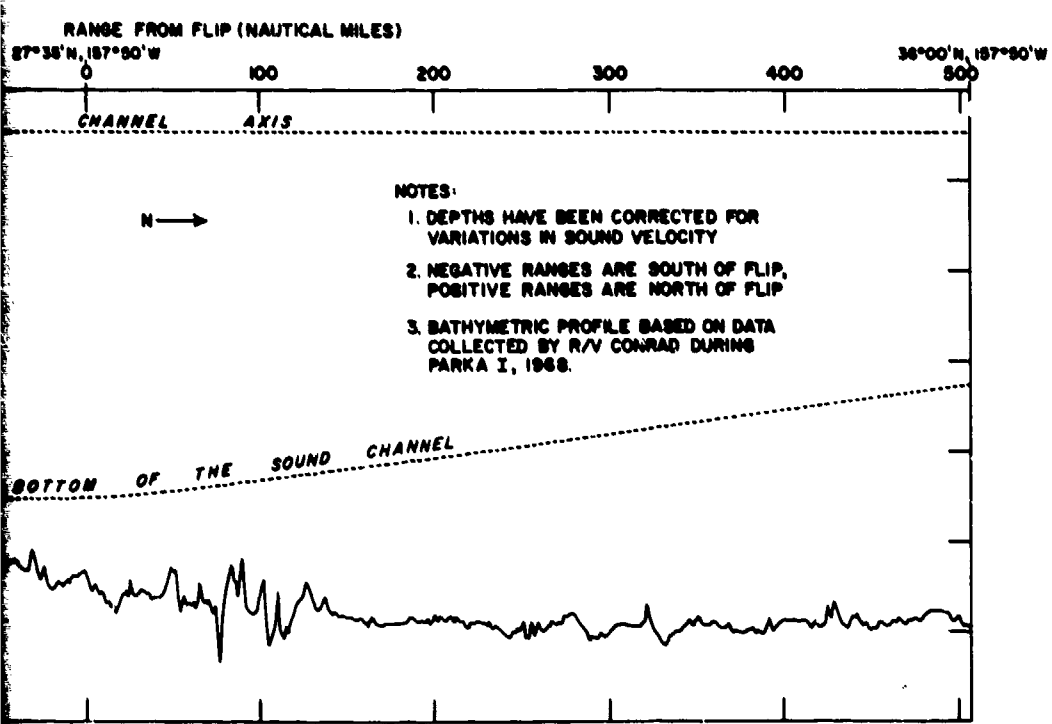

– Bathymetric Profile, PARKA North-South Track

(Page 32 Blank)

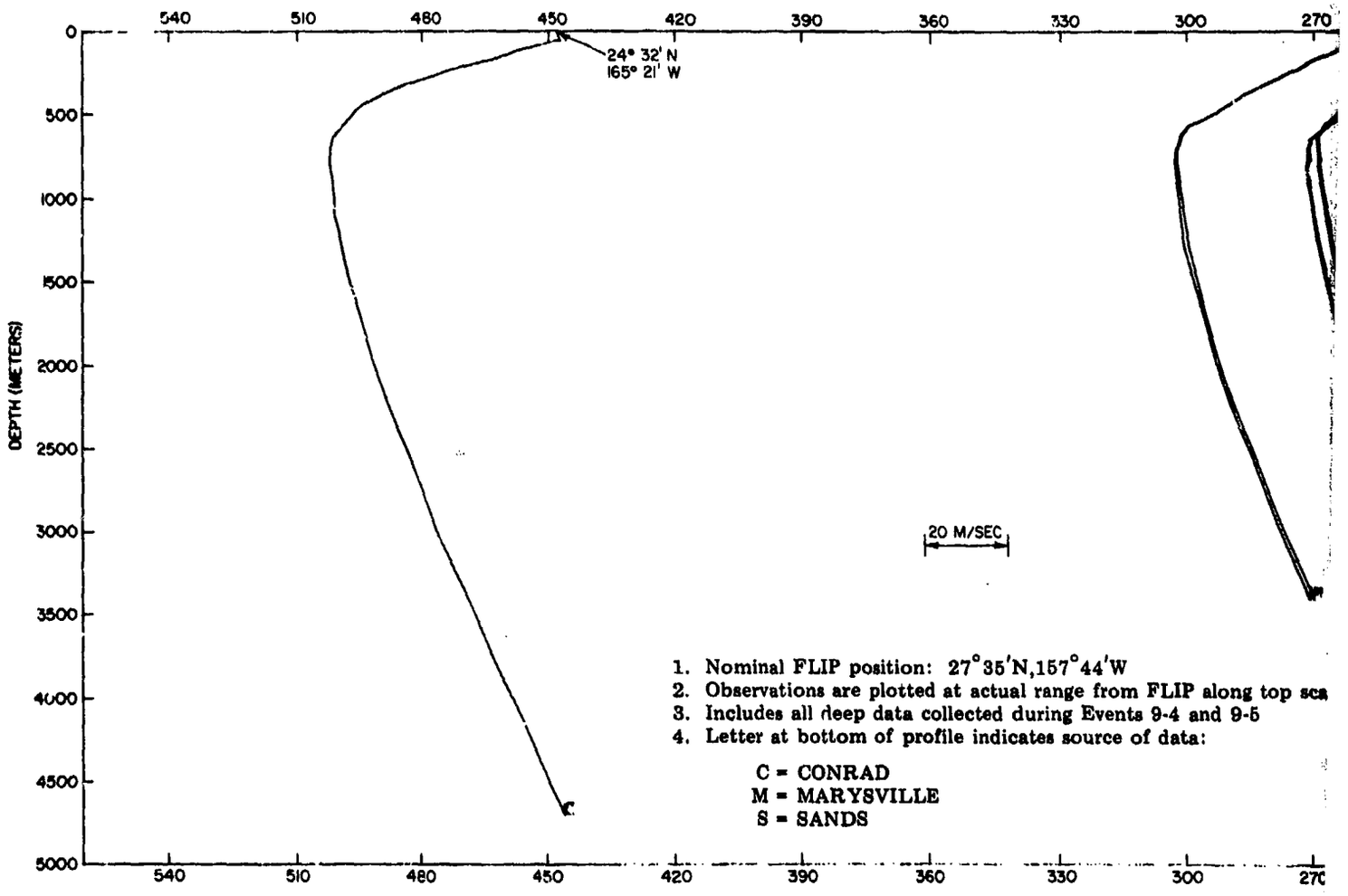

Fig. 19 — Deep Soun

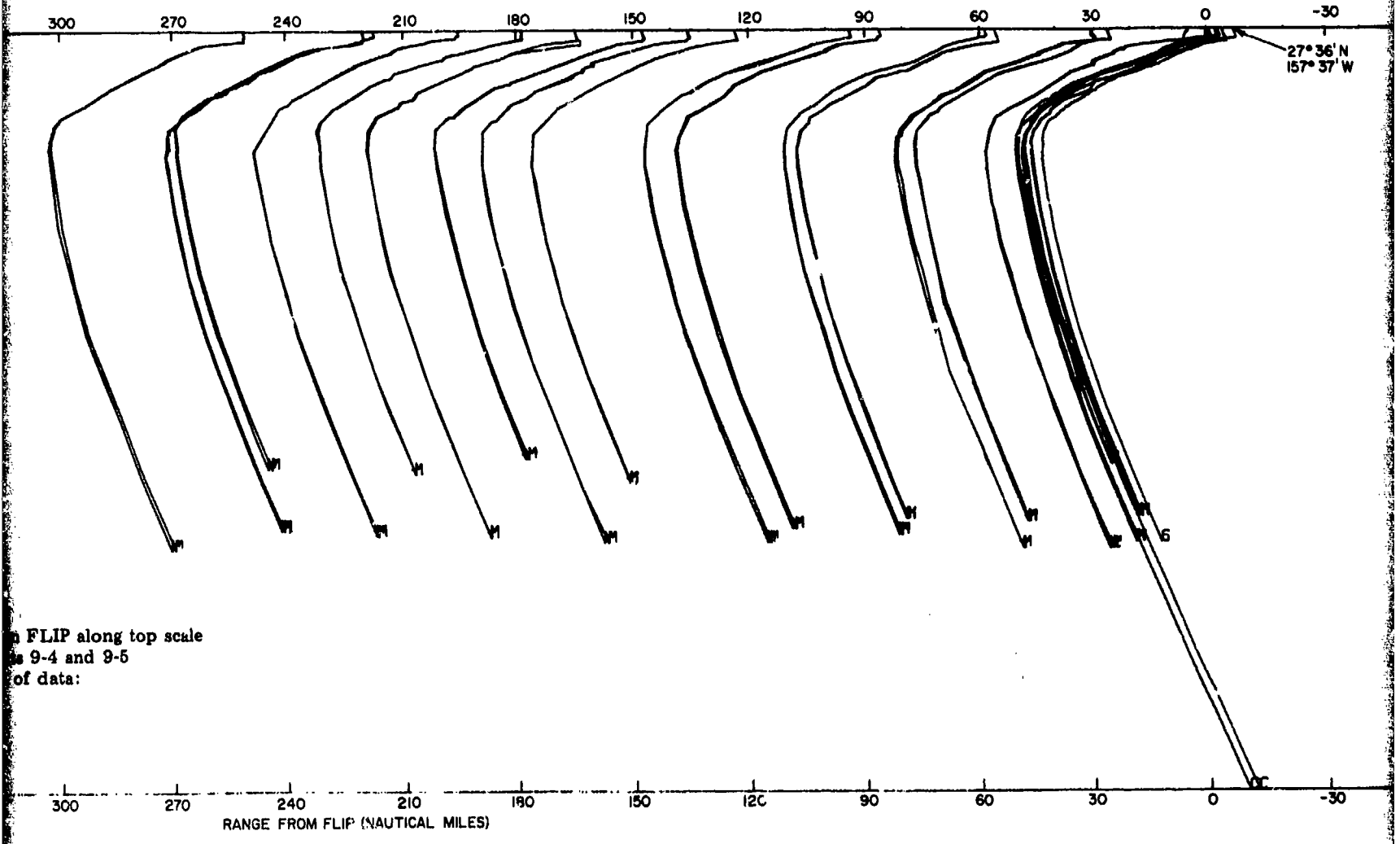

n FLIP along top scale
e 9-4 and 9-5
of data:

ig. 19 — Deep Sound Velocity Profiles Along PARKA II-A Southwest Track

(Page 34 Blank)

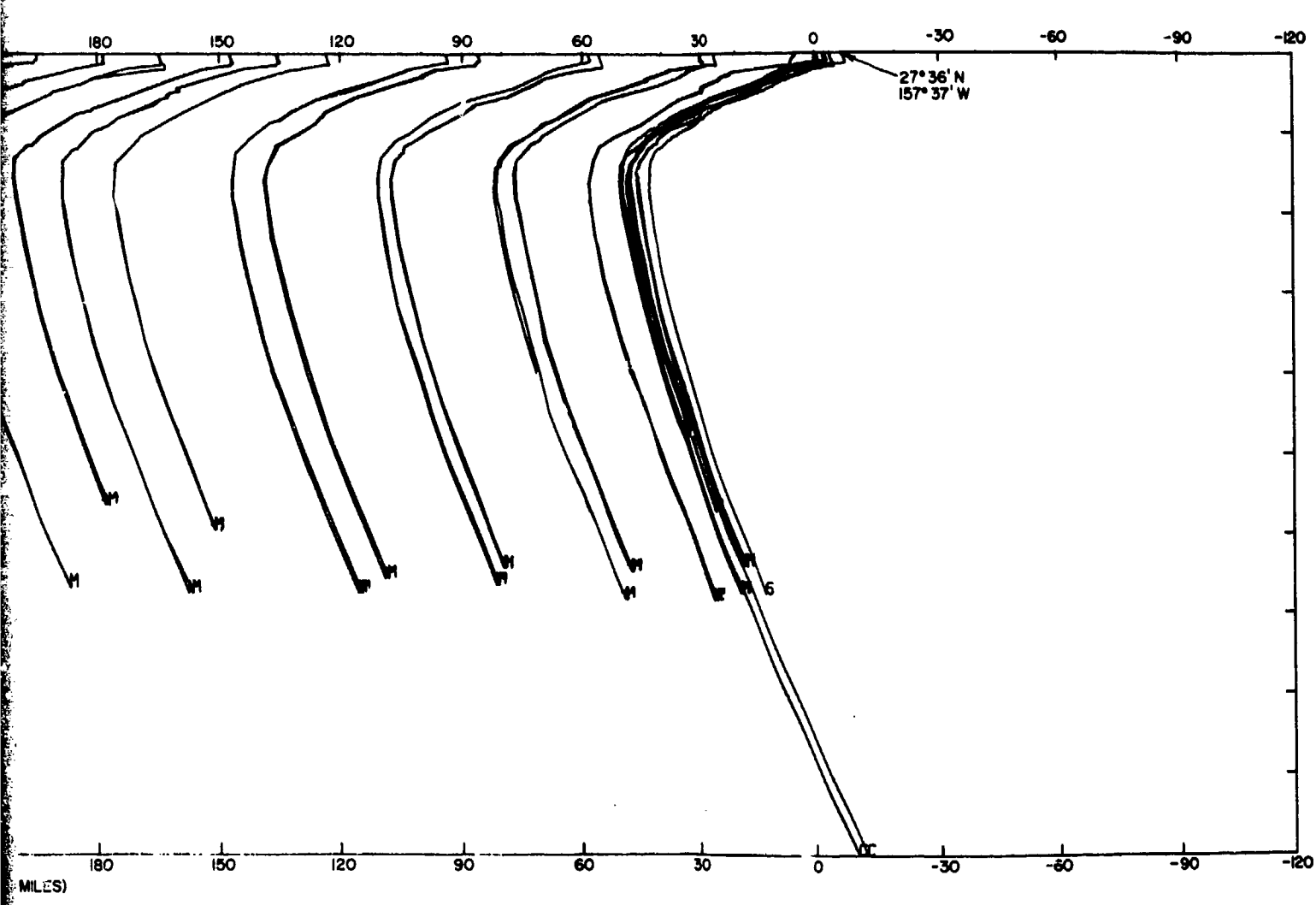

RKA II-A Southwest Track

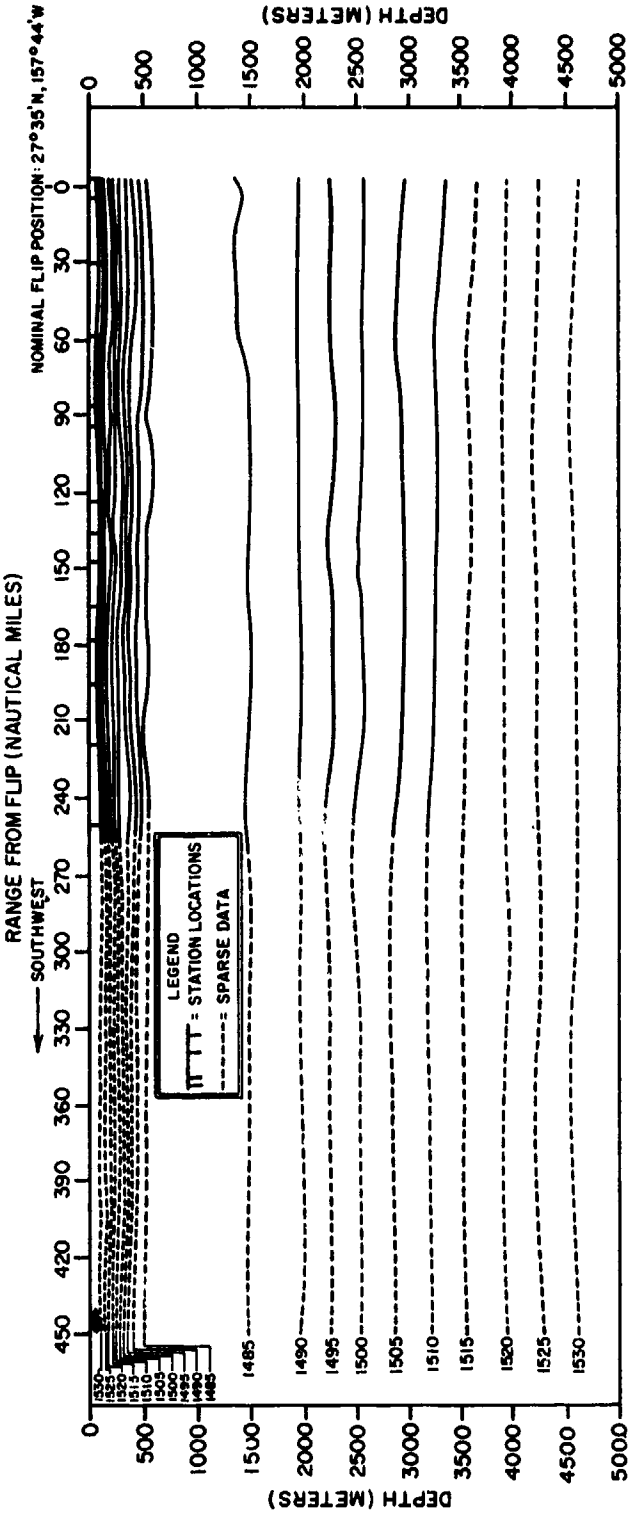

Fig. 20 — Contoured Deep Cross Section of Sound Velocity Along PARKA II-A Southwest Track

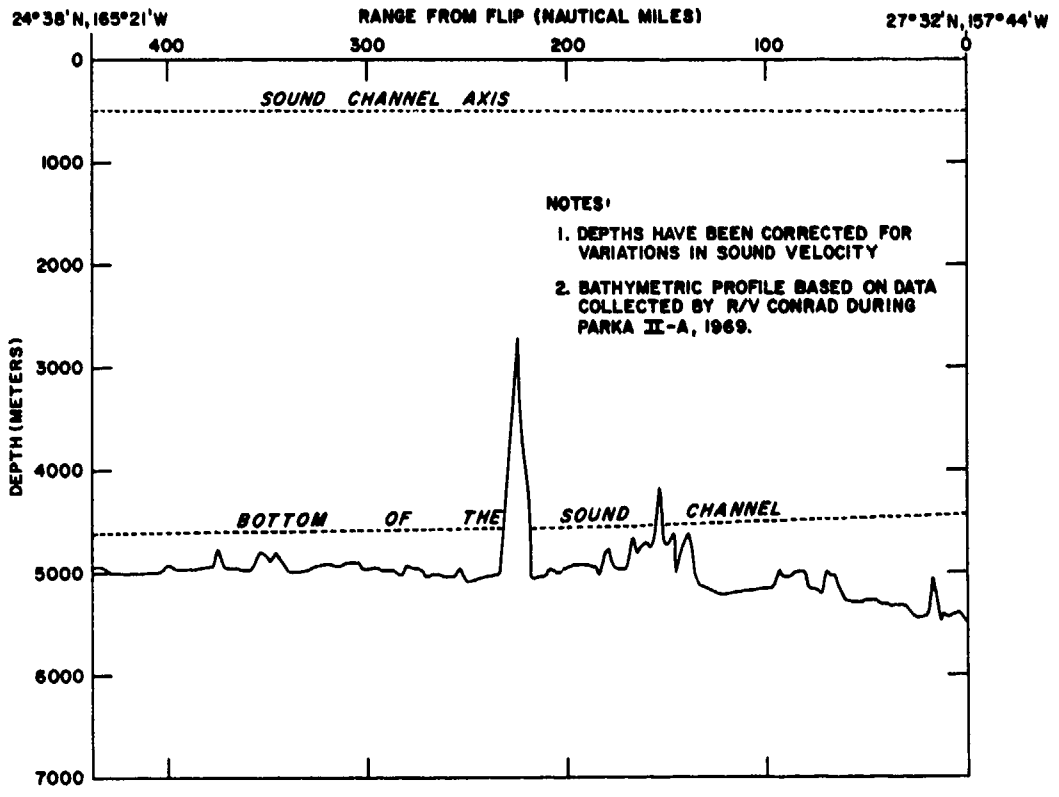

Fig. 21 — Bathymetric Profile, PARKA II-A Southwest Track

2. Contoured Cross Sections of Sound Velocity

A series of six shallow cross sections of sound velocity have been plotted for the same acoustic events and are based on the same data as the profiles discussed above. These were constructed by contouring machine-plotted sound velocity values as a function of depth and range from FLIP. The paper size, height and width of numbers, etc., required the deletion of some observations to prevent overplotting.

The individual stations were computer-sorted by ship, depth, and time of observation. Each plot, therefore, includes only the environmental data collected during the particular acoustic event. Preference in plotting was given to deep data (e.g., CONRAD STD, SANDS and MARYSVILLE velocimeter), with shallow data (REXBURG thermistor chain, or XBT's from any ship) used to fill in the blank spaces.

Stations from the various PARKA ships were plotted in the following order: CONRAD, SANDS, MARYSVILLE, REXBURG. The plotting program did not permit two stations to be plotted in the same location; consequently, the deeper observations from the first ship took precedence over the shallower information from the others. As SANDS stayed in essentially the same location during the entire experiment, only one or two of her stations were included.

The contour interval is 5 m/sec. The plots used to construct these cross sections were machine-printed with no more than one station every two nautical miles in the horizontal, and

one data point every seven meters in the vertical. Consequently, the smallest feature that can be shown is about four miles wide by fourteen meters deep. Ranges from FLIP are shown in nautical miles.

The series of 750-meter illustrations covers the water column above the axis of the sound channel. This region typically displays the largest fluctuations in velocity structure. The cross sections are a static presentation of a dynamic medium, and are influenced by the sampling method and contour interval. Although the data points were plotted along the track to facilitate contouring, they are *not* in chronological order. Therefore, some of the perturbations shown by the isotachs may be caused by changes in the near-surface sound velocity structure during the time that elapsed between the occupation of adjacent stations. This may also partially account for the noticeable lack of agreement between these contours and those constructed from the NURDC thermistor chain temperature measurements in Section III, Part B. Each event covers between two and a half and three days, and considerable variability in the near-surface environment may occur over such a period. The different methods of data collection and coding may also introduce minor perturbations of the isotachs.

Shallow Sound Velocity Structure North and South of FLIP (Events 9-1, 9-2, and 9-3)

As has been stated, the depth interval between the surface and the axis of the deep sound channel displays more variability than any other part of the water column. In addition, the characteristics of the sound velocity structure in this depth region are particularly important since in most situations the source and/or receiver lie within the domain. Figures 22 through 24 display the gross sound velocity conditions along the north-south PARKA track from 22°N to 36°N, from the surface to a depth of 750 meters. This depth approximately marks the base of the permanent thermocline, which coincides with the axis of the deep sound channel. Figure 22 includes all observations made during Event 9-1, from 22°N to FLIP (at 27°35'N). Figure 23 shows profiles collected during Event 9-2 from FLIP north to 36°N, and Fig. 24 shows profiles collected during Event 9-3 from 36°N south to FLIP. Each profile is plotted at the appropriate range from FLIP and carries a ship indicator letter at the bottom of the trace.

These sound velocity profiles display varying degrees of detail caused by differences in the vertical sampling intervals used aboard different ships. Considerable detail is evident in the 220-meter profiles computed from temperature data collected by the NURDC thermistor chain aboard REXBURG. The consistently negative gradients between the mixed layer and about 700 to 800 meters are typical of the thermocline region where temperature is the controlling factor. This region forms the upper portion of the deep sound channel.

The mixed layer (in agreement with temperature observations) extends from the surface to depths of 70 to 80 meters, both north and south of FLIP. A comparison of the profiles shown in these three figures indicates that there is very little difference in the sound velocity gradient over the length of the north-south track. A slight positive sound velocity gradient appears in the mixed layer in most of the profiles, regardless of their location on the track. As isothermal conditions usually prevail in this layer, this slight positive gradient results from increasing pressure. The positive gradient produces upward refraction of sound and can lead to repeated surface reflections for a source in this layer. Any perturbations in the depth of the mixed layer will tend to distort the cyclic symmetry of this mode of propagation.

In a few cases, slightly negative gradients exist within the mixed layer. This situation can best be observed at approximately 100 to 150 nautical miles north of FLIP (Figs. 23 and 24). A change in gradient of this type frequently reflects spatial or temporal fluctuations of the medium. Such perturbations in the velocity structure within the mixed layer can have a significant effect upon sound transmission both within and below the layer. When both sound source and receiver are located within the layer, a negative gradient will produce the classic shadow zone phenomenon. Thus, the existence of isolated reversals in gradient within the layer indicates that the character of sound refraction observed in this region may be particularly sensitive to the depth of the source, and that transmission via the surface duct may be unreliable or impossible.

Figures 25 through 27 display contoured cross sections of the same data included in Figs. 22 through 24 above. Figure 25 includes data from Event 9-1, Fig. 26 from Event 9-2, and Fig. 27 from Event 9-3. These cross sections indicate the non-isothermal character of the mixed layer at a range of about 100 to 150 nautical miles north of FLIP (Figs. 26 and 27). The existence of such pockets or tongues of warmer (higher velocity) water in the mixed layer probably caused the appearance of the negative sound velocity gradients observed in this same area on Figs. 23 and 24. It is very likely, therefore, that propagation via the surface duct would be interrupted through this area.

The surface sound velocity along the track south of FLIP (Fig. 25) averages about 1534.0 m/sec. North of FLIP, (Figs. 26 and 27), a decrease in the surface sound velocity of over 20 m/sec occurs over the 500 nautical miles between FLIP and the northern end of the track, with most of the change occurring between 32°N and 36°N. This trend reflects the transition zone north of 32°N. However, this transition zone water mass, which is similar to the subarctic water found farther north, forms only the uppermost part of the water column (Roden, 1970). Roden also suggests that the persistence of this shallow water mass is accounted for principally by winds and air/sea energy exchange. Consequently, this noticeable change in sound velocity is restricted to the upper layers of the water colum. Below a depth of about 250 meters, the nearly horizontal and parallel isotachs predominate over all other features that occur along the tracks (see also Fig. 17).

Figures 26 and 27 depict the sound velocity conditions along the same track but differing in time by about three days. Comparison of these two illustrations shows that, although very similar, the two figures are not identical, even below 500 meters. Because of the arbitrary method of construction, these contour plots do not depict the environment precisely, though they can reveal the type and the magnitude of perturbations to be expected. The irregularities present here suggest time-dependent fluctuations of the medium. As noted in Volume 1 of this report, the changes in contours between Event 9-2 and 9-3 did not result in observable differences in the measured acoustic propagation loss.

Above the depth of the permanent thermocline, temperature is the major factor in determining sound velocity. The steepest sound velocity gradient shown in Figs. 25 through 27 is located at a depth of 60 to 90 meters, and coincides with the strongest temperature gradient displayed in the temperature cross sections in Figs. 11 through 15 in Section III, Part B.

Shallow Sound Velocity Structure Southwest of FLIP (Events 9-4 and 9-5)

Events 9-4 and 9-5 were conducted in opposite directions along a 400-nautical mile great circle track on a bearing of 247°T from FLIP. The shallow sound velocity profiles show

1. Nomin
2. Obser
3. Letter

C
M
R
S
P

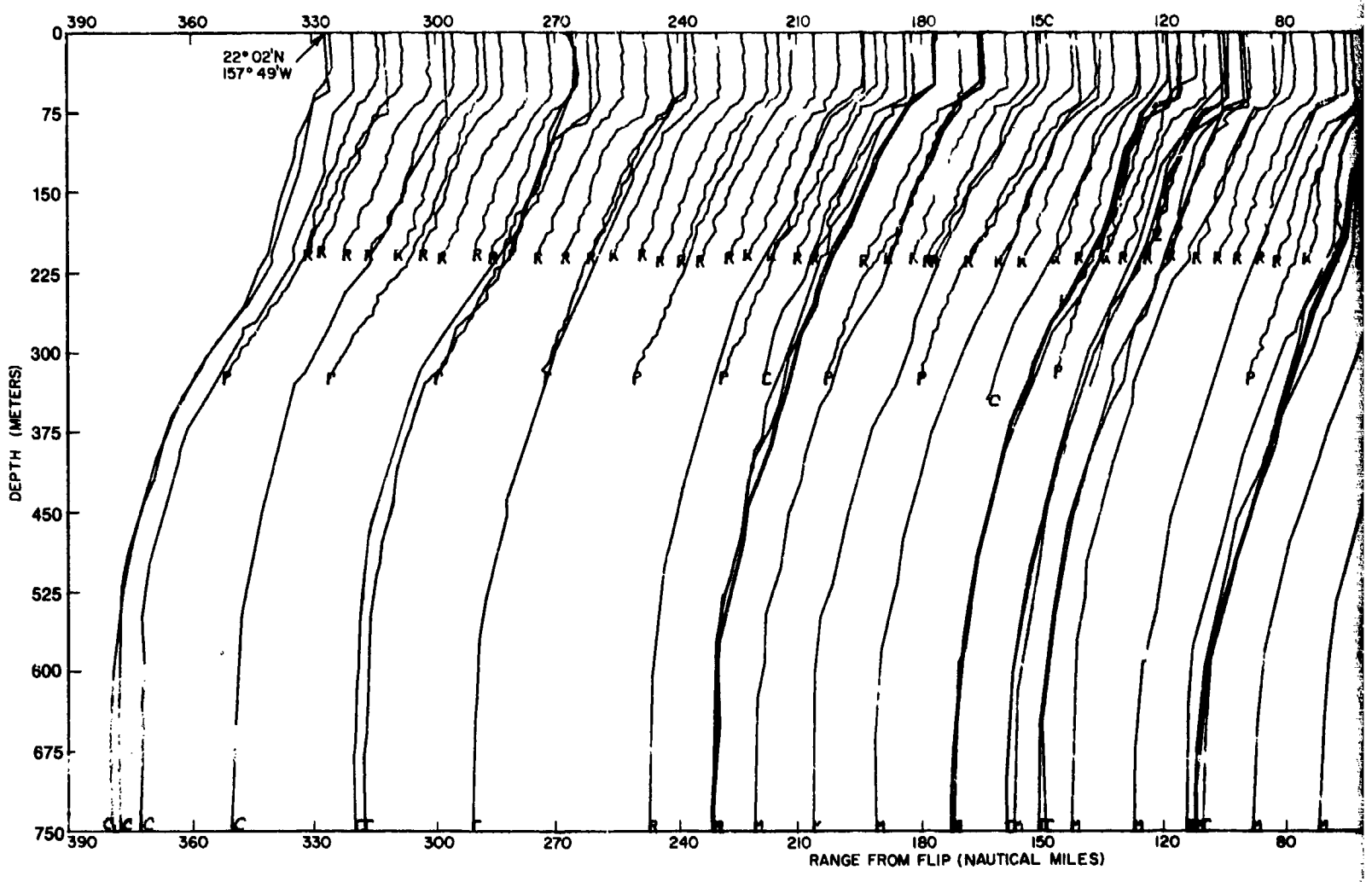

Fig. 22 - Shallow Sound Velocity Profiles, Event 9-1 (Propagation Loss and Arrival Structure), 22

(Page 40 Blank)

1. Nominal FLIP position: 27°35'N,157°44'W
2. Observations are plotted at actual range from FLIP along top scale
3. Letter at bottom of profile indicates source of data:

C = CONRAD
M = MARYSVILLE
R = REXBURG
S = SANDS
P = PARKA AXBT

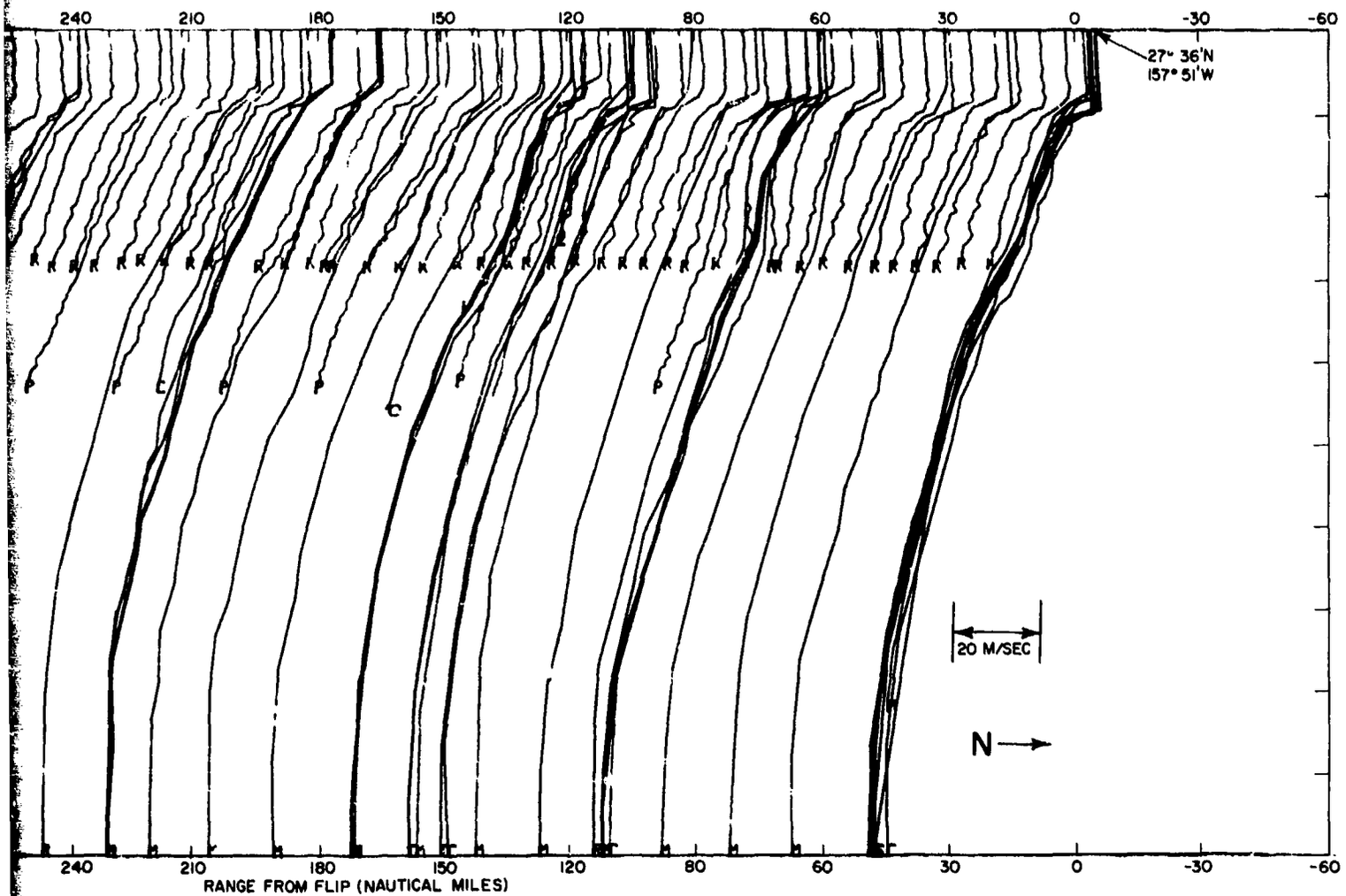

ound Velocity Profiles, Event 9-1 (Propagation Loss and Arrival Structure), 22°N to FLIP

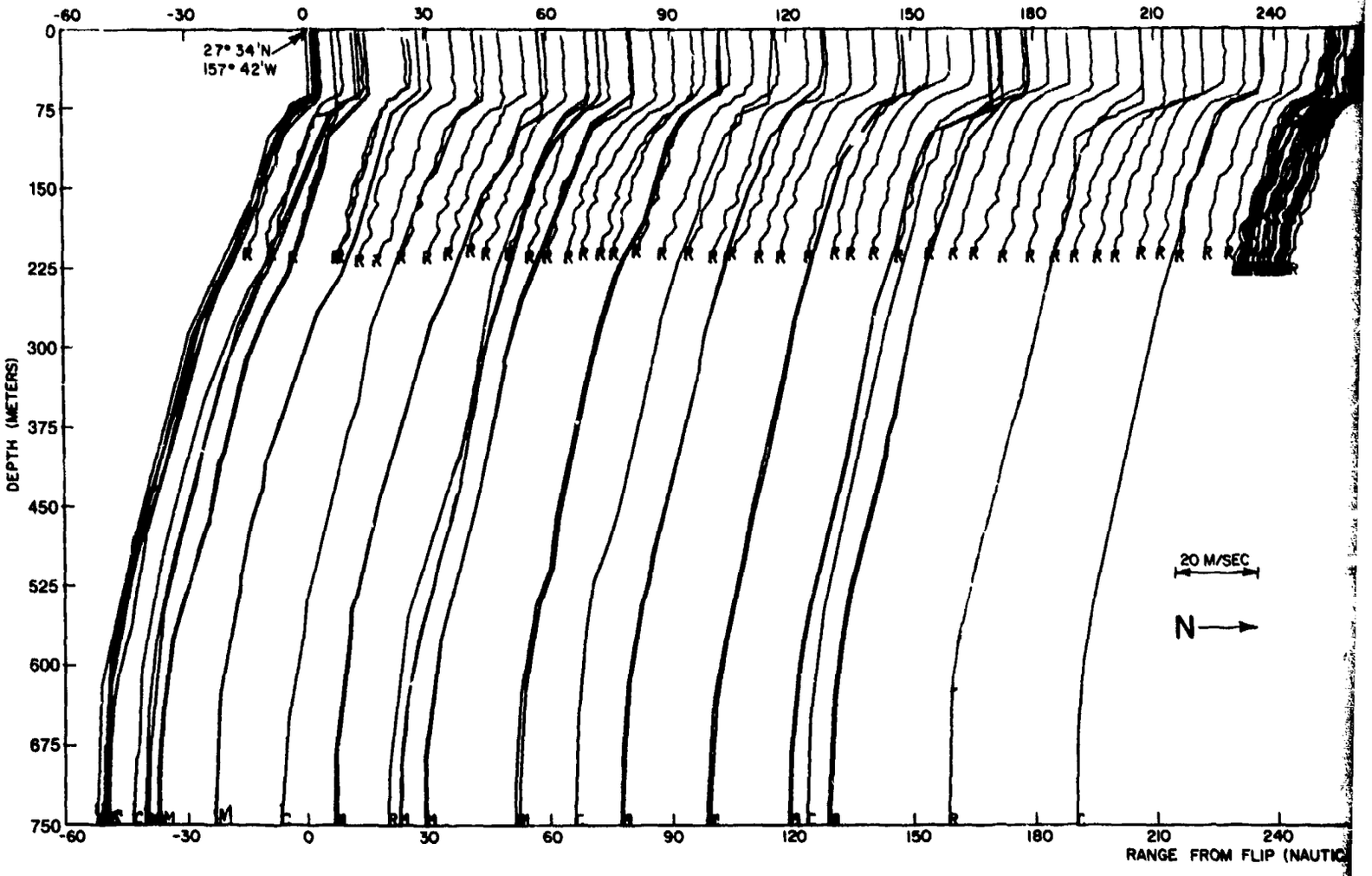

Fig. 23 — Shallow Sound Velocity Profiles, Event 9-2 (Propagati

(Page 42 Blank)

1. Nominal FLIP position: 27°35'N,157°44'W
2. Observations are plotted at actual range from FLIP along top sc
3. Letter at bottom of profile indicates source of data:

C = CONRAD
M = MARYSVILLE
R = REXBURG
S = SANDS

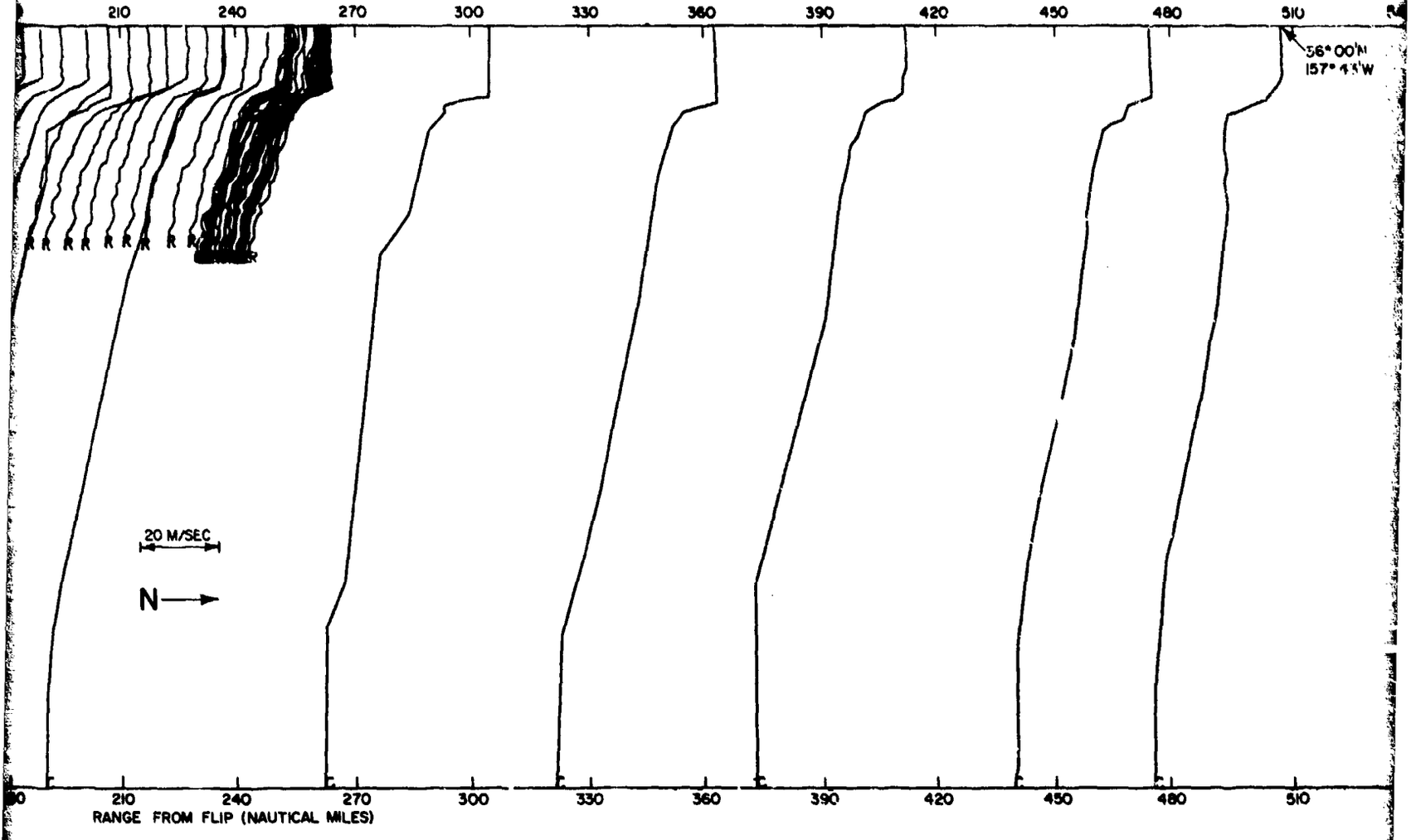

ity Profiles, Event 9-2 (Propagation Loss and Arrival Structure), FLIP to 36°N

(Page 42 Blank)

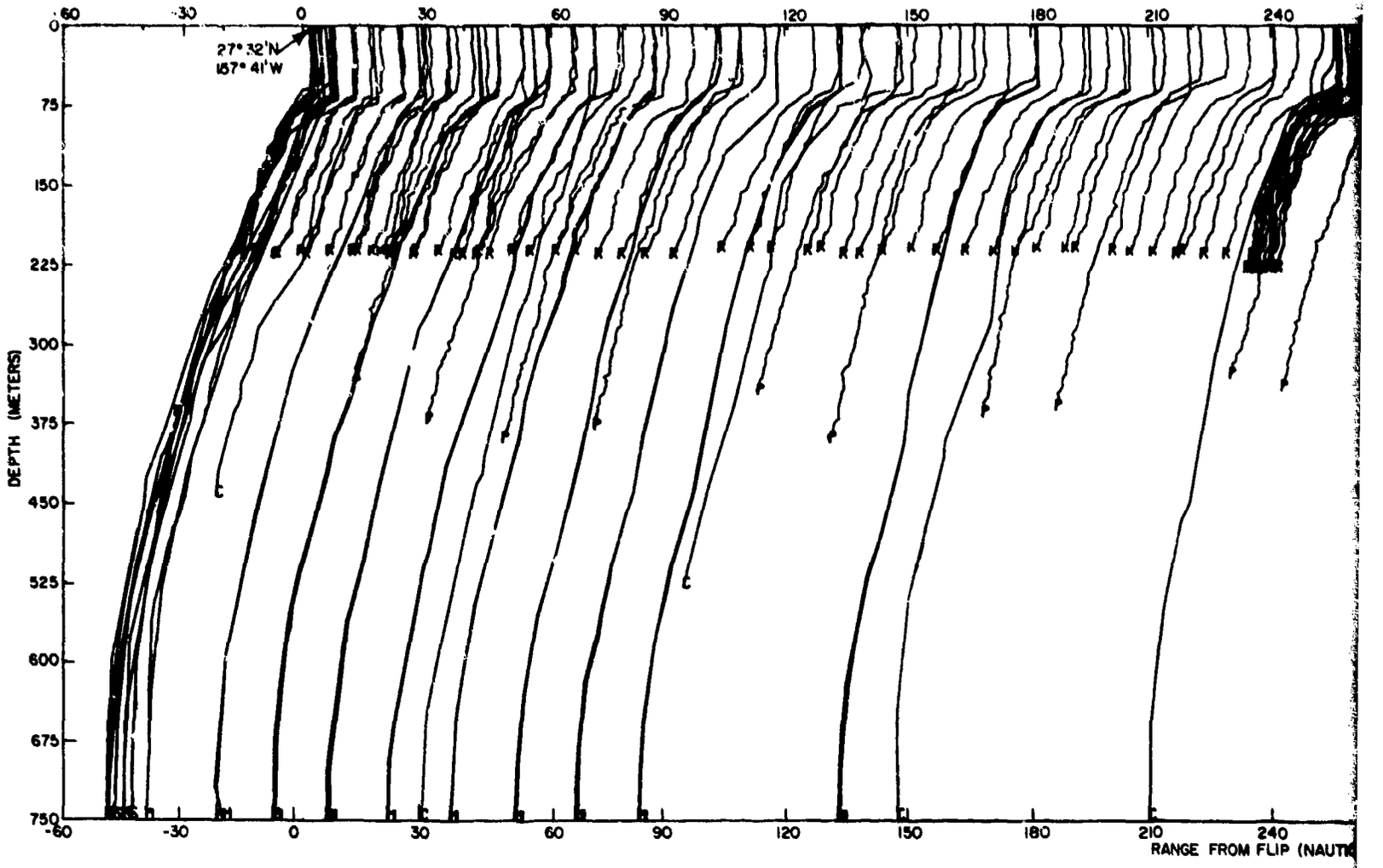

Fig. 24 — Shallow Sound Velocity Profiles, Event 9-3 (Propag

(Page 44 Blank)

1. Nominal FLIP position: 27°35'N,157°44'W
2. Observations are plotted at actual range from FLIP along top scale
3. Letter at bottom of profile indicates source of data:

C = CONRAD
M = MARYSVILLE
R = REXBURG
S = SANDS
P = PARKA AXBT

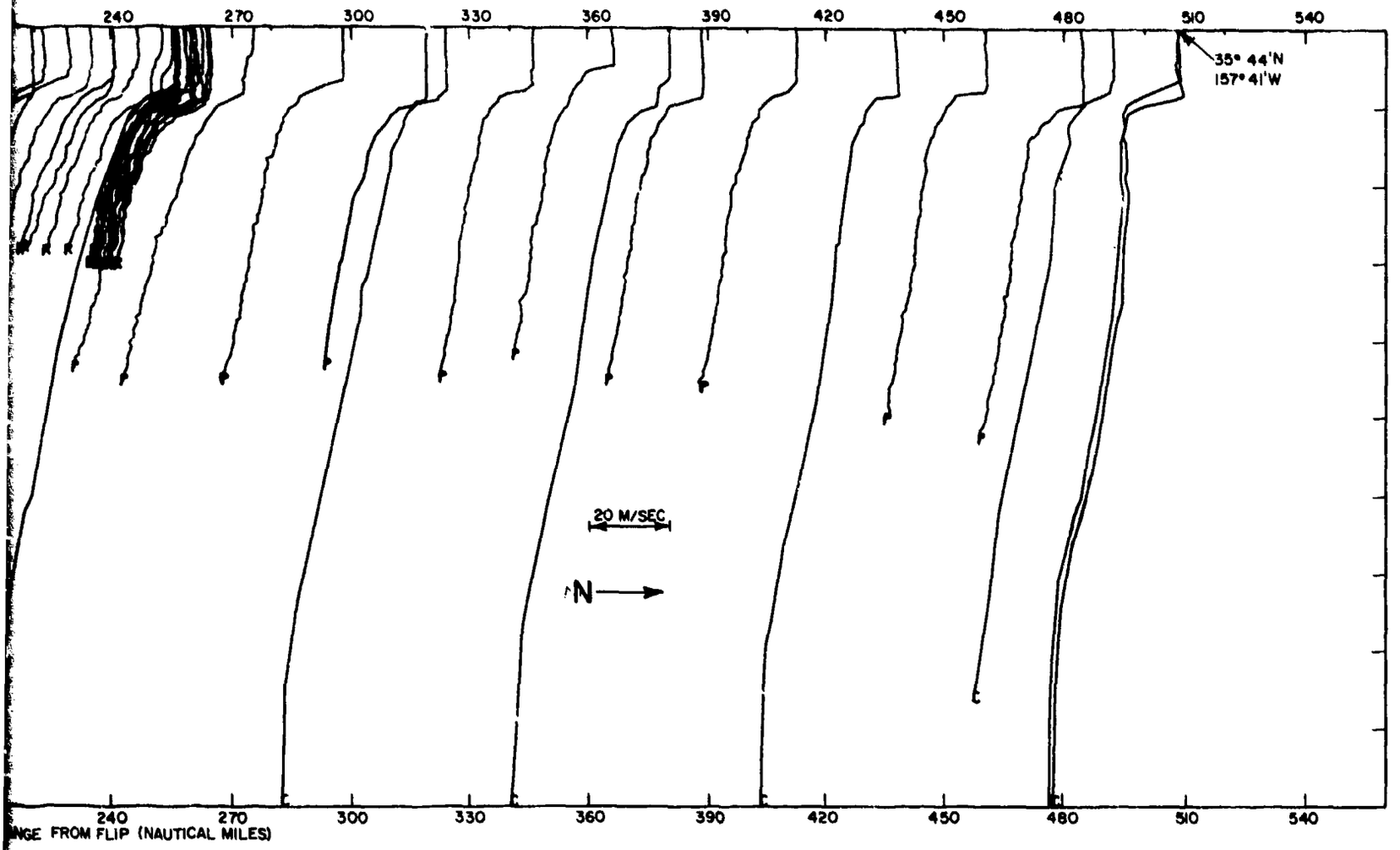

, Event 9-3 (Propagation Loss and Arrival Structure), 36°N to FLIP

(Page 44 Blank)

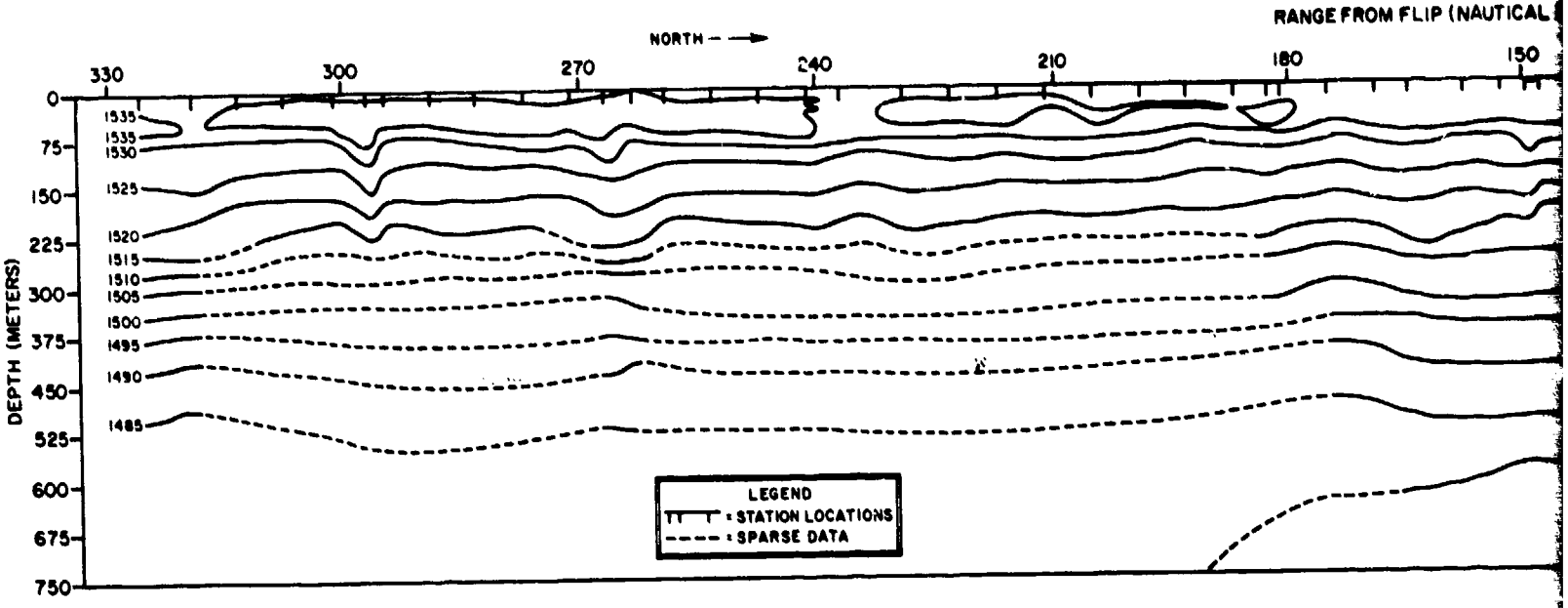

Fig. 25 — Contoured Shallow Cross Section of Sound Velocity,

(Page 46 Blank)

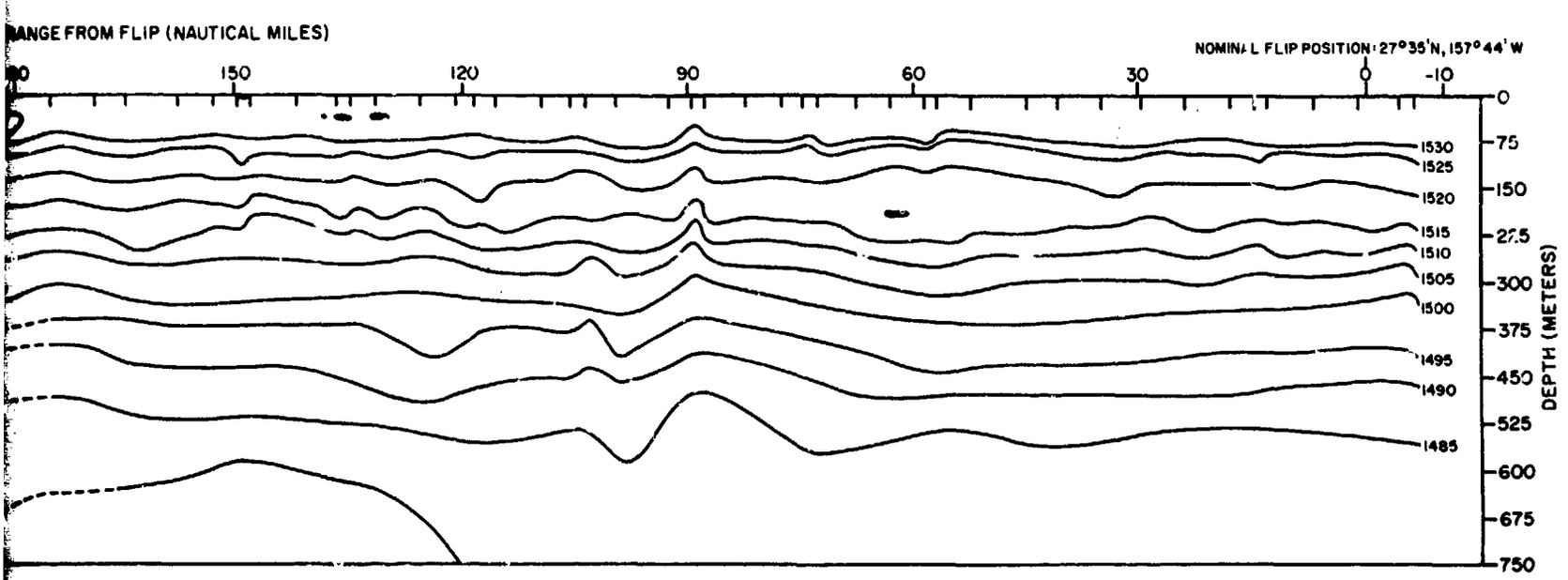

ion of Sound Velocity, Event 9-1 (Propagation Loss and Arrival Structure), 22°N to FLIP

(Page 46 Blank)

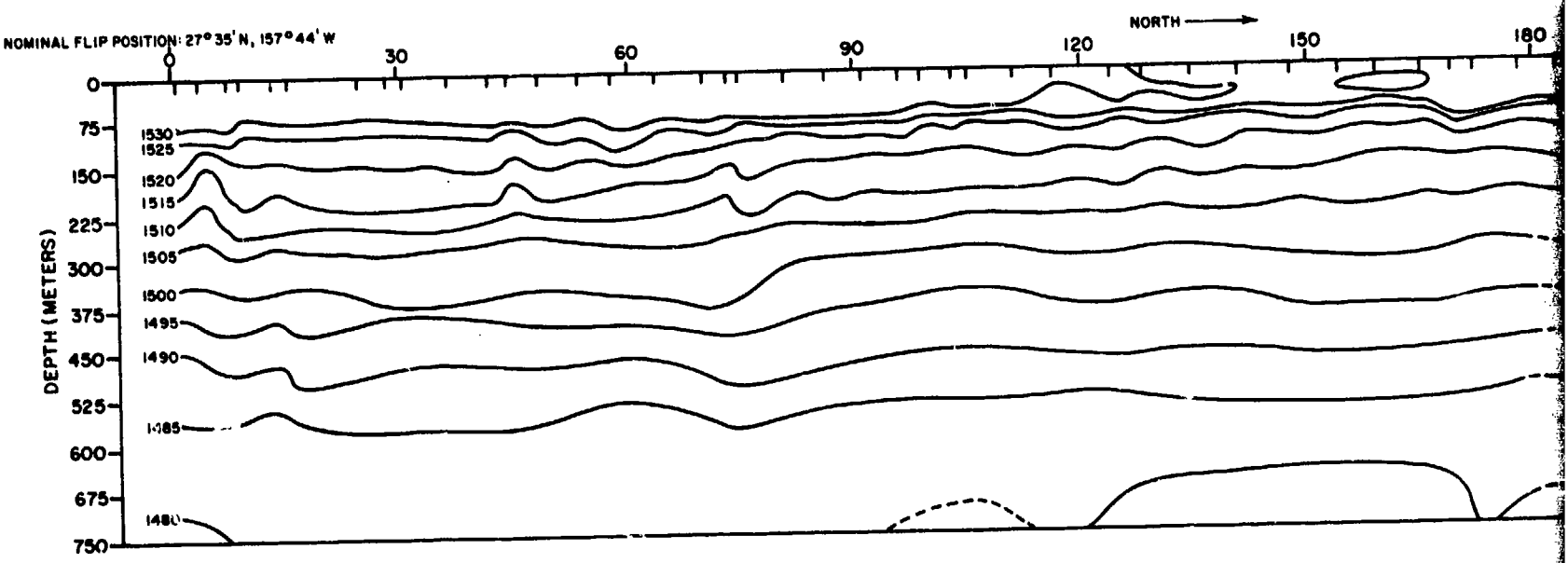
NOMINAL FLIP POSITION: 27°35'N, 157°44'W
NORTH
0
30
60
90
120
150
180
0
75
150
225
300
375
450
525
600
675
750
DEPTH (METERS)
1530
1525
1520
1515
1510
1505
1500
1495
1490
1485
1480

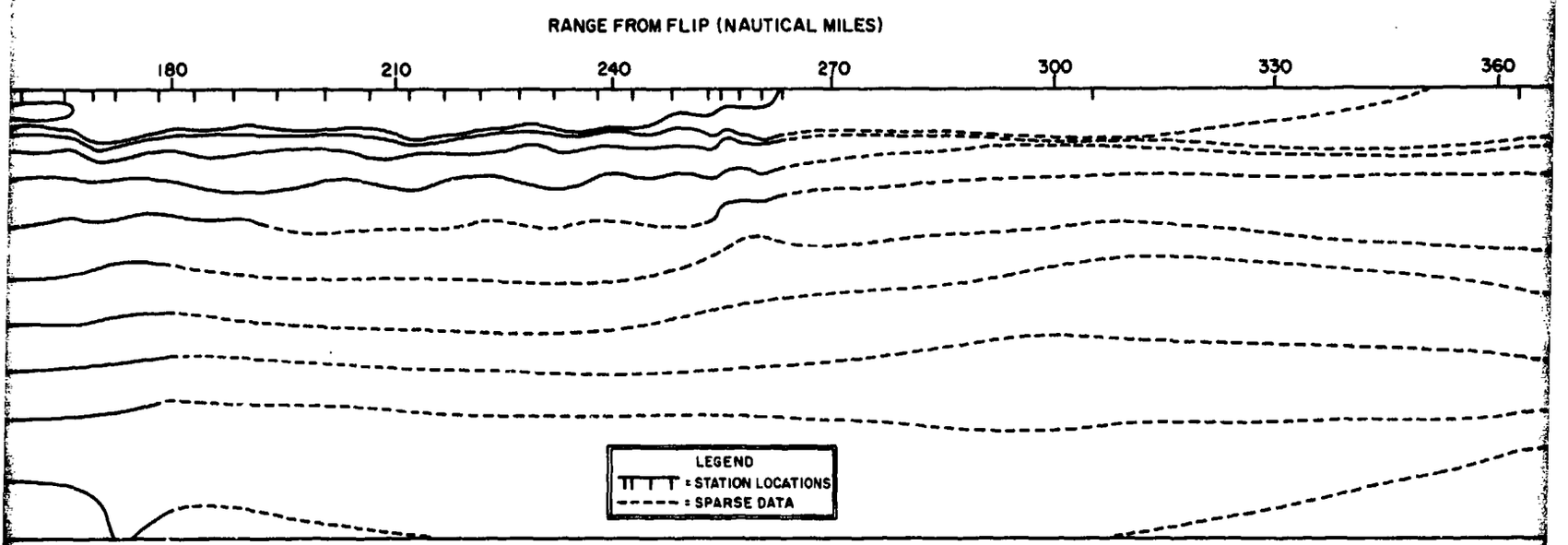

Fig. 26 — Contoured Shallow Cross Section of Sound Velocity, Event 9-2 (Propagation Loss and Arrival Structure), FLIP to 36°N

(Page 48 Blank)

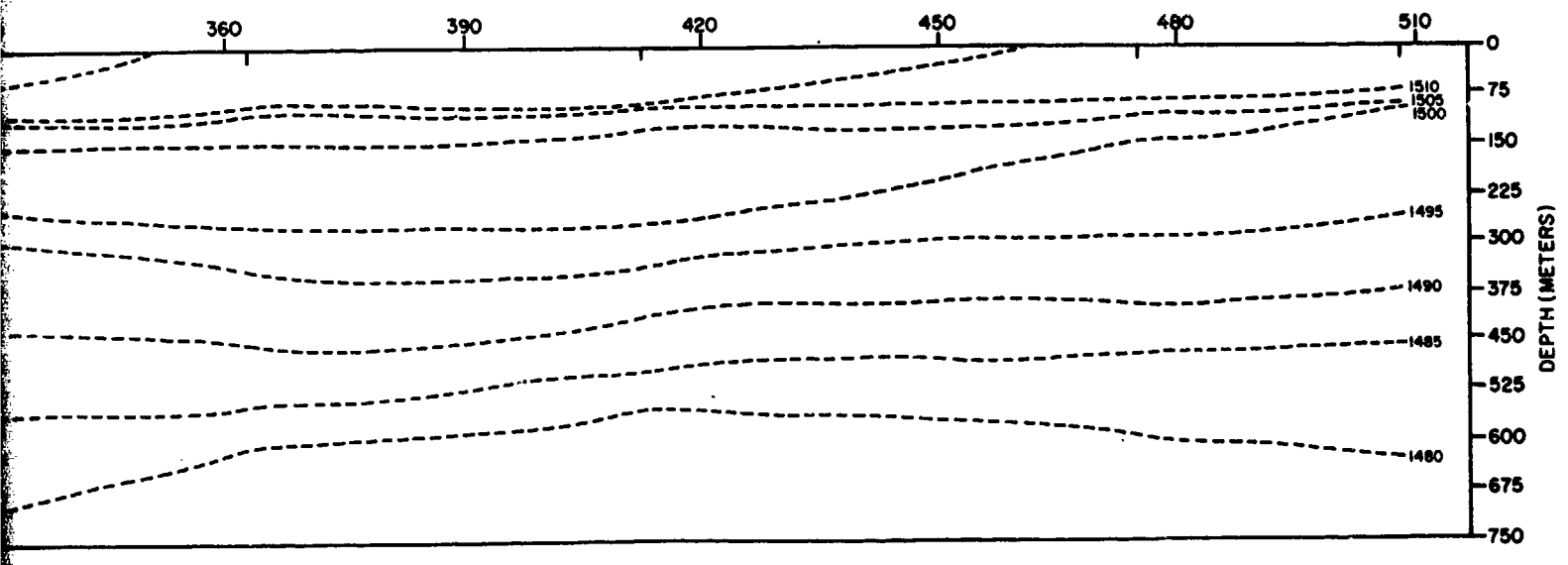

ucture), FLIP to 36°N

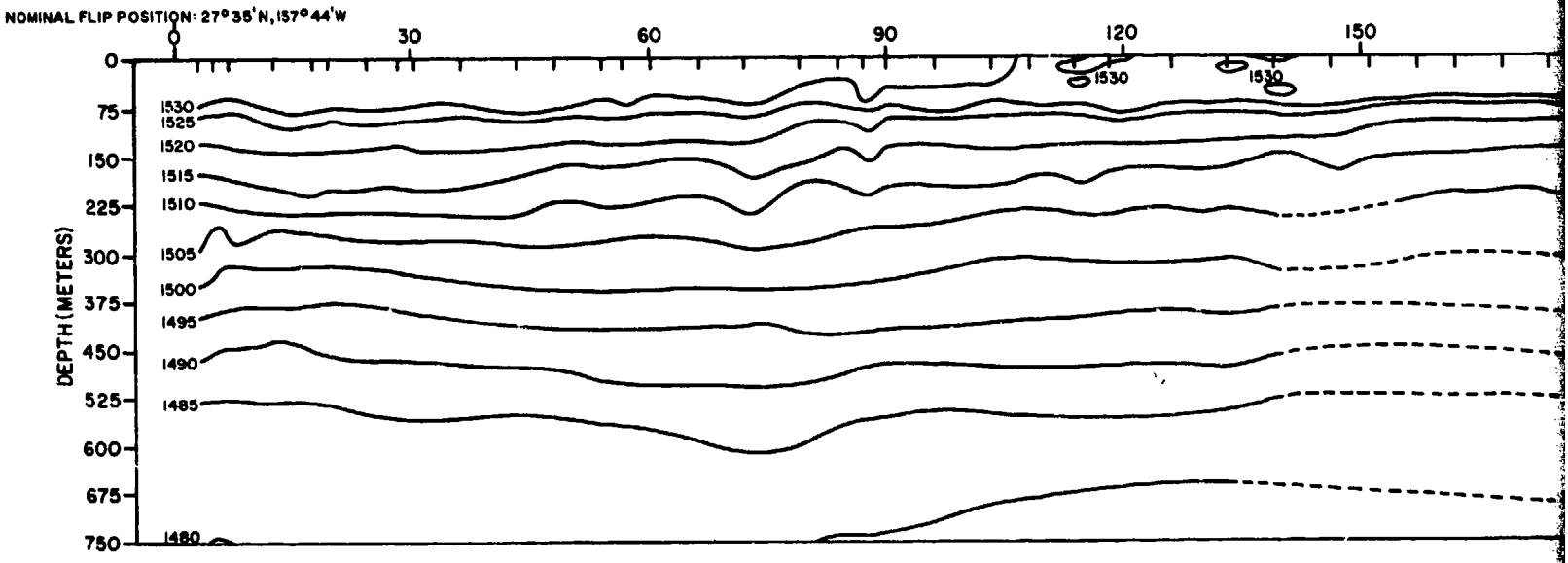
NOMINAL FLIP POSITION: 27°35'N, 157°44'W
0
30
60
90
120
150
0
75
150
225
300
375
450
525
600
675
750
DEPTH (METERS)
1530
1525
1520
1515
1510
1505
1500
1495
1490
1485
1480
1530
1530

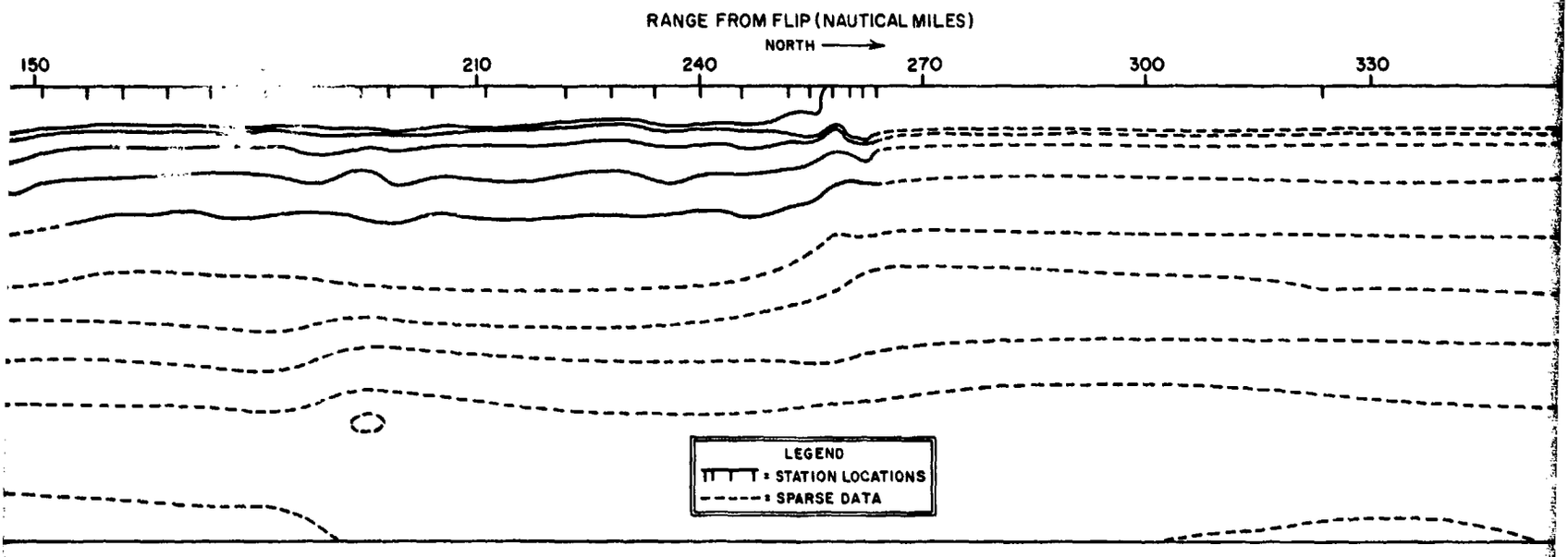

Fig. 27 — Contoured Shallow Cross Section of Sound Velocity, Event 9-3 (Propagation Loss and Arrival Structure), 36°N to

(Page 50 Blank)

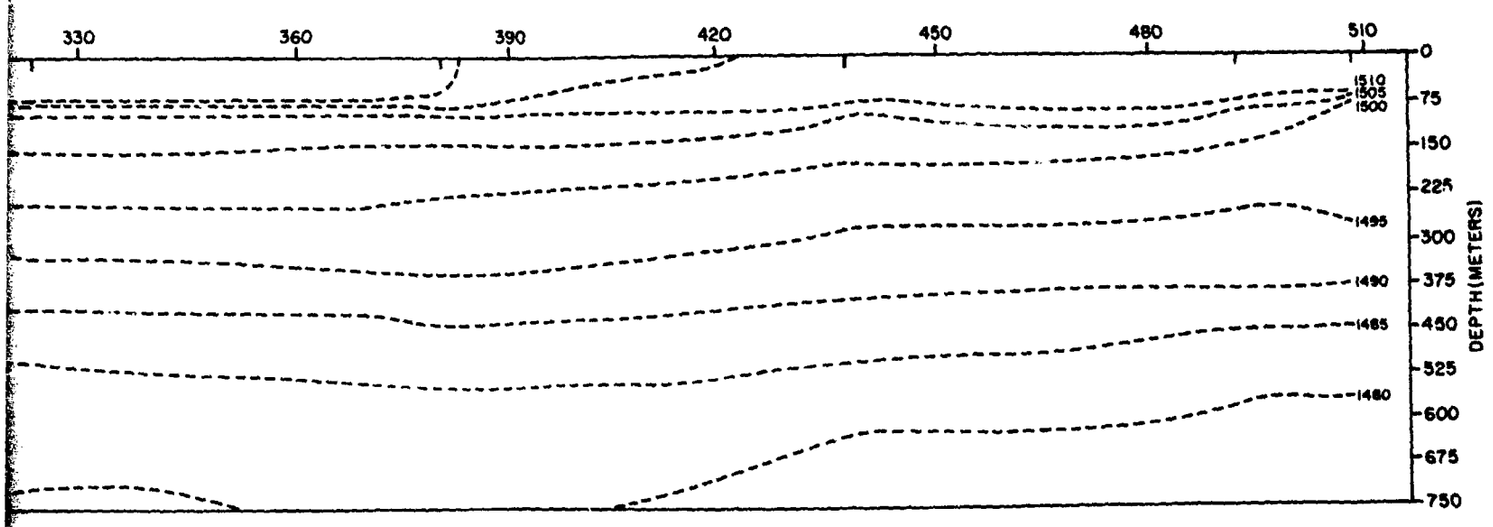

rival Structure), 36°N to FLIP

that isovelocity or near-isovelocity conditions prevail in the mixed layer, except where the mixed layer deepens at a point about 320 nautical miles southwest of FLIP (Fig. 28 for Event 9-4 and Fig. 29 for Event 9-5). The gradients displayed in these profiles are similar to those along the north-south track (Figs. 22, 23, and 24). A slight sound velocity minimum appears in several profiles at a depth of about 75 meters on both runs along the southwest track. This minimum produces a secondary sound channel which could enchance detection of a target in the layer, although the effect would be restricted to short ranges at isolated locations.

Figures 30 and 31 display contoured cross sections of the same data included in Figs. 28 and 29. These values are similar to those contoured in Fig. 25 for the track from Oahu to FLIP. The figures for the southwest track show virtually parallel and almost horizontal isotachs with no surfacing of the near-surface contours except near maximum range, beyond 350 nautical miles. In this area, the isotachs indicate a confused velocity structure in the mixed layer, with possible interruptions of the surface duct. Although the layer is apparently not isothermal in this region, no negative gradients are apparent on the near-surface portion of the profiles given in Figs. 28 and 29.

Shallow Sound Velocity Structure North of MAHI (Events 11-1 and 11-2)

Figures 32 and 33 show all data collected during both Events 11-1 and 11-2, and are included primarily for record. After FLIP had been disabled, these acoustic runs were carried out on a north-south track utilizing MAHI as the receiving ship. The profiles and the corresponding contoured cross section are based on few observations, and provide little new information concerning the sound velocity structure.

LONG RANGE PROPAGATION LOSS, AIRCRAFT RUNS (EVENT 13)

Summary

During Event 13 aircraft dropped explosive charges for propagation loss studies along five runs on three long-range tracks radiating from FLIP (Fig. 2). The tracks to Adak (Events 13-1 and 13-2) and San Diego (Events 13-3 and 13-4) were completed in both directions, with charges dropped inbound and outbound, but AXBT's dropped inbound to FLIP only. The run along the PARKA I track due north to 55°N was completed using charges only (Event 13-5). The return trip plus a planned round trip to Seattle were eliminated after FLIP was disabled on 1 December. Because of equipment failures and other problems, environmental data in the form of good AXBT traces were collected to only limited ranges on Events 13-1 and 13-3. Figures 34 and 35 show sound velocity profiles along these tracks constructed from the PARKA AXBT data combined with archival salinity information. In order to describe the sound velocity conditions along the entire length of all of the acoustic runs, some supplementary profiles have been constructed. Figures 36 through 39 display a series of sound velocity profiles computed by FNWC from archival Nansen cast data for the four Event 13 tracks. Bathymetric profiles collected by the PARKA ships prior to the experiment are also shown on these figures.

The ocean environment on the tracks radiating northward from FLIP to Alaska (Figs. 36 and 37) is characterized by a deep sound channel that shoals rapidly in the vicinity of the Subarctic Convergence (about 42°N). The critical depth decreases rather uniformly from FLIP northward to Alaska.

In contrast, the axis of the sound channel remains relatively deep on the track eastward to

San Diego (Fig. 38). However, sound velocity conditions do not remain constant along the entire track. In the vicinity of the California Current a marked boundary region exists between two water masses (Fig. 4) at about 1300 nautical miles range. Propagation loss measured at FLIP should generally increase with range until this transition zone is reached, where significant perturbations may occur. Partial interruption of acoustic propgation by seamounts and other complex bathymetry is possible everywhere on this track from a range of 500 nautical miles to the coast of California.

Adak and Due North Aircraft Runs (Events 13-1, 13-2, and 13-5)

The oceanographic features and the sound velocity structure along the Adak and "due north" runs are similar and will be considered together. North-northwestward from FLIP there is a typical substropical sound velocity structure which extends to about 32°N (Figs. 36 and 37). It consists of a well-defined deep sound channel with an average axial depth of 750 meters (410 fathoms). Between 32°N and 42°N, the Mid-Pacific Transition Zone is encountered. This zone couples a deep, 750-meter sound channel having a large velocity difference to the south with a much shallower, 200-meter subarctic sound channel having a considerably smaller difference to the north. Much of this change in the character of the sound channel apparently takes place near the northern edge of this transition zone, near 42°N. As indicated earlier in this Section, the bottom of the sound channel at the FLIP site occurs at about 4500 meters (2460 fathoms); at 50°N it occurs around 500 meters (270 fathoms). Although the critical depth decreases gradually with increasing latitude from FLIP, it also shows a sharp decrease around 42°N. From 42°N northward to the Alaskan coast, the axis shoals gradually to about 100 meters (55 fathoms) near the northern end of the tracks. As shown in Figs. 36 and 37, the critical depth drops to less than 600 meters (330 fathoms) off Alaska, which is just below the axis. With depth excess increasing from 1000 meters at FLIP to 4200 meters off the Alaskan coast, convergence zone propagation is unimpeded over the length of both of these tracks.

The Mid-Pacific Transition Zone is characterized by near-surface instabilities and a complex vertical structure in the upper several hundred meters of the water column. Farther north a characteristic vertical temperature structure prevails over most of the Subarctic Pacific region. This structure (termed "dichothermal" by Uda, 1963) is characterized by a temperature minimum at a depth of about 100 meters, and can be formed in two ways. First, just north of the Subarctic Convergence, warmer subsurface water of tropical origin may intrude into the subarctic water mass, resulting in a temperature minimum immediately above the intrusion (about 100 meters), and a temperature maximum at the depth of the intrusion. Water associated with this temperature maximum is called "mesothermal" by Uda when found in the subarctic region. Second, a similar temperature structure found to the north-northwest is probably caused by seasonal heating effects.

The dichothermal/mesothermal structure accounts in part for the shallow sound channel found in the area described above. The strength of the channel and the critical depth (bottom of the channel) should be seasonally dependent. Increased surface temperature in summer and the associated near-surface negative gradient intensifies the sound channel; in winter the surface layer becomes isothermal, and as the near-surface temperature maximum decreases, the critical depth becomes shallower, and the maximum velocity difference decreases. Regardless of seasonal changes, topography does

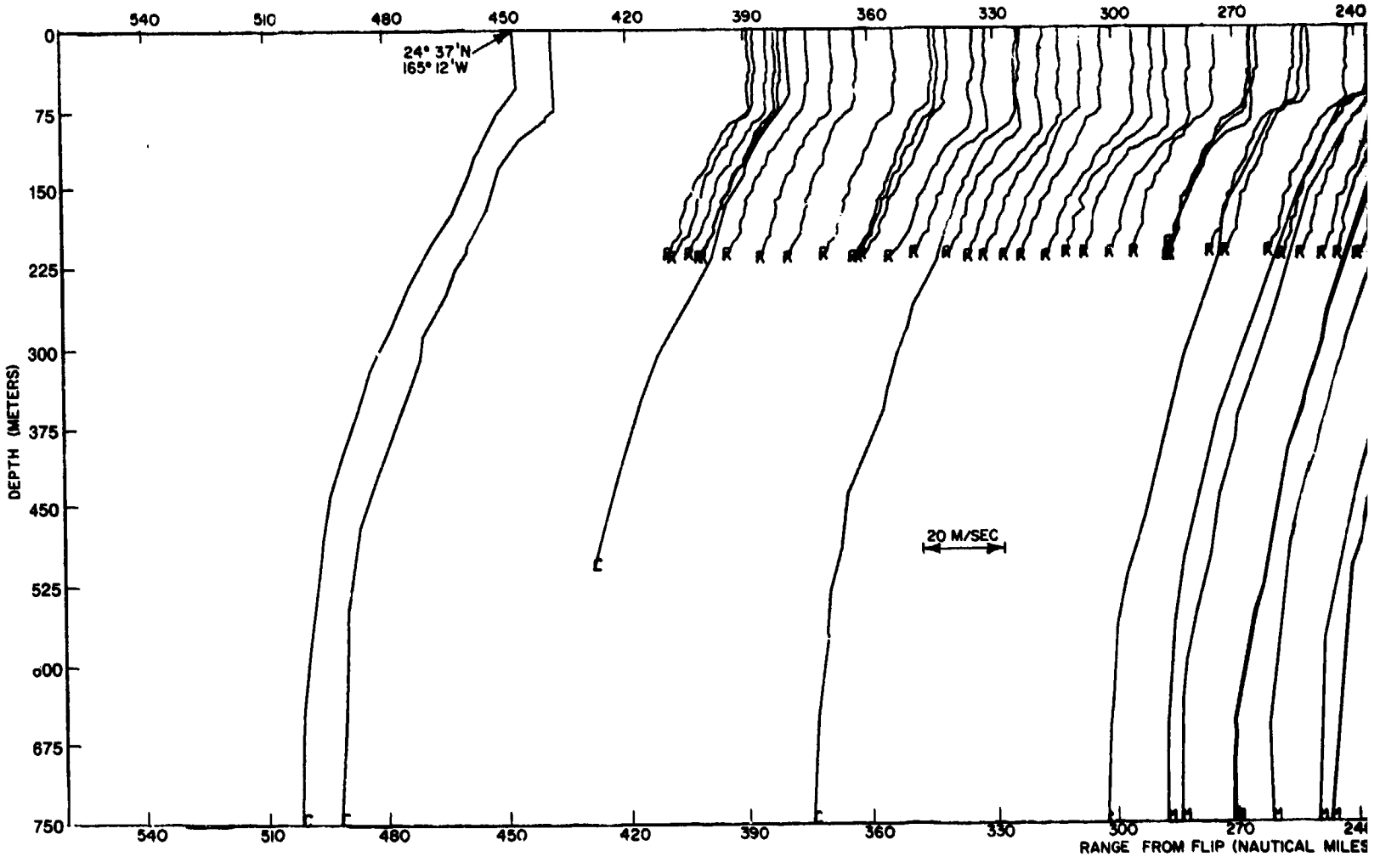

Fig. 28 — Shallow Sound Velocity Profiles, Event 9-4 (Propagation Loss and

(Page 54 Blank)

1. Nominal FLIP position: 27°35'N,157°44'W
2. Observations are plotted at actual range from FLIP along top scale
3. Letter at bottom of profile indicates source of data:

C = CONRAD
M = MARYSVILLE
R = REXBURG
S = SANDS

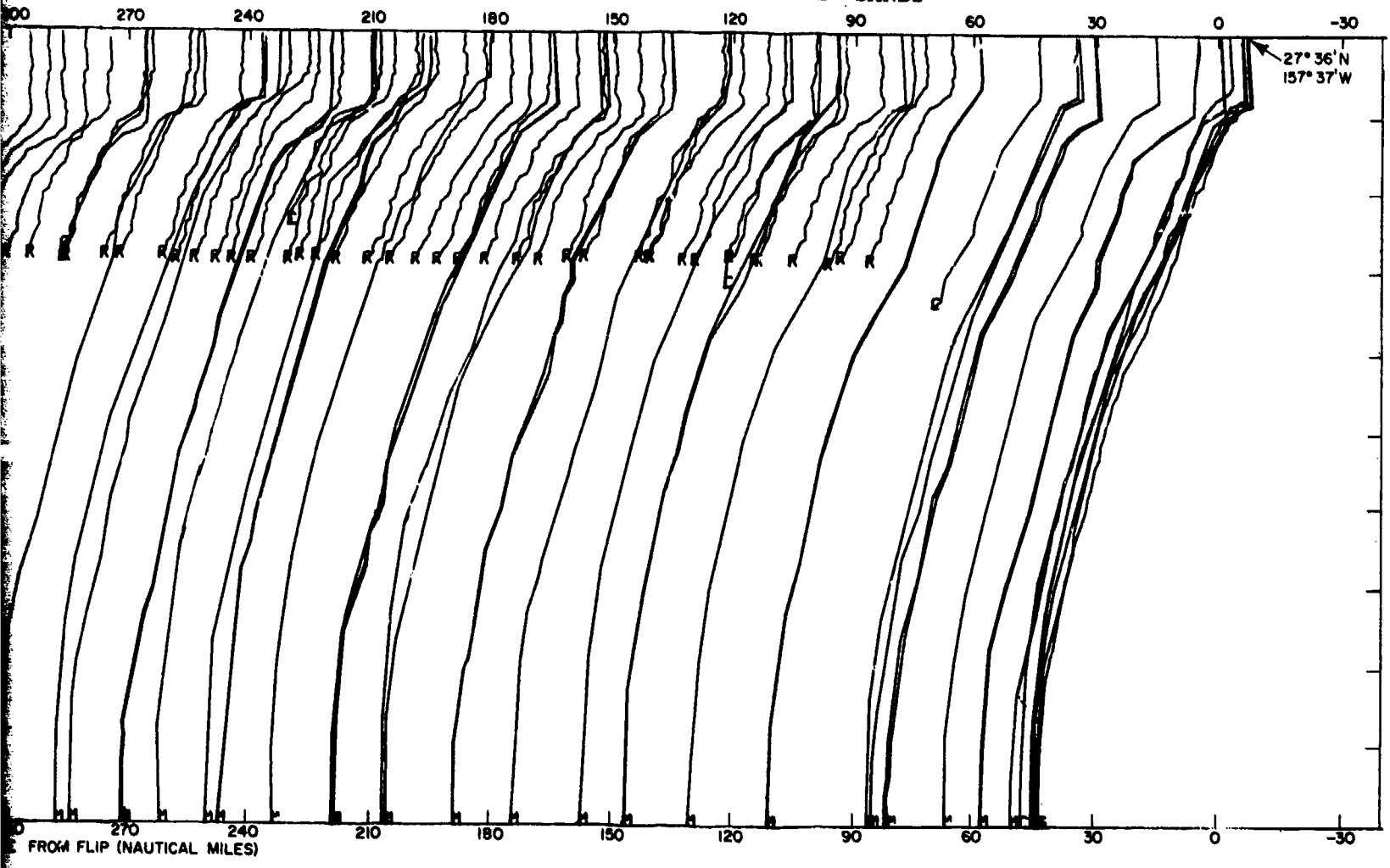

9-4 (Propagation Loss and Arrival Structure), from FLIP to about 24°30'N,165°20'W

(Page 54 Blank)

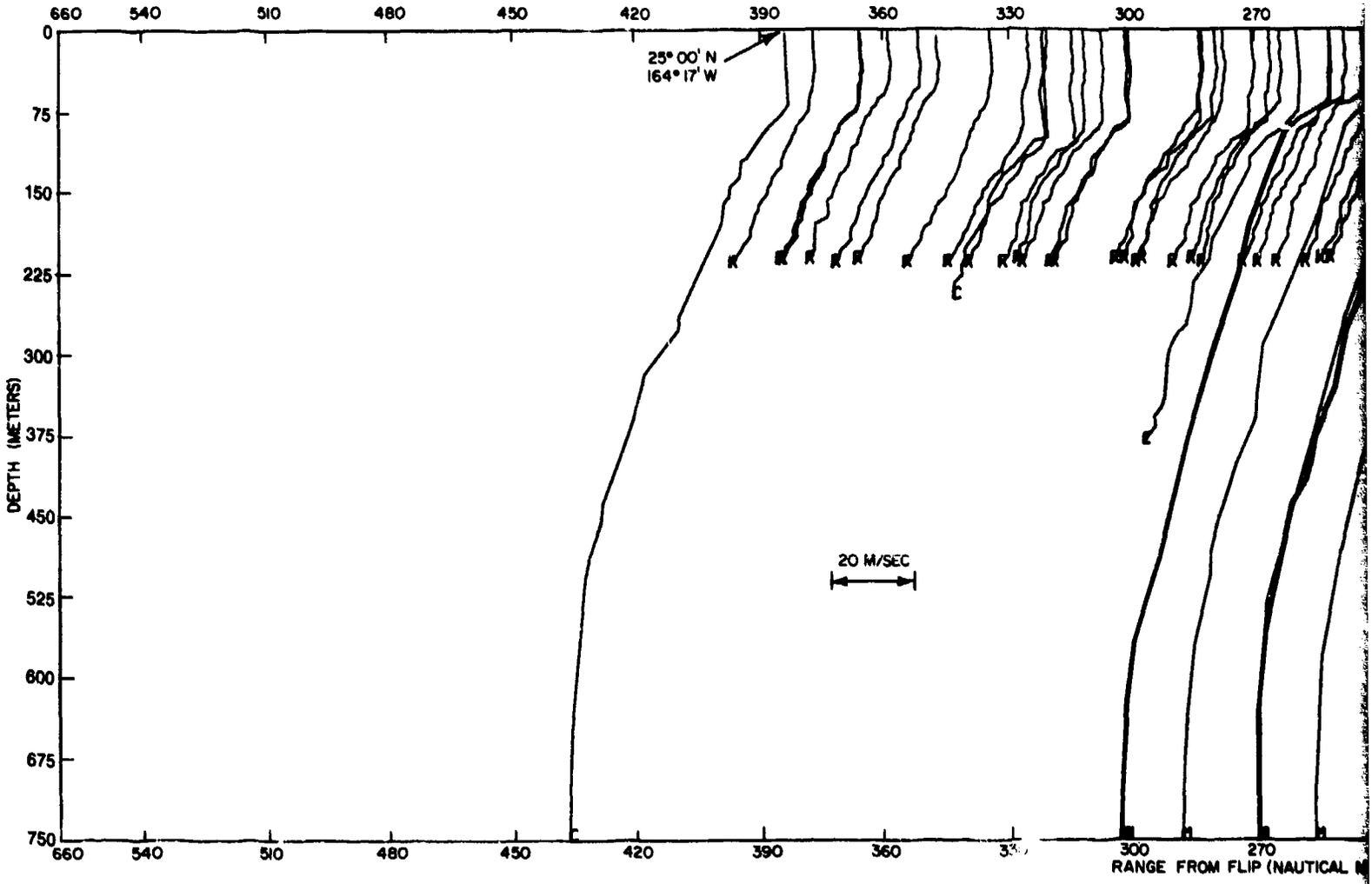

Fig. 29 — Shallow Sound Velocity Profiles, Event 9-5 (Propagation Loss and

(Page 56 Blank)

1. Nominal FLIP position: 27°35'N,157°44'W
2. Observations are plotted at actual range from FLIP along top scale
3. Letter at bottom of profile indicates source of data:

C = CONRAD
M = MARYSVILLE
R = REXBURG
S = SANDS

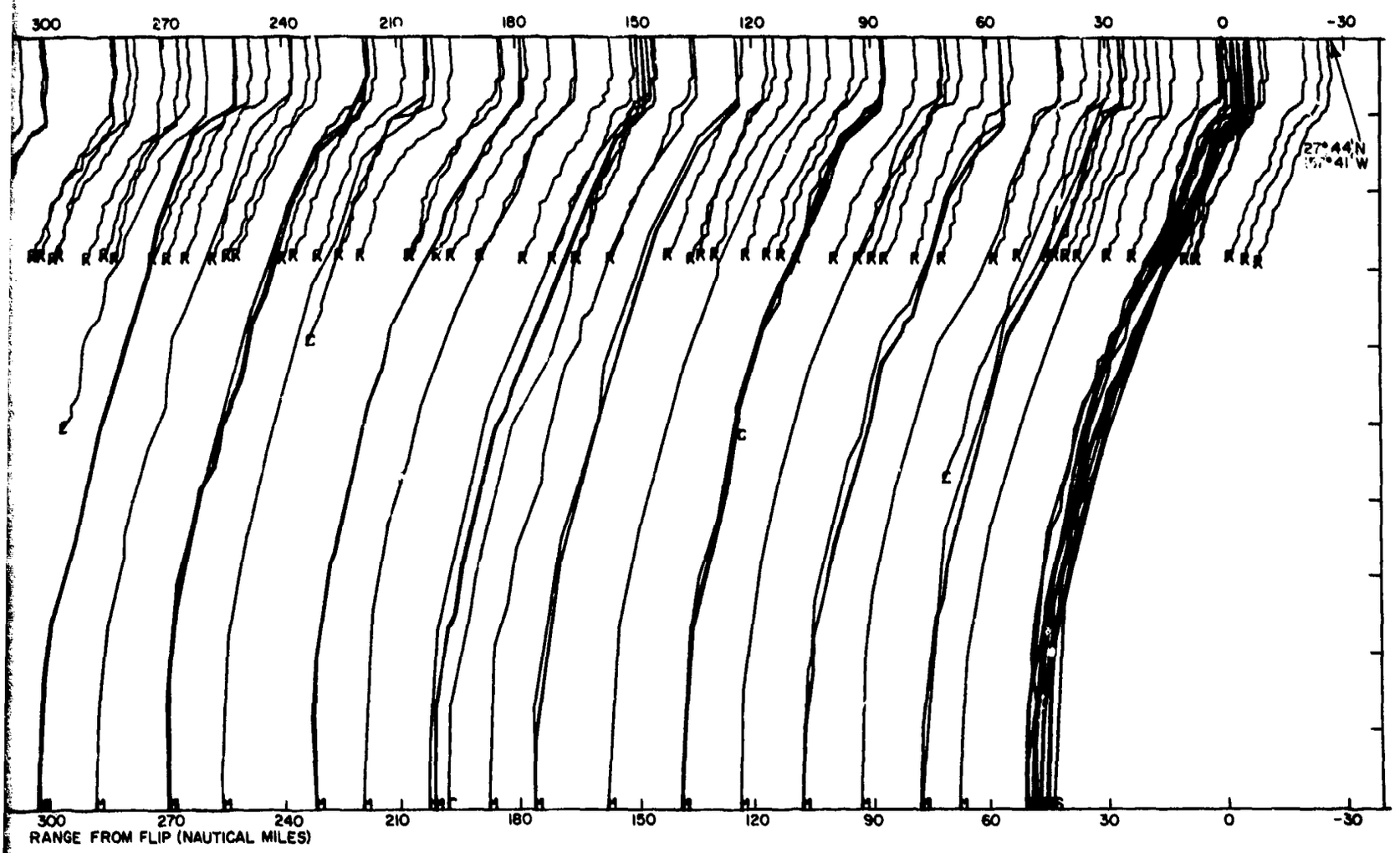

t 9-5 (Propagation Loss and Arrival Structure), from about 24°30'N,165°20'W to FLIP

(Page 56 Blank)

2

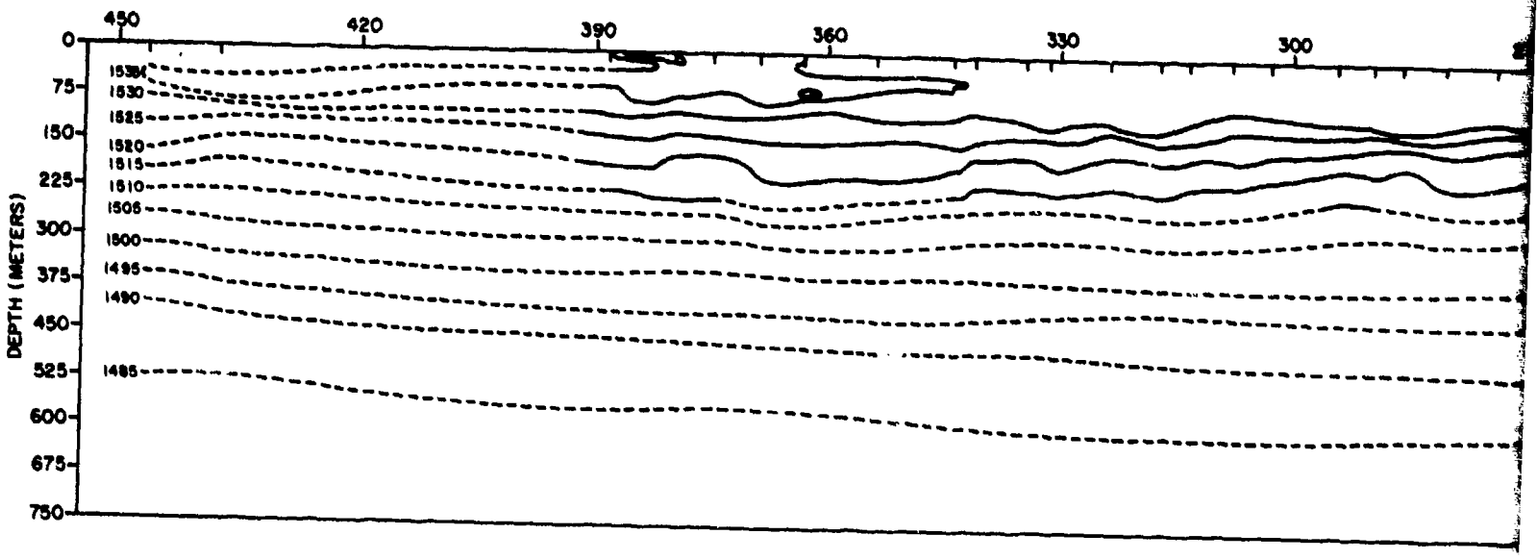

Fig. 30 — Contoured Shallow Cross Sec

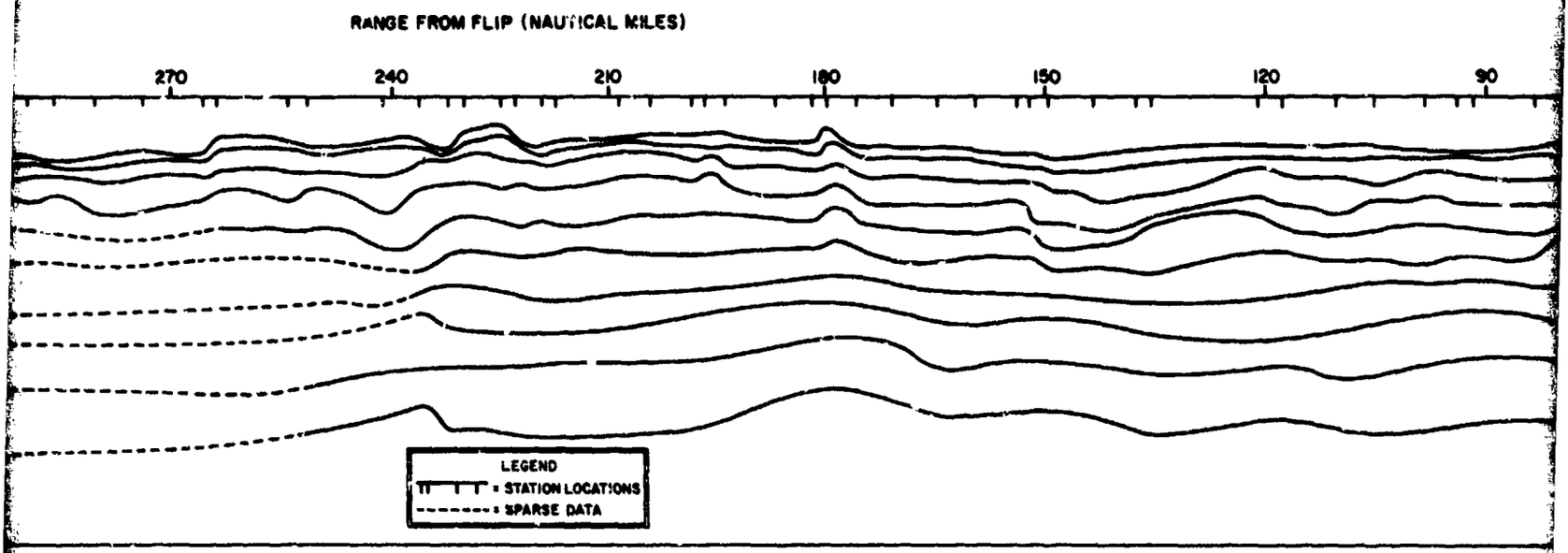

allow Cross Section of Sound Velocity, Event 9-4 (Propagation Loss and Arrival Structure), from FLIP to about 24°30′N,165°20′W

(Page 58 Blank)

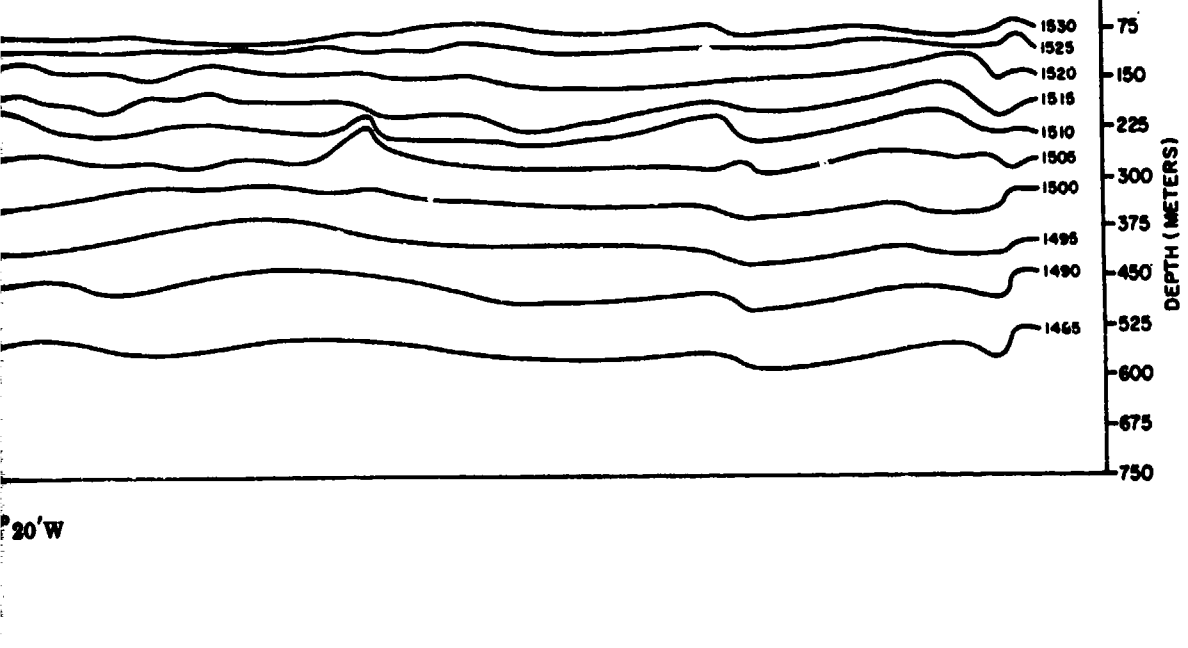
NOMINAL FLIP POSITION: 27°35'N, 157°44'W
120
90
60
30
0
-10
0
75
150
225
300
375
450
525
600
675
750
DEPTH (METERS)
1530
1525
1520
1515
1510
1505
1500
1495
1490
1485

°20'W

3

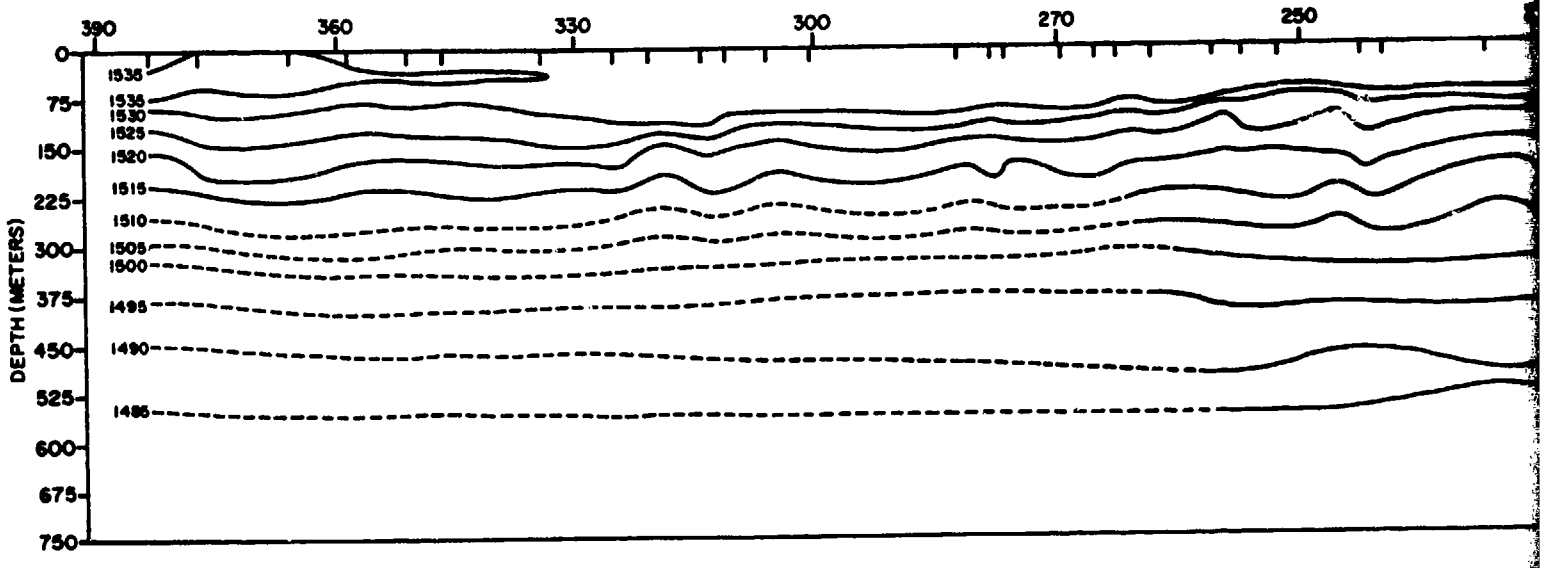

Fig. 31 — Contoured Shallow Cross Section of Sound Ve

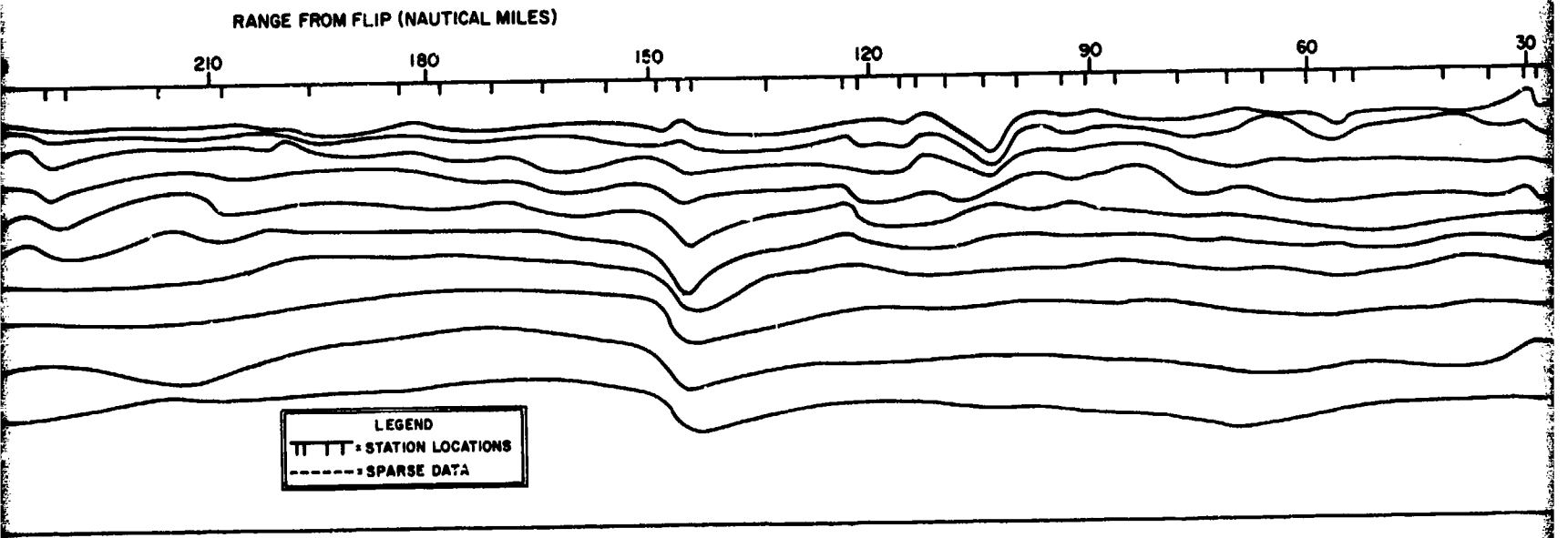

ection of Sound Velocity, Event 9-5 (Propagation Loss and Arrival Structure), from about 24°30'N,165°20'W to FLIP

(Page 60 Blank)

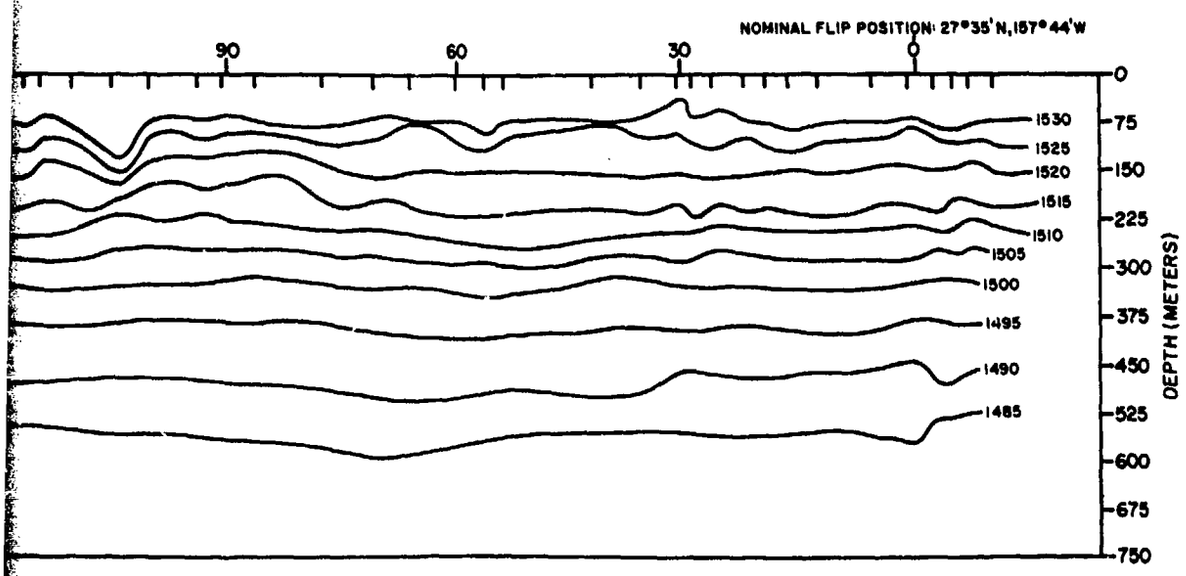

24°30'N,165°20'W to FLIP

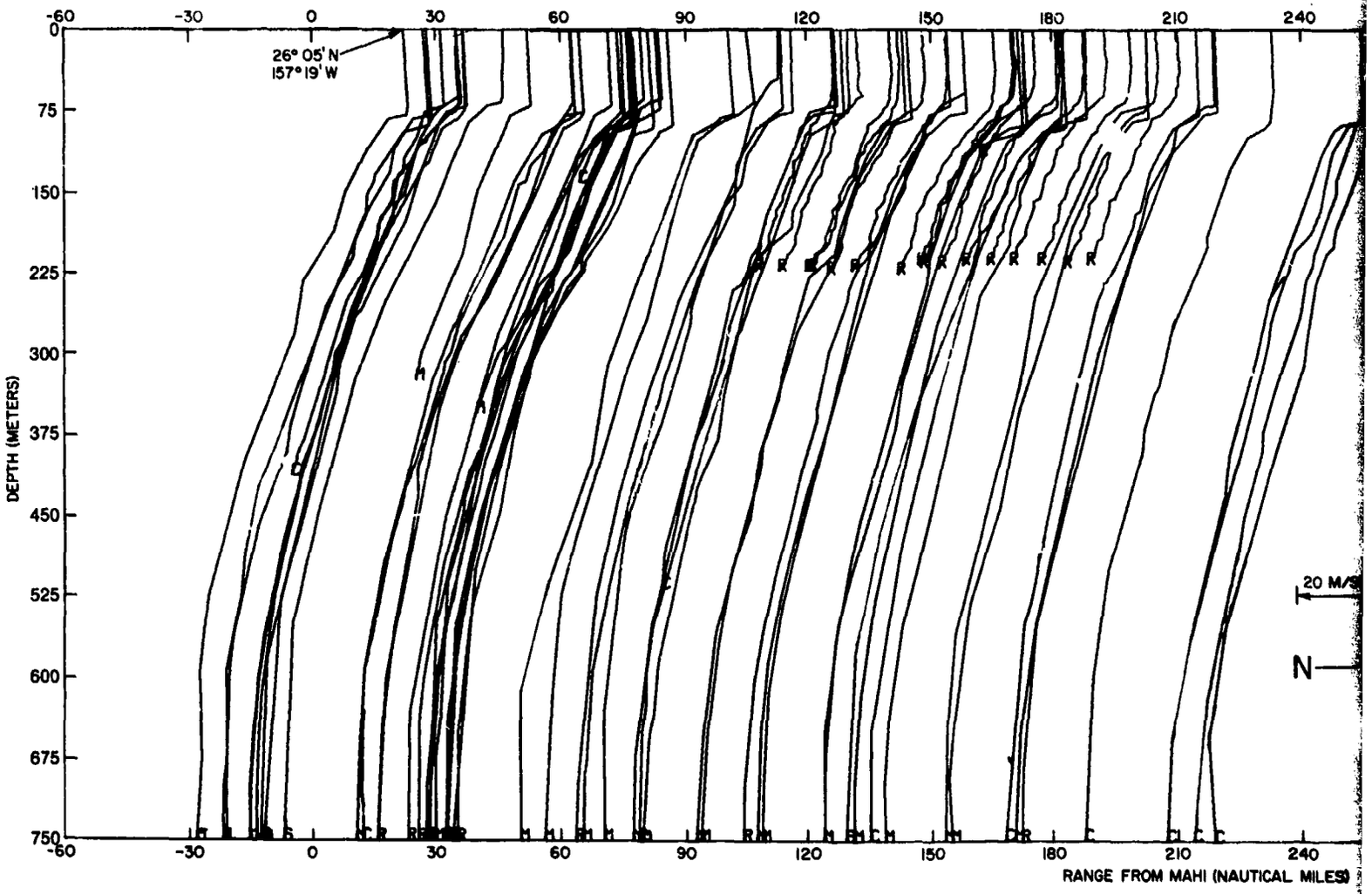

Fig. 32 — Shallow Sound Velocity Profiles, Events 11-1 and 11-2 (Propagation Loss and Temporal F

(Page 62 Blank)

1. MAHI position: 26°09'N,157°41'W
2. Observations are plotted at actual range from MAHI along top scale
3. Letter at bottom of profile indicates source of data:

   C = CONRAD
   M = MARYSVILLE
   R = REXBURG
   S = SANDS

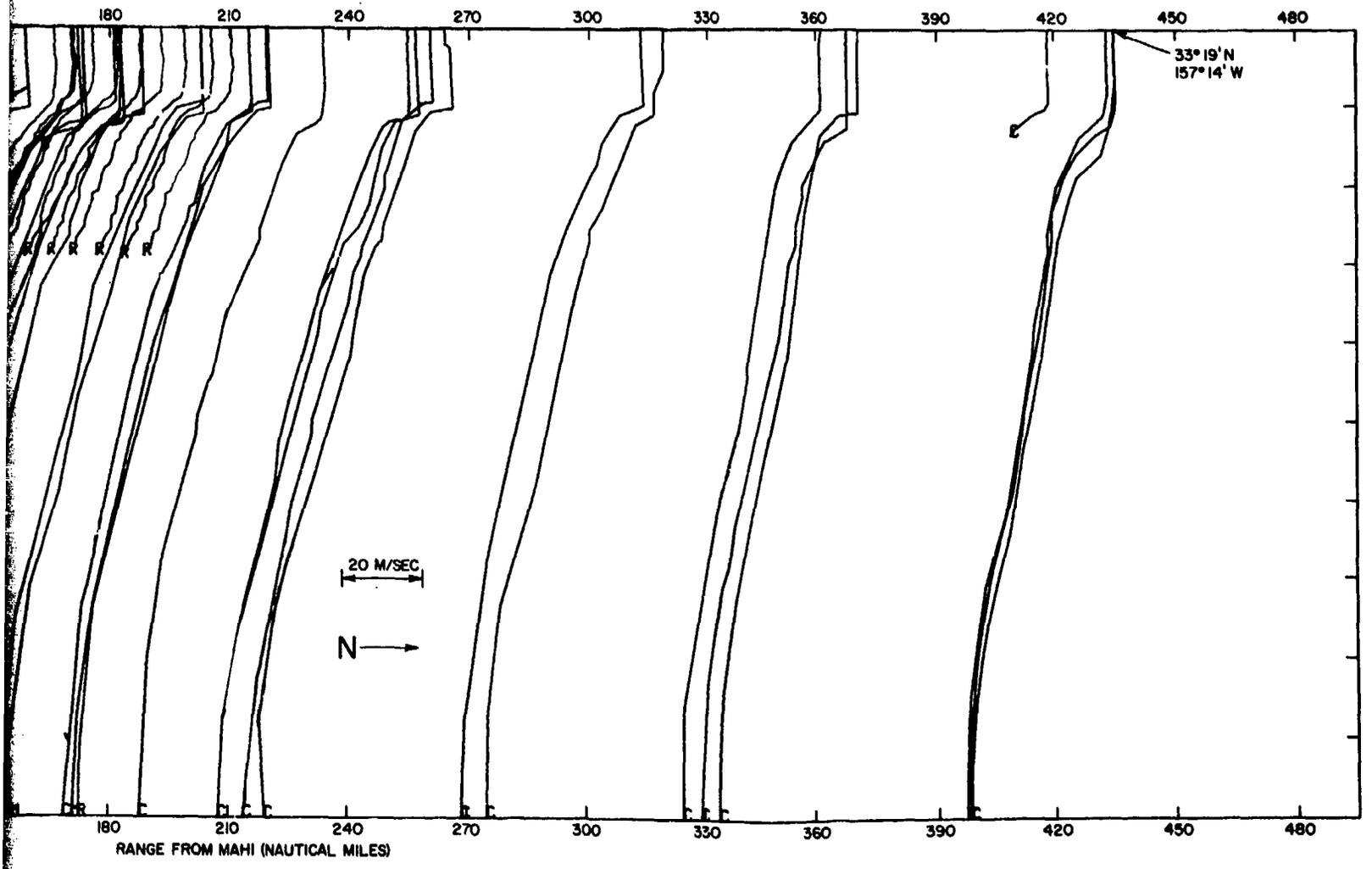

nd 11-2 (Propagation Loss and Temporal Fluctuation of CW Signals, MAHI to about 33°20'N and Return

(Page 62 Blank)

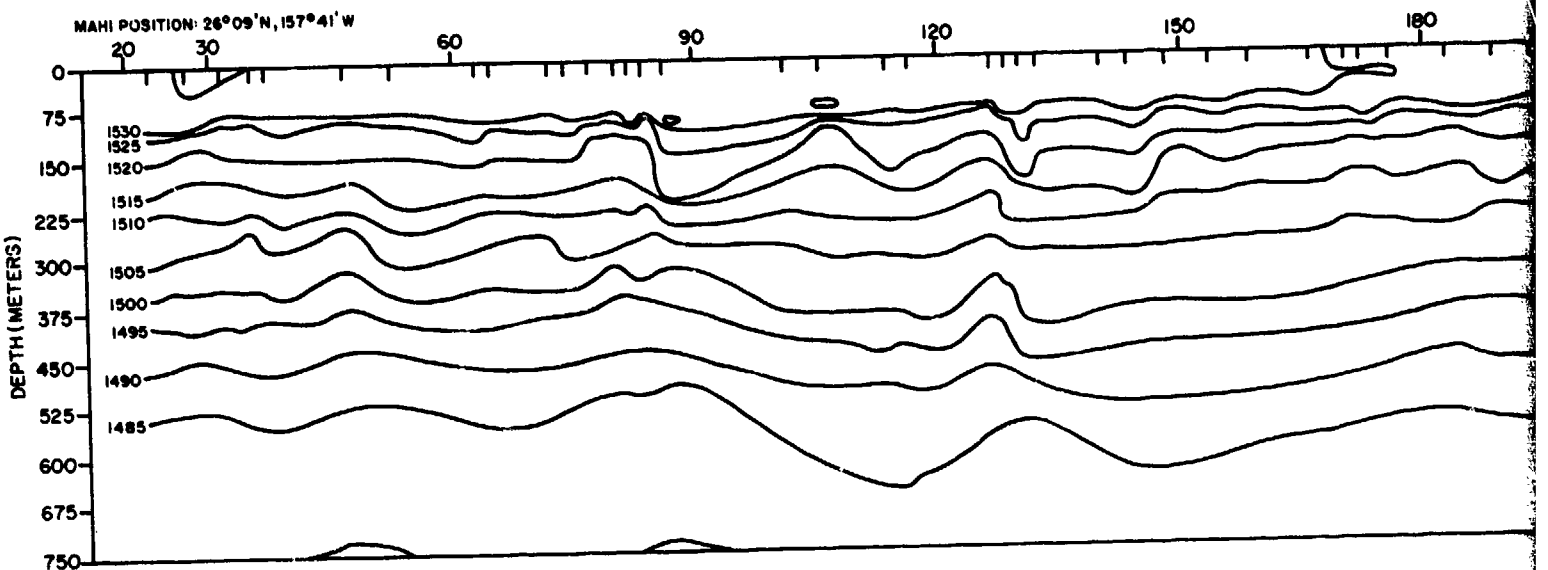

Fig. 33 — Contoured Shallow Cross Section of Sound Velocity,

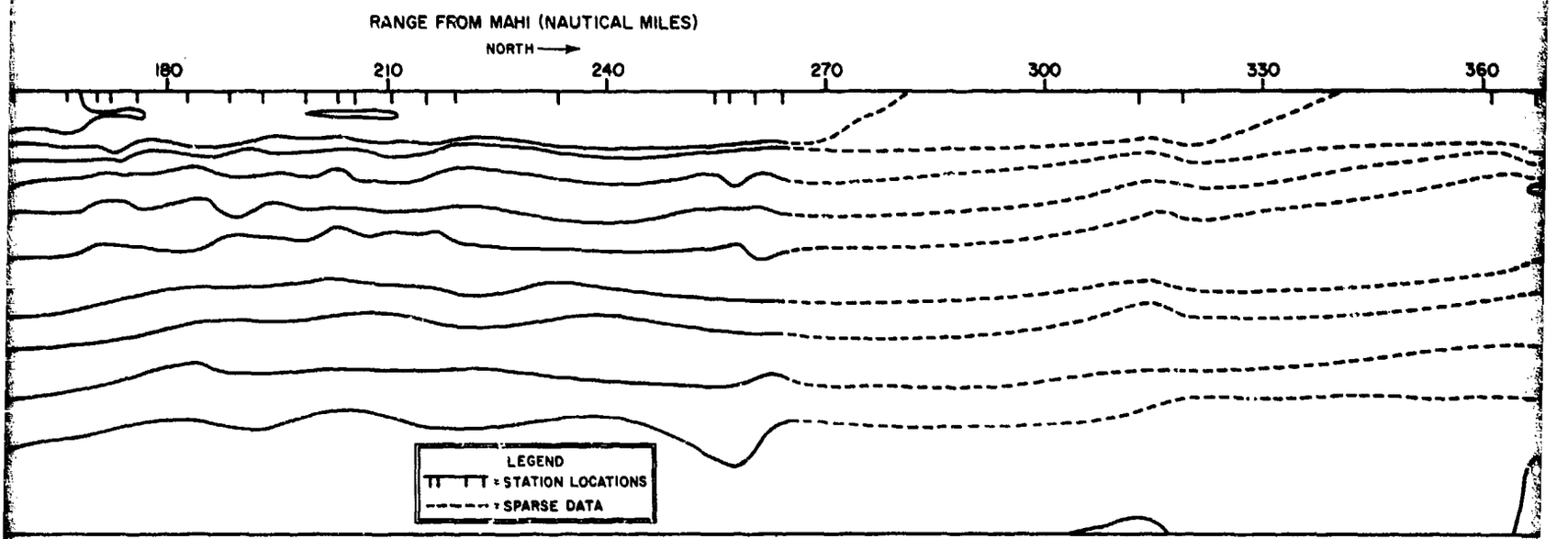

ction of Sound Velocity, Events 11-1 and 11-2 (Propagation Loss and Temporal Fluctuation of CW Signals), MAHI to about 33°20'N and Return

(Page 64 Blank)

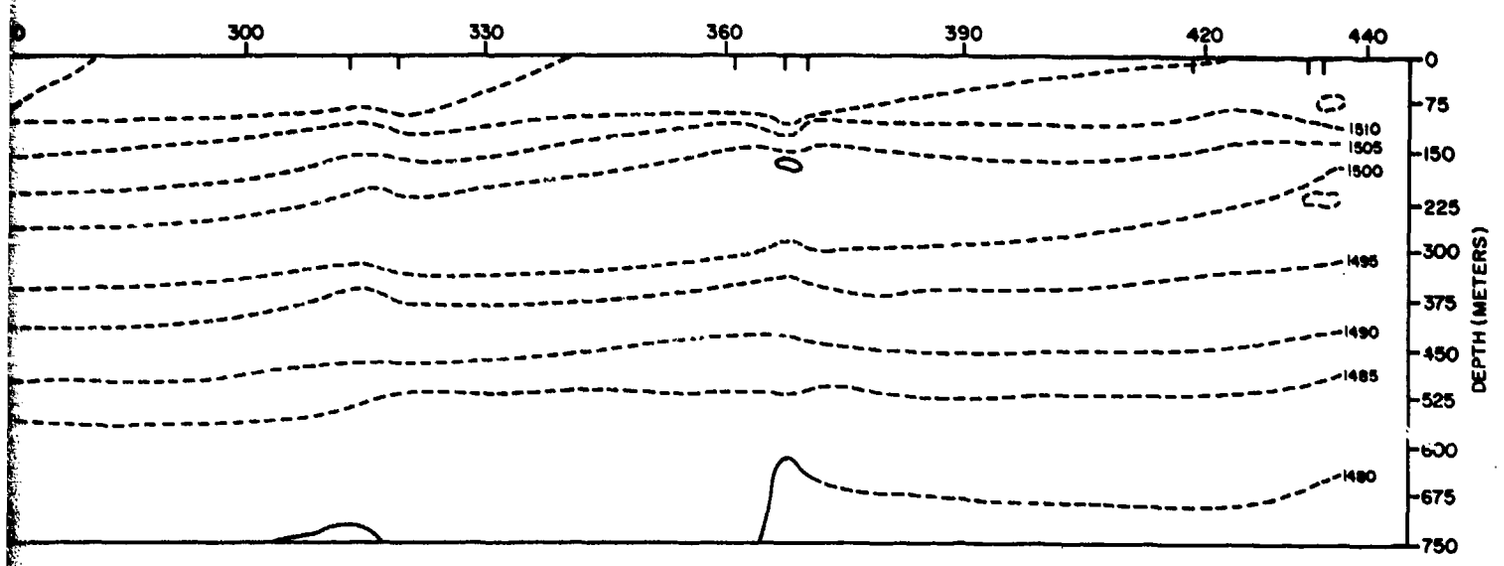

ituation of CW Signals), MAHI to about 33°20′N and Return

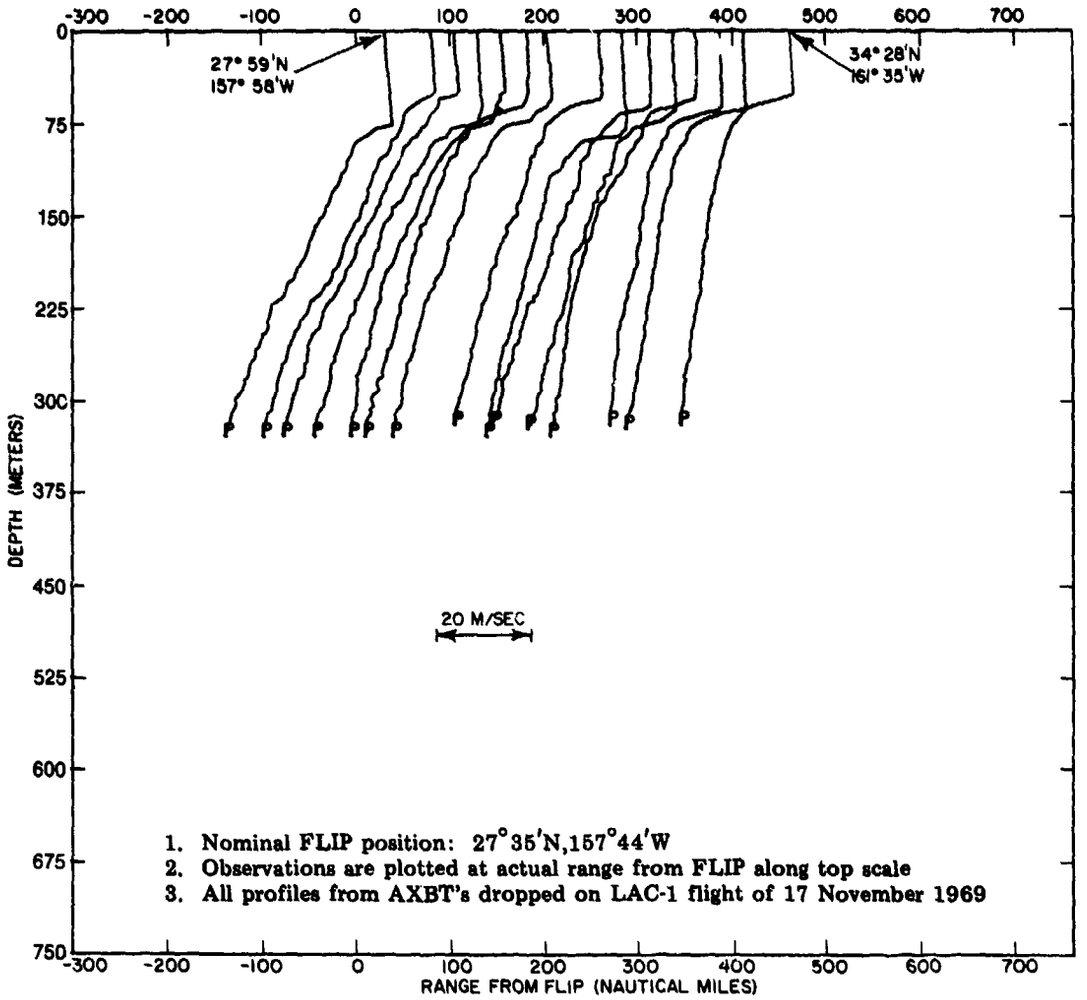

Fig. 34 — Shallow Sound Velocity Profiles, Event 13-1 (Long Range Propagation Loss, Aircraft), Adak to FLIP

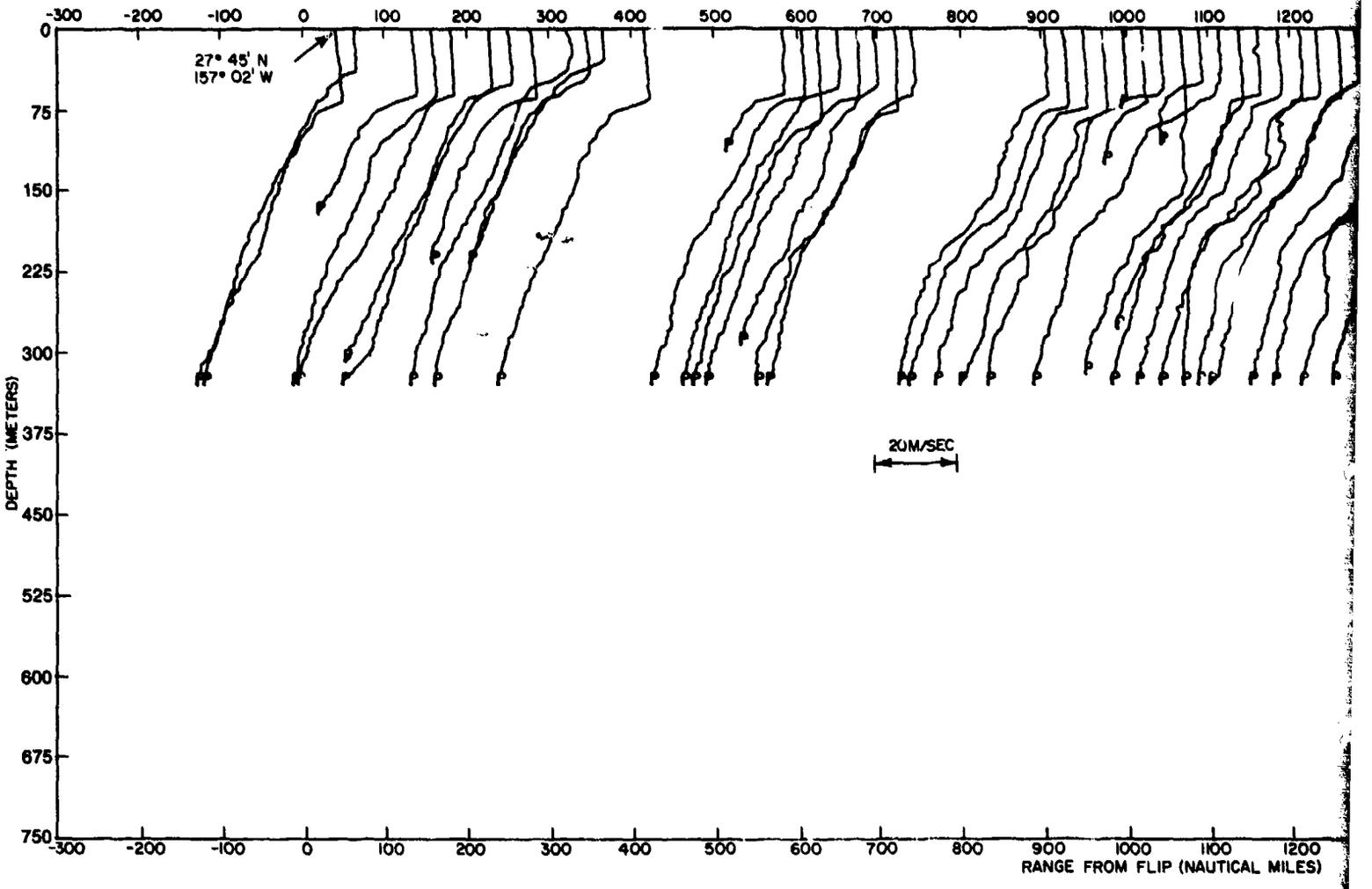

Fig. 35 — Shallow Sound Velocity Profiles, Event 13-3 (Long Range Propagatio

(Page 68 Blank)

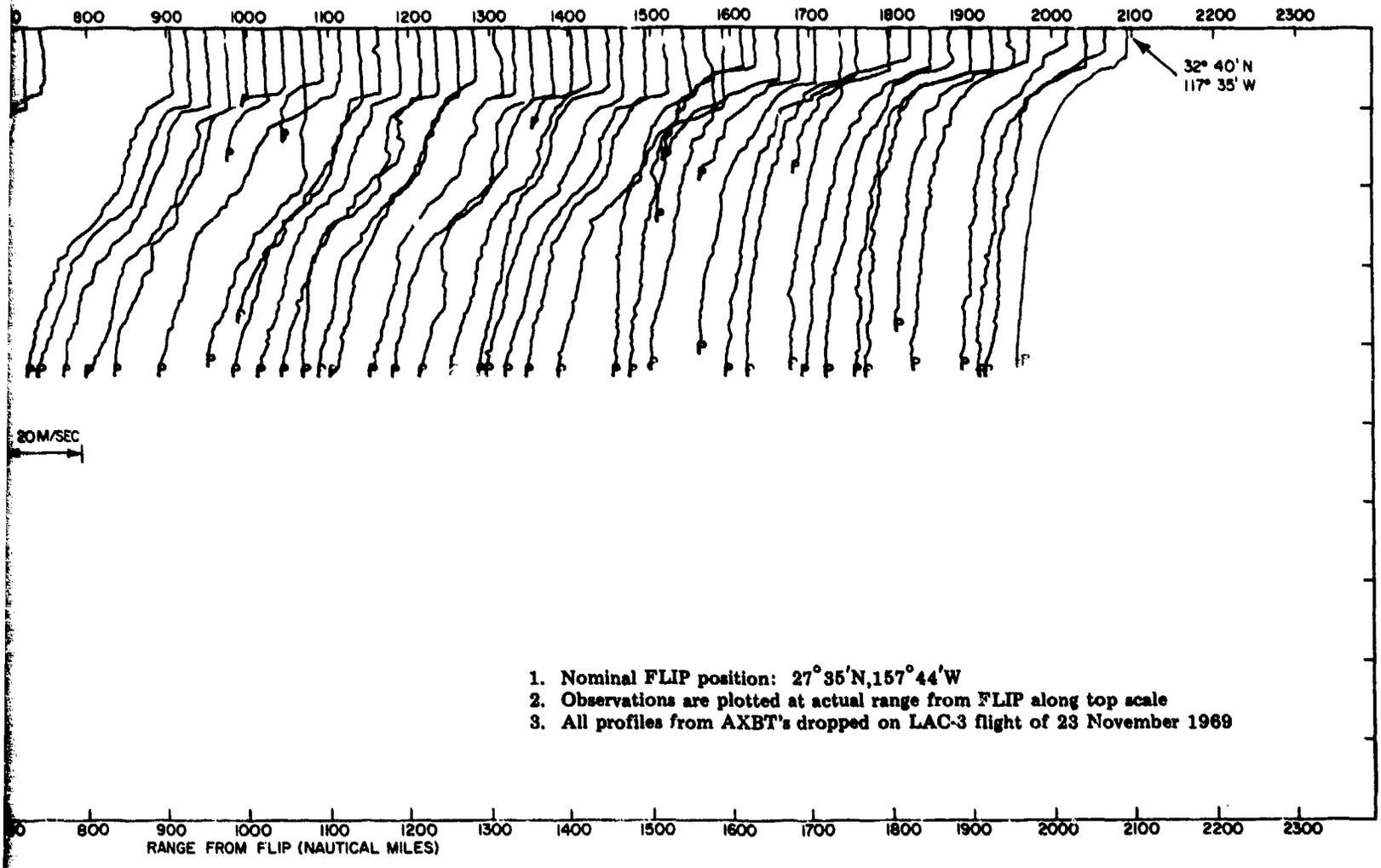

city Profiles, Event 13-3 (Long Range Propagation Loss, Aircraft), San Diego to FLIP

(Page 68 Blank)

These classified figures are to be used in conjunction with Maury Center Report 006, Volume 2, PARKA II-A, The Oceanographic Measurements. They are being distributed separately to permit the basic publication to be used on an unclassified basis.

CONFIDENTIAL

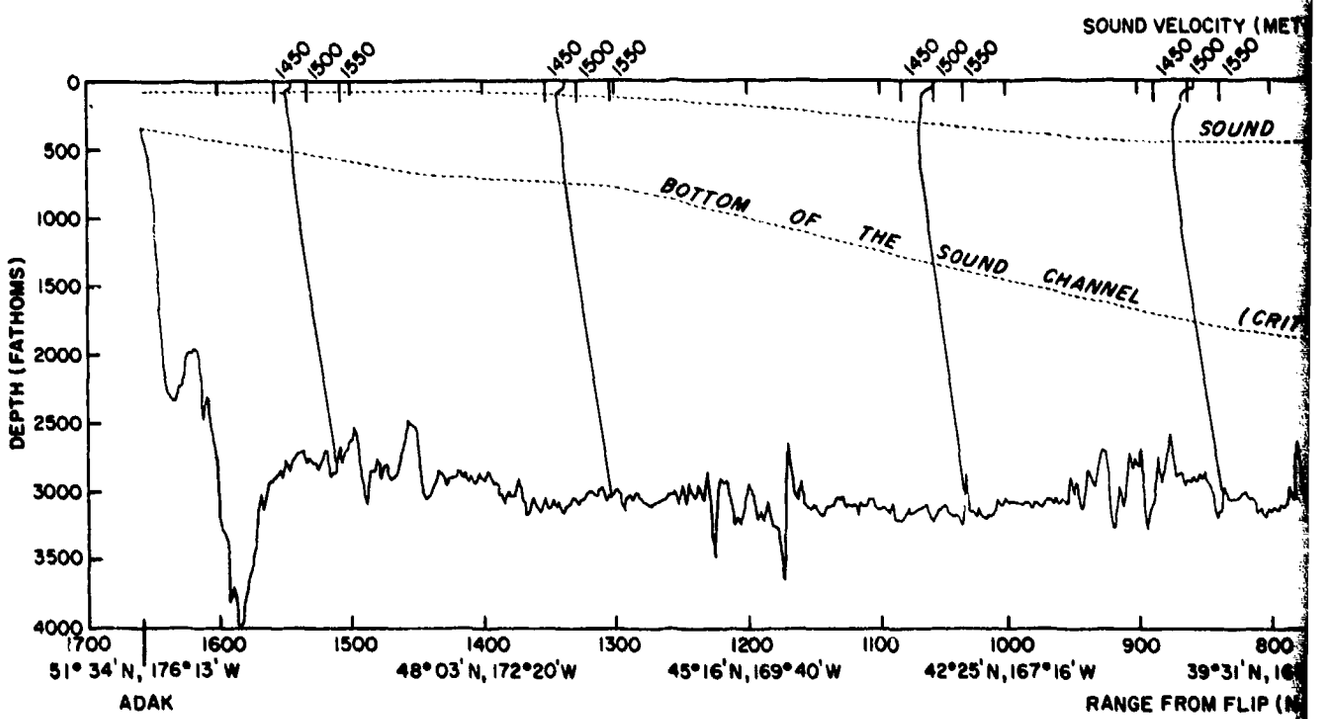

Fig. 36 — Bathymetric Profile and Predicted

CONFIDENTIAL

Secret

J. B. HERSEY
Deputy Assistant Oceanographer for
Ocean Science

JECT TO GENERAL
EXECUTIVE ORDER ... AUTOMATICALLY DOWNGRADED AT
TWO YEAR INTERVALS AND DECLASSIFIED ON 31 DEC 1979
(insert ye

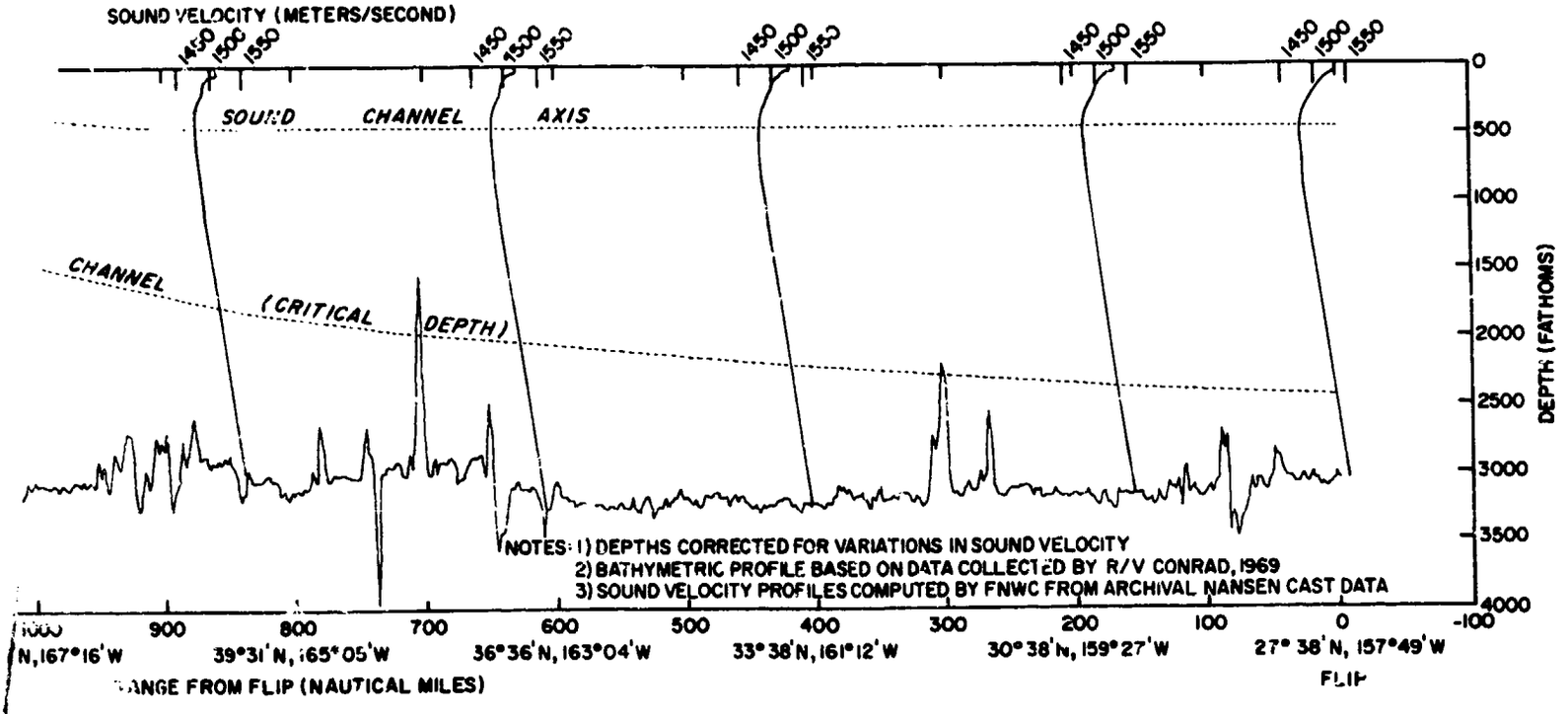

ymetric Profile and Predicted Sound Velocity Structure, FLIP to Adak

(Page 70 Blank)

CONFIDENTIAL

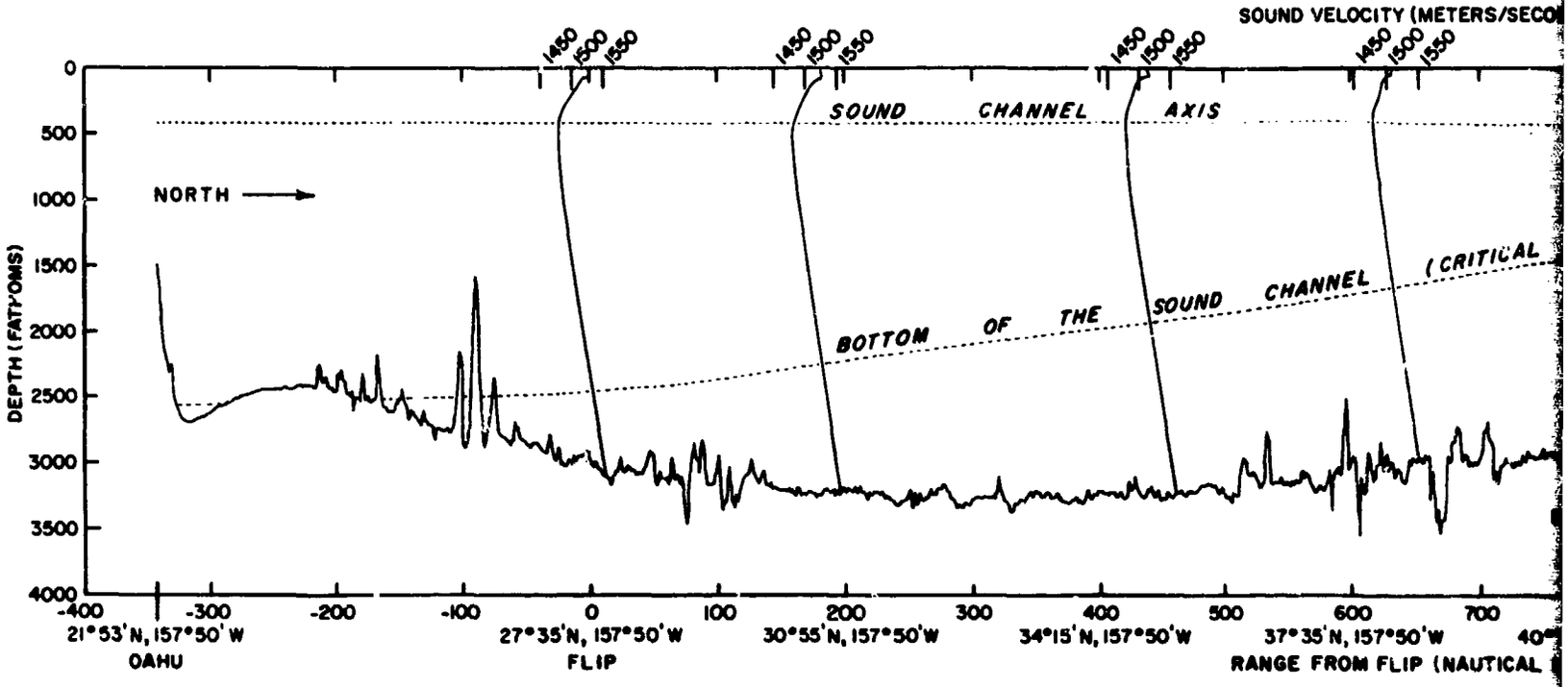

Fig. 37 — Bathymetric Profile and Predicted Sound Velo

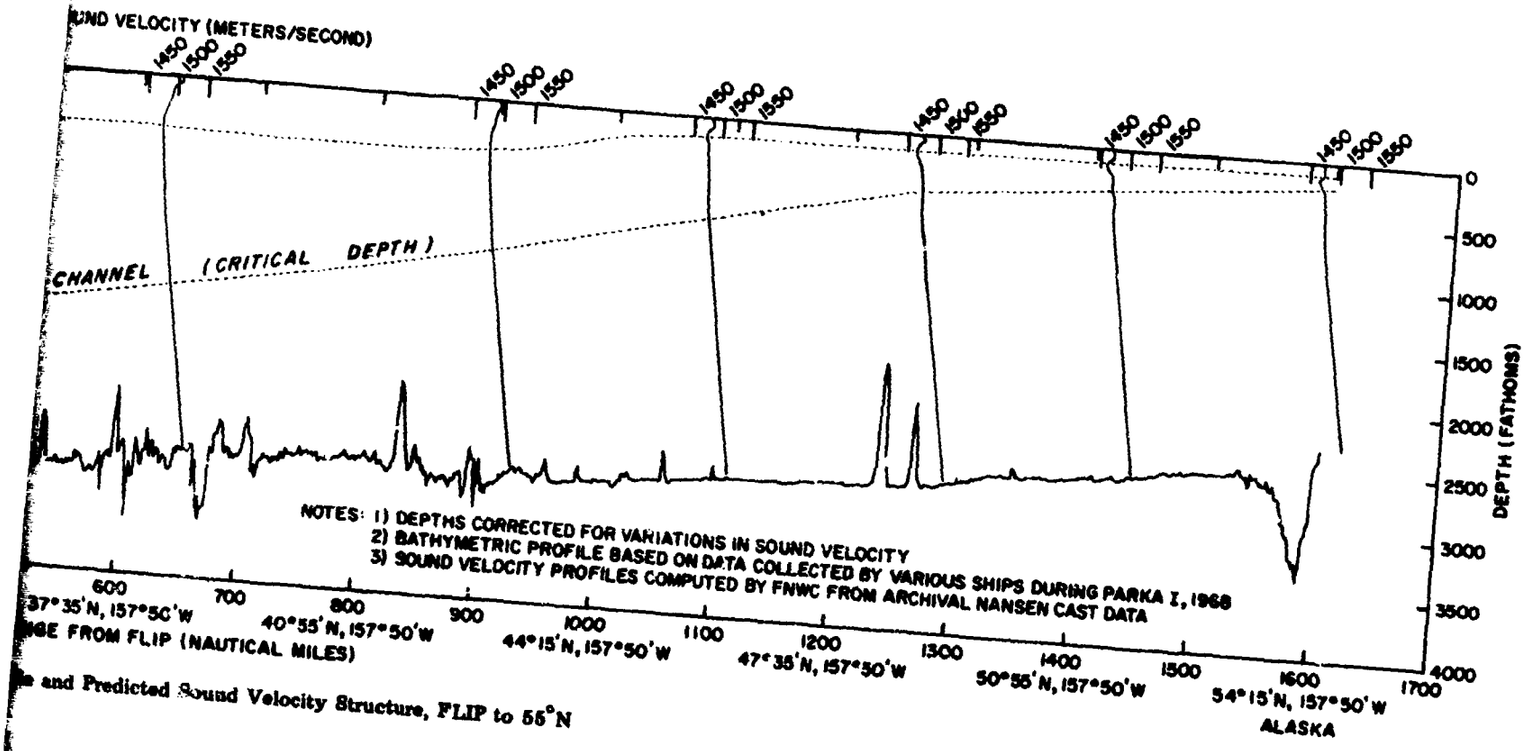

e and Predicted Sound Velocity Structure, FLIP to 55°N

(Page 72 Blank)

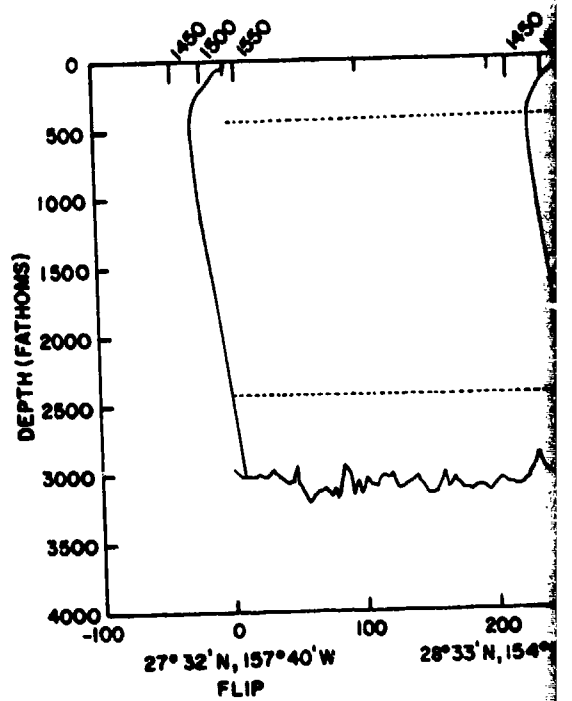

CONFIDENTIAL

Secret, Sensitive

J. B. HERSEY
Deputy Assistant Oceanographer for
Ocean Science

TO BE CANCELLED AT 31 DEC 1979.
(insert year)

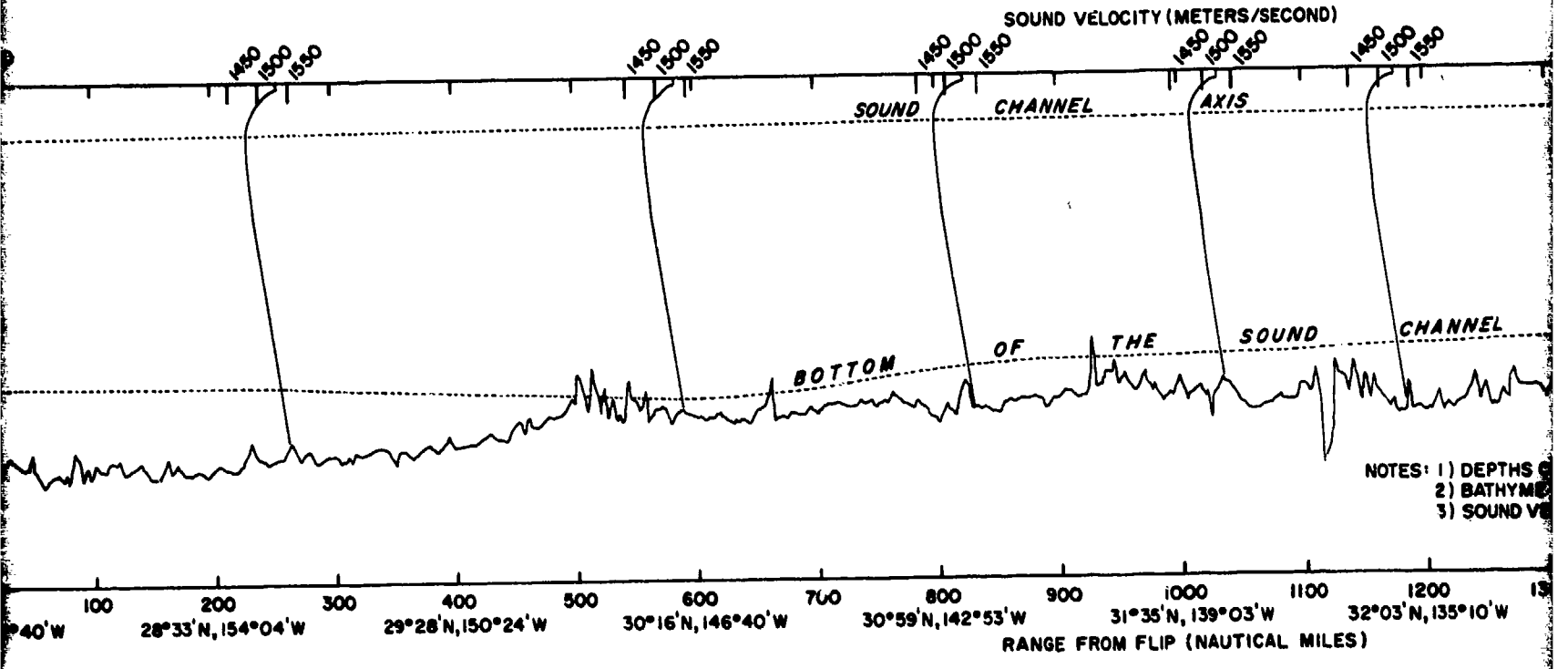

Fig. 38 — Bathymetric Profile and Predicted Sound Velocity Structure, FLIP to

(Page 74 Blank)

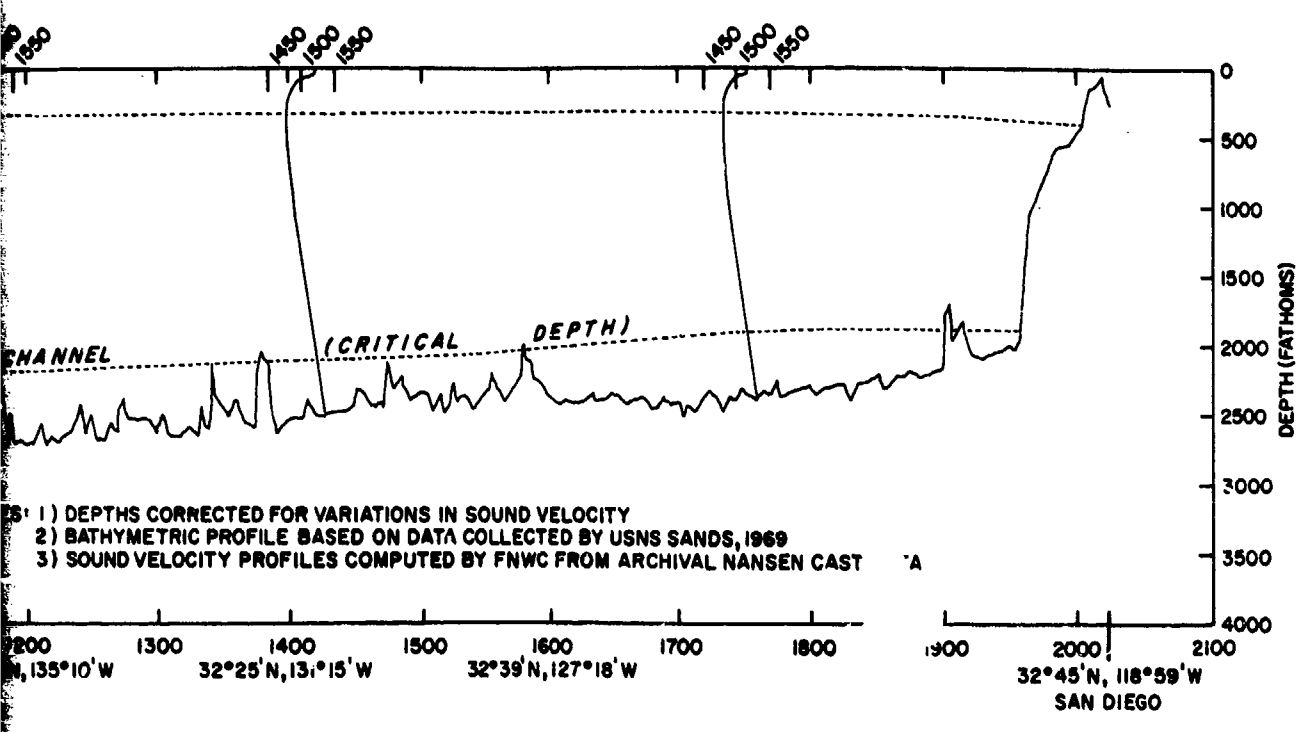

ure, FLIP to San Diego

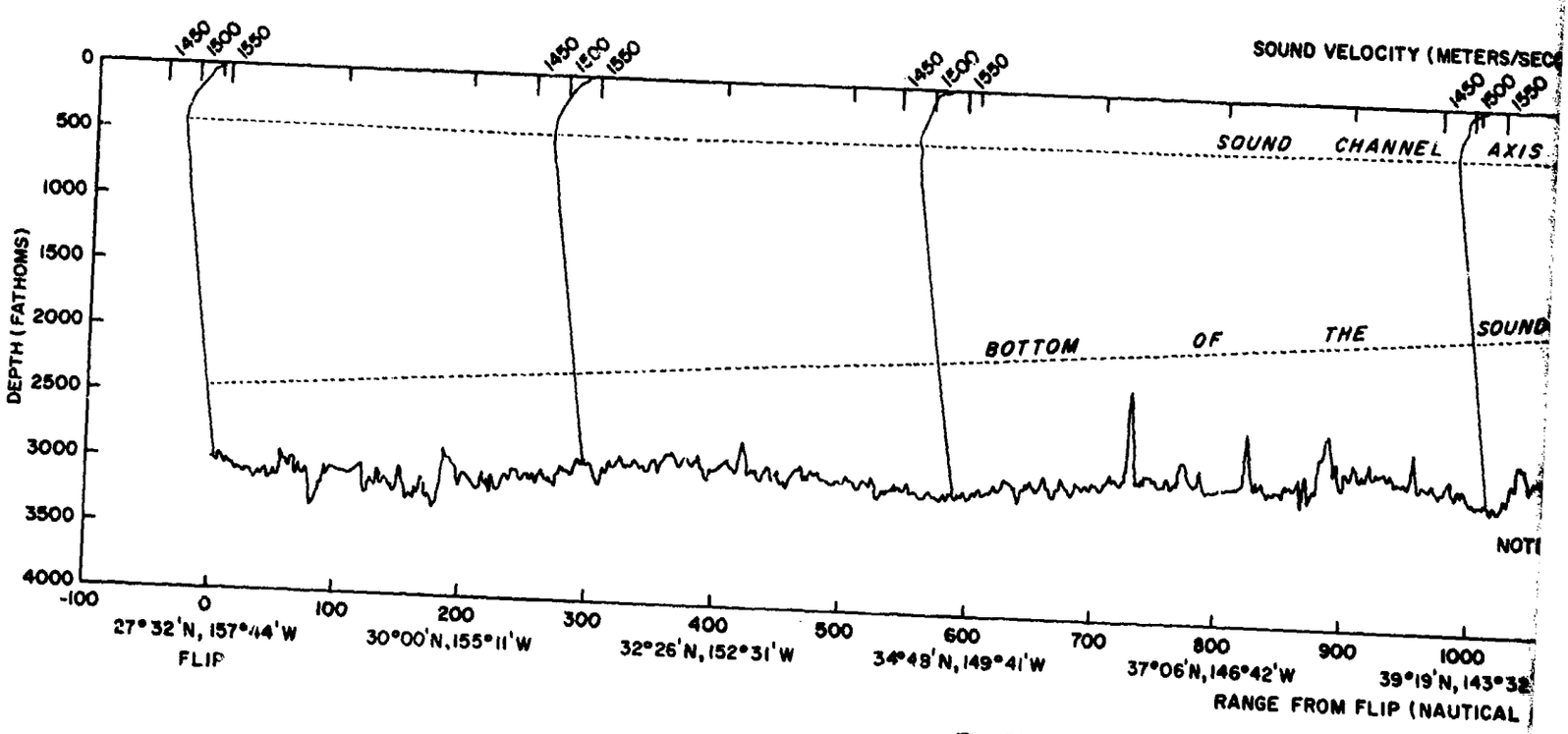

Fig. 39 — Bathymetric Profile and Predicted Sound Velo

, Secret, Sc

J. B. HERSEY
Deputy Assistant Oceanographer for
Ocean Science

CT TO GE
TIVE ORDE
YEAR INTERVALS A 31 DEC 1979.
(insert year)

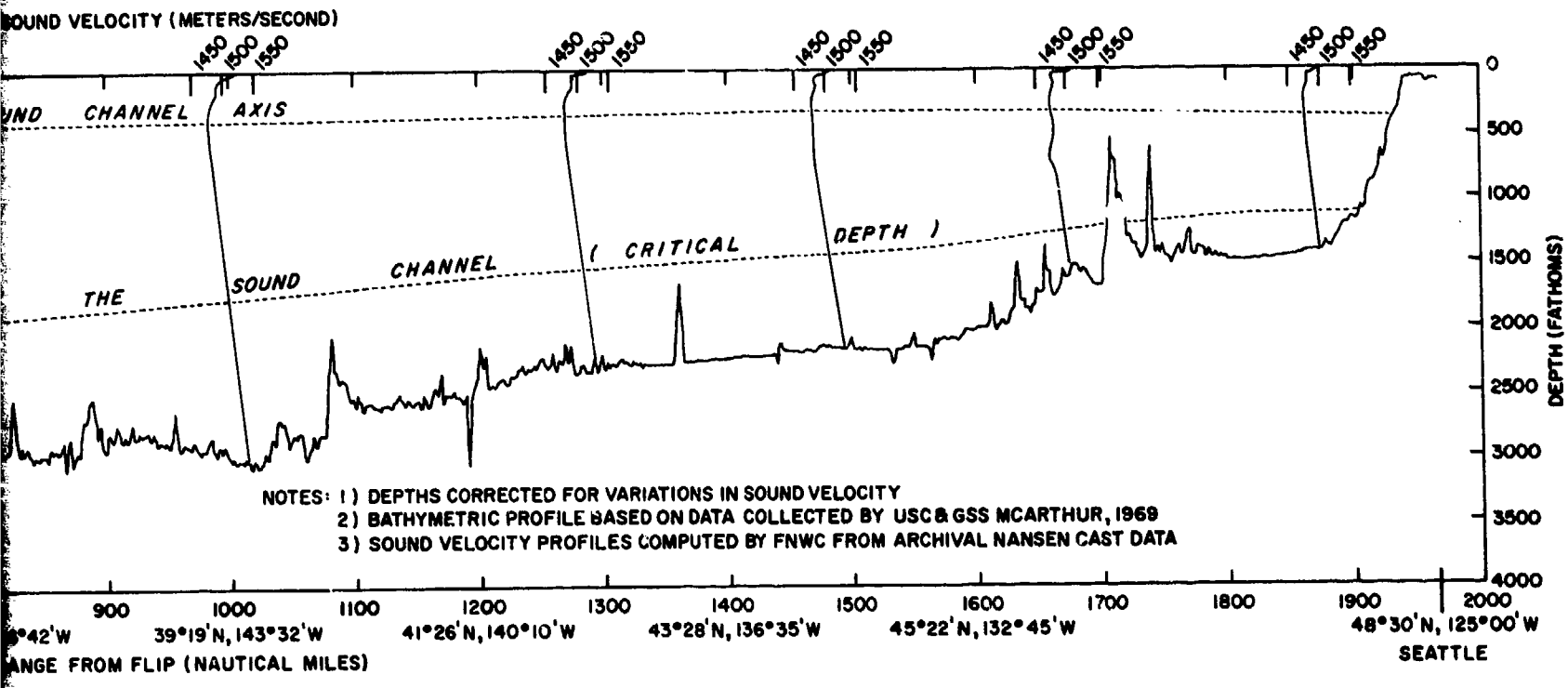

ile and Predicted Sound Velocity Structure, FLIP to Seattle

(Page 76 Blank)

not intrude into the sound channel in this region. The presence of dichothermal/mesothermal conditions are evident in Fig. 37 and to a lesser extent in Fig. 36.

In summary, along the two PARKA tracks in particular, but also more generally over a large portion of the northern North Pacific, we can expect improvement of coupling of the source to the sound channel as the source moves northward. The improvement is a consequence mainly of a shoaling axis, and a decrease in the critical depth. This funneling effect should begin to be prominent when the source reaches 42°N

San Diego Aircraft Run (Events 13-3 and 13-4)

Three water masses affect sound propagation along the great circle track between FLIP and San Diego. These water masses extend to a depth of several hundred meters. North Pacific Central Water, described in Section II, is located along the western part of the track, and Transition Water is found adjacent to the coast of Southern California. Boundary Water lies between these two water masses and has a horizontal extent of several hundred miles at the latitude of San Diego. The Boundary Water zone coincides closely with the California Current, whose effects also extend to a depth of several hundred meters.

The major features of the vertical sound velocity structure in the presence of North Pacific Central Water can be seen in Fig. 38 and are generally similar to those described below for the FLIP area. The axis of the sound channel remains deep (between 700 and 800 meters) from FLIP all the way east to the California coast. The critical depth, however, deepens from about 4500 meters (2460 fathoms) at FLIP to over 4600 meters (2520 fathoms) at a range of 600 nautical miles, then shoals gradually to about 3500 meters (1910 fathoms) off San Diego. This 1000-meter decrease in the critical depth is more than matched by a 1500-meter decrease in the average bottom depth between FLIP and San Diego. The amount of excess depth is usually only about 500 meters, and in some places is zero. At a range of about 500 nautical miles and at several other greater ranges, convergence zone propagation is seriously hindered by seamounts penetrating the sound channel.

At a range of about 1300 nautical miles, the presence of Boundary Water in the upper several hundred meters of the water column could affect acoustic propagation through the area. Figure 38 lacks sufficient profile density and detail to display adequately the velocity conditions in this region, but the near-surface sound velocity structure is typically more complex here than that found on either side of the boundary zone. Transitory secondary sound channels in the near-surface layer are frequently found in and near the boundary region. Figure 40 (from Christensen and Lee, 1965) indicates the different vertical structures that may be found in the area.

Transition water dominates the area near San Diego: Figs. 35 and 38 provide representative sound velocity profiles for this water mass.

FEATURES OF SOUND VELOCITY PROFILES AT THE FLIP/SANDS SITE

Figure 41 shows a sequence of four sound velocity profiles spanning a period of about three weeks. These profiles were taken by SANDS near FLIP, and, for illustrative purposes, may be considered a times-series. The only distinguishable change during the three-week period is a slight reduction in the sound velocity maximum in the mixed layer, which reduces the value for critical depth and slightly improves propagation via the convergence zone path.

There is a noticeable positive sound velocity gradient in the mixed layer, representing isothermal conditions dominated by the pressure gradient. The positive gradient in the layer would support propagation via the surface duct, the mean depth of which is approximately 70 meters. A time series plot of SANDS XBT's, shown in Fig. 42, indicates the variability of the near surface environment during PARKA II-A.

Many complexities of the profiles in the depth interval between the mixed layer and the sound channel axis are reflected in corresponding temperature-salinity (T-S) diagrams. Some illustrative T-S plots are presented in Fig. 5a in Section III, Part A. The sound channel axis mean depth of about 750 meters, and mean velocity of about 1480 m/sec agree closely with archival data. The slight shoaling of the critical depth during the period of observation is undoubtedly the result of seasonal cooling. The average depth excess (the distance between the bottom of the sound channel and the bottom of the ocean) is about 1000 meters, and thus convergence zone transmission is reliable for this time of year.

COMPARISON OF SOUND VELOCITY DATA FROM DIFFERENT SYSTEMS

XBT's Compared with STD System

Figure 43 displays the shallow portion of two CONRAD temperature profiles, one from an XBT and the other from an STD station. Two obvious discrepancies between these profiles can be seen: a change in the depth of the layer, and an offset of the profile in the region of the thermocline.

The large change in layer depth (22 meters) and the noticeable thermocline offset may both result from a number of factors: the difference between the times and locations of the two observations, instrument error, environmental variability, differences in the way the data were coded, or any combination of these. Figure 44 shows a comparison between another pair of temperature profiles resulting from a CONRAD STD observation and a coincident XBT. The agreement shown here is excellent, with the greatest difference (four meters) occurring at the bottom of the mixed layer. In general, the CONRAD system agreed quite well with data from other systems taken at approximately the same location and time.

XBT's, however, can be quite erratic; a thorough analysis of XBT data taken during PARKA I (Whalen and Northrop, 1971) indicates that individual XBT probes will sometimes give erroneous results, and that these discrepancies can be difficult to detect. Also, as mentioned in Section III, Part A above, layer depths in this region *do* change by more than 22 meters over a period of time (Fig. 10); internal waves could cause such a change. Therefore, the cause of the difference between the two traces given in Fig. 43 cannot definitely be identified.

Comparison of Computed and Measured Sound Velocities

During the PARKA II-A Experiment, an attempt was made to compare values of sound velocity measured with velocimeters aboard SANDS and MARYSVILLE with other data computed using measured temperature and salinity data in Wilson's equation (Wilson, 1960). SANDS employed an NUS Model TR4 velocimeter and an NUS Model 1210-004 depth gauge. MARYSVILLE employed an NUS Model 1630-002 sound velocity/temperature/pressure sensor. STD measurements from CONRAD were used as the inputs to Wilson's equation to compute sound speed. The Lamont-Doherty Geological Observatory provided corrected salinity and depth data for use in Wilson's equation. The computations were

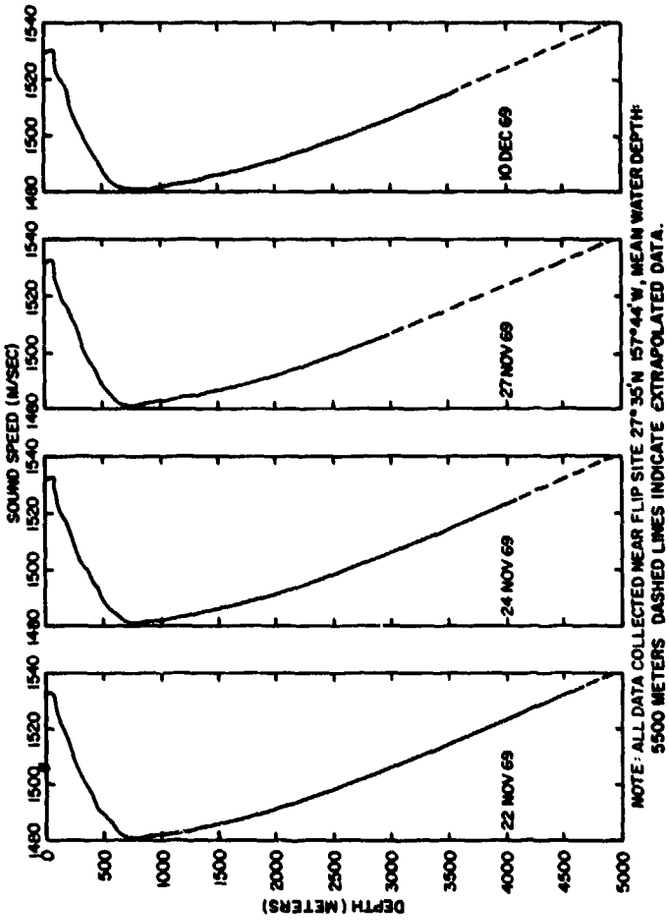

Fig. 41 — SANDS Deep Sound Velocity Profiles

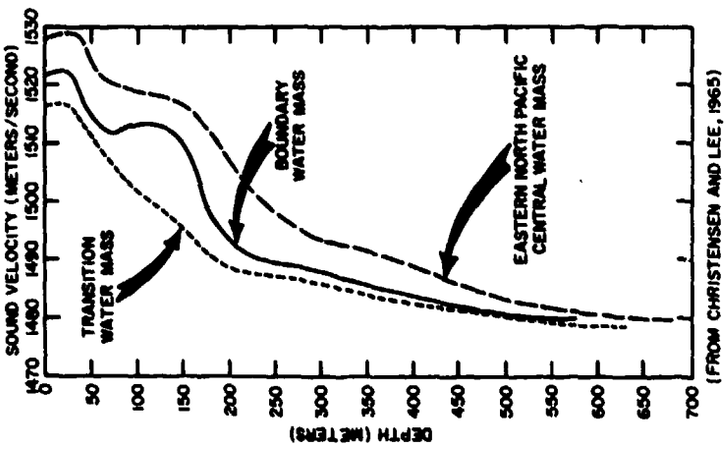

Fig. 40 — Sound Velocity Profiles in Region of California Current and Associated Water Masses

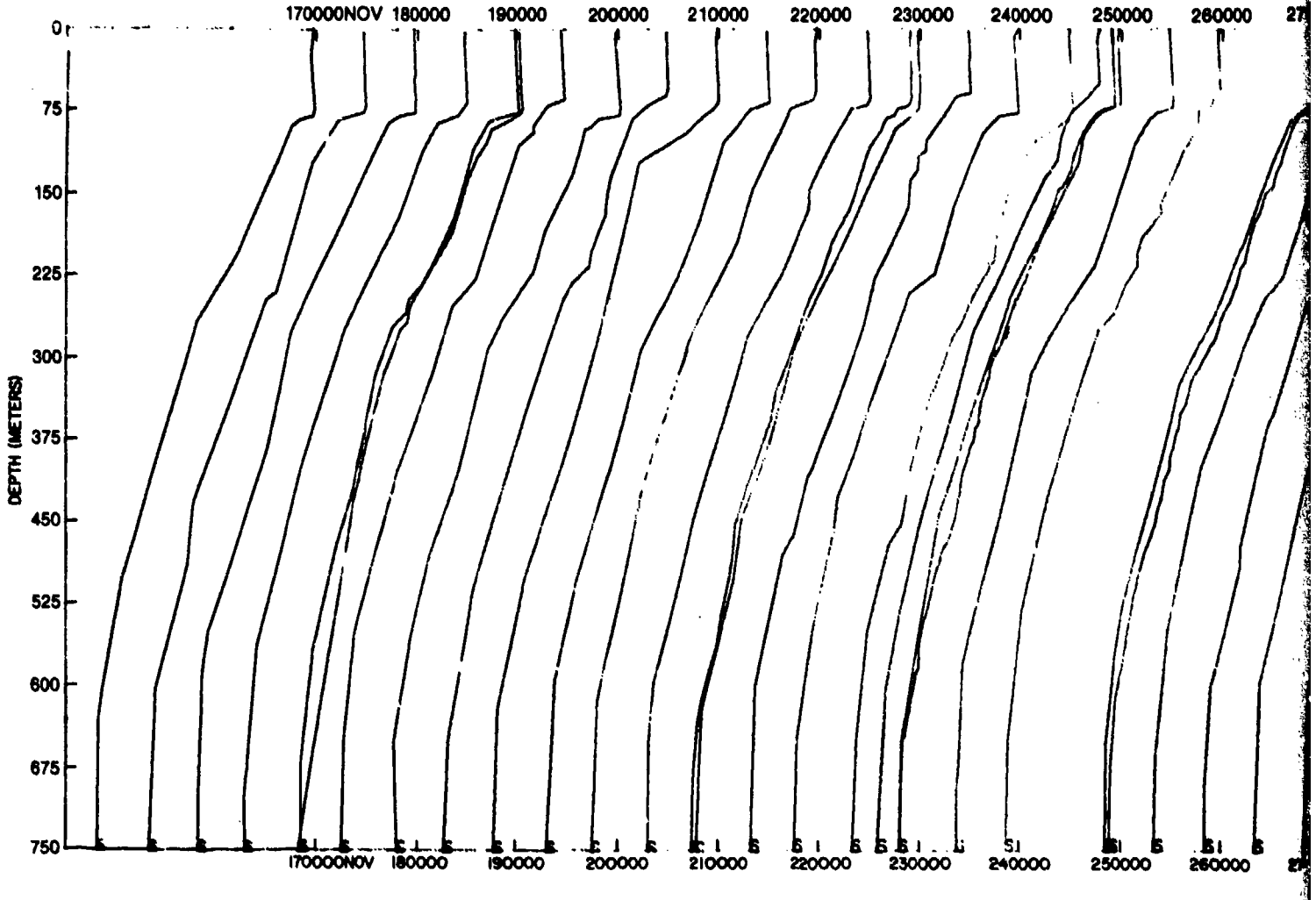

Fig. 42 — SANDS T

1. Profiles are plotte
2. All profiles from

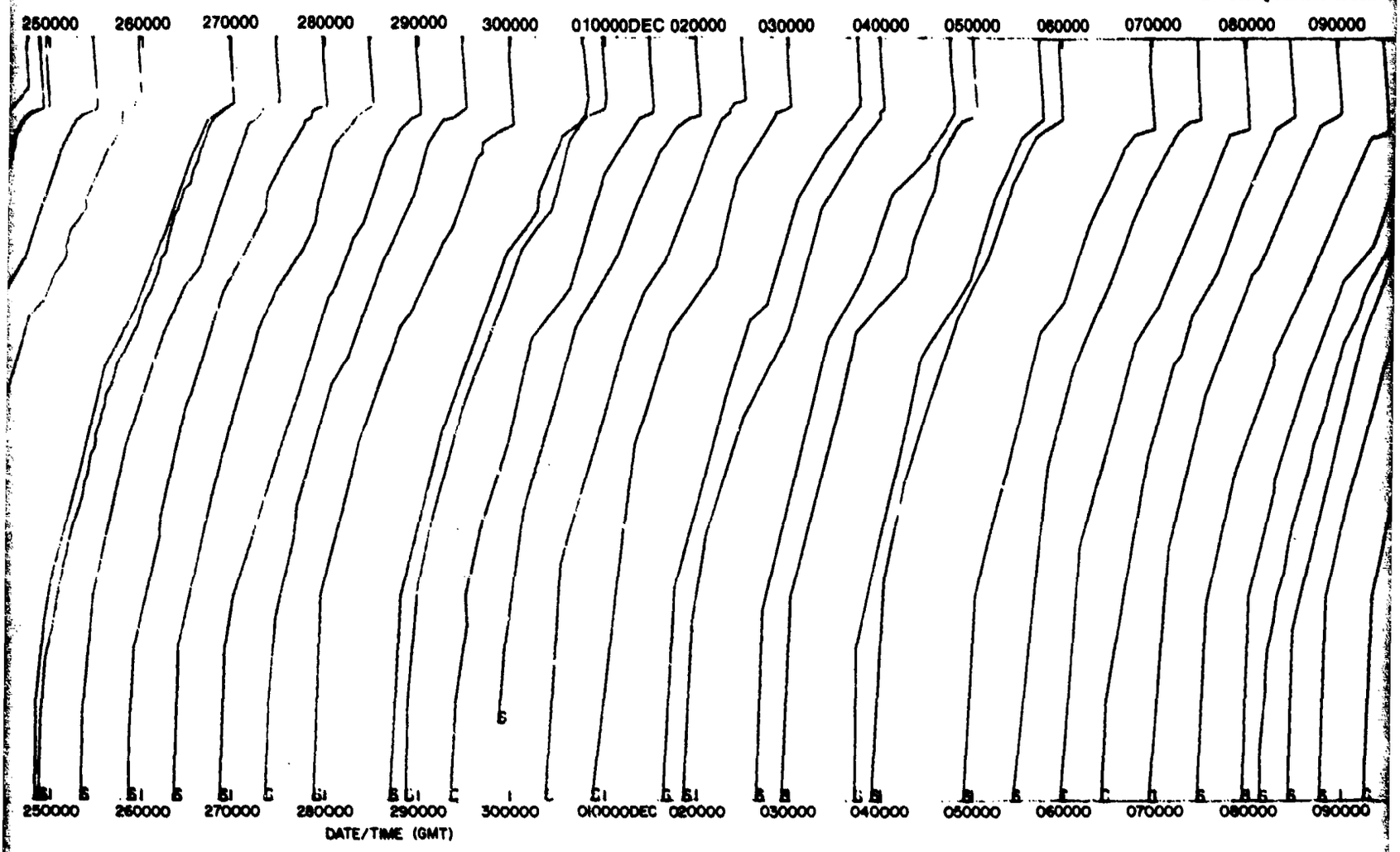

Fig. 42 — SANDS Time-Series Plot of Shallow Sound Velocity Profiles

(Page 82 Blank)

1. Profiles are plotted at time (GMT) observation made
2. All profiles from SANDS XBT data

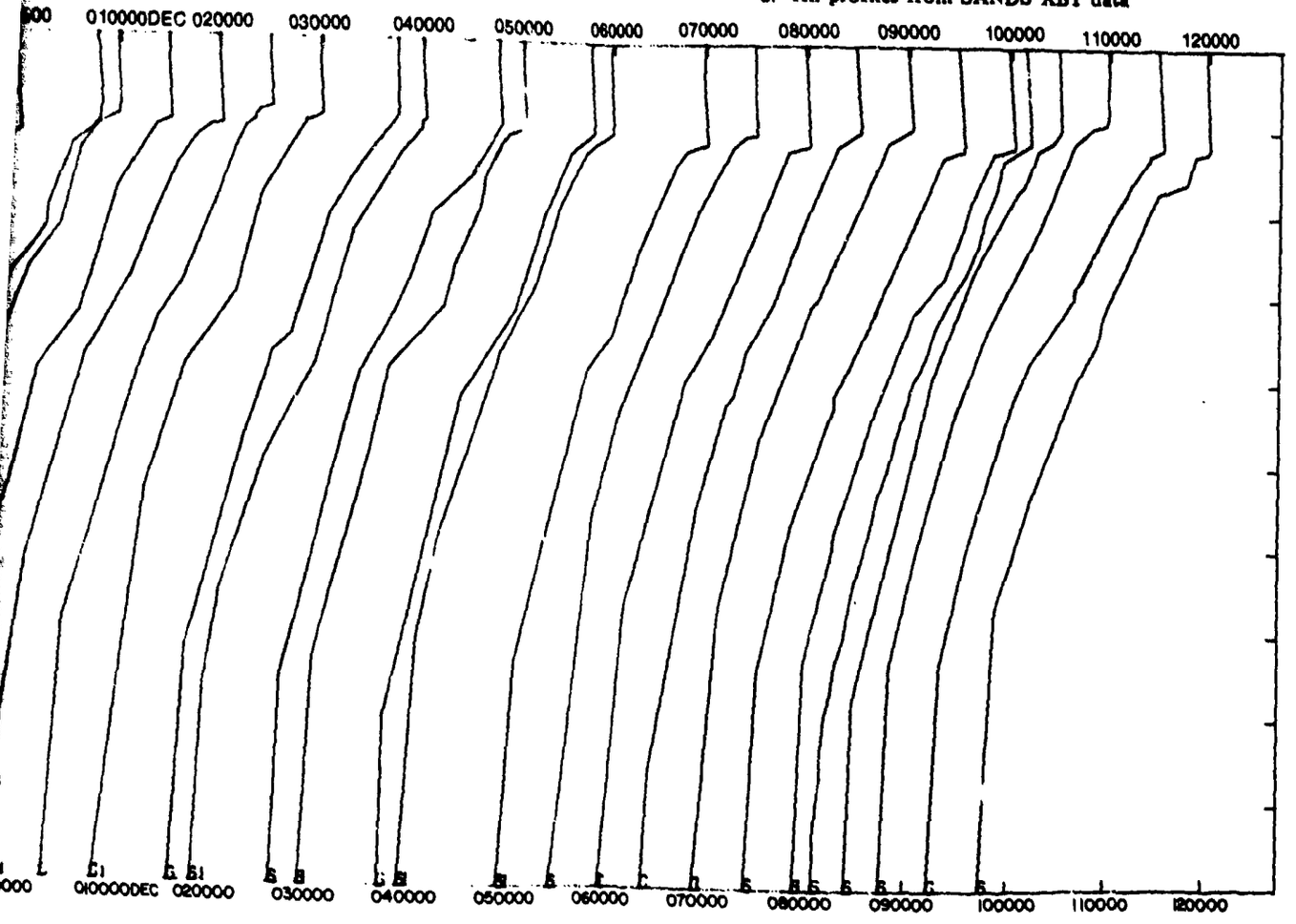

d Velocity Profiles

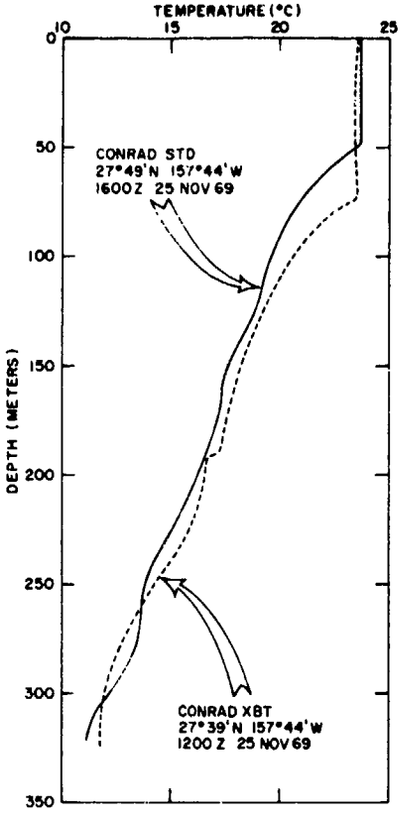

Fig. 43 — Example of Variability of the Near-Surface Temperature Structure

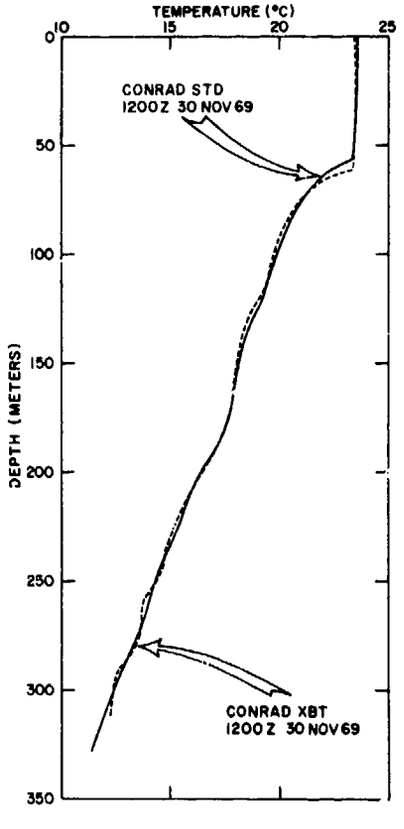

Fig. 44 — Example of Agreement Observed Between Temperature Profiles Obtained by Different Systems

carried out in accordance with U.S. Naval Oceanographic Office Special Publication 58 (1962).

Because questions arose concerning the precision and consistency of the sound velocity measurements that were made during the PARKA I Experiment (Whalen and others, 1971), considerable care was taken during the PARKA II-A Experiment to ensure that the sound velocimeter systems aboard SANDS and MARYSVILLE were kept in accurate calibration. The basic difference between the PARKA I and PARKA II-A results is that there was better compensation in the depth gauge electronics for the second experiment. Also, the SANDS velocimeter was calibrated prior to the operation and no significant changes were found when it was recalibrated upon completion of the exercise. The depth gauge was calibrated only prior to the operation, because the initial pressure setting had not changed since the original calibration. The complete sound velocimeter system aboard MARYSVILLE was calibrated before and after the PARKA II-A Experiment.

Figure 45 shows three superimposed velocity profiles, two from direct measurements and one constructed from Wilson's equation. The abscissa scale has been expanded in order to display more clearly the differences in sound velocity between the profiles. The profiles from SANDS and MARYSVILLE were recorded by velocimeter about two hours and seven nautical miles apart. The CONRAD STD profile was taken in the same area, but about 20 hours later. Table 2 lists velocity values from the three systems.

In Fig. 46 a MARYSVILLE measured profile and a CONRAD computed profile (via Wilson's equation) are shown. These two sets of values, also quasisynoptic and taken within a few miles of each other, are listed in Table 3.

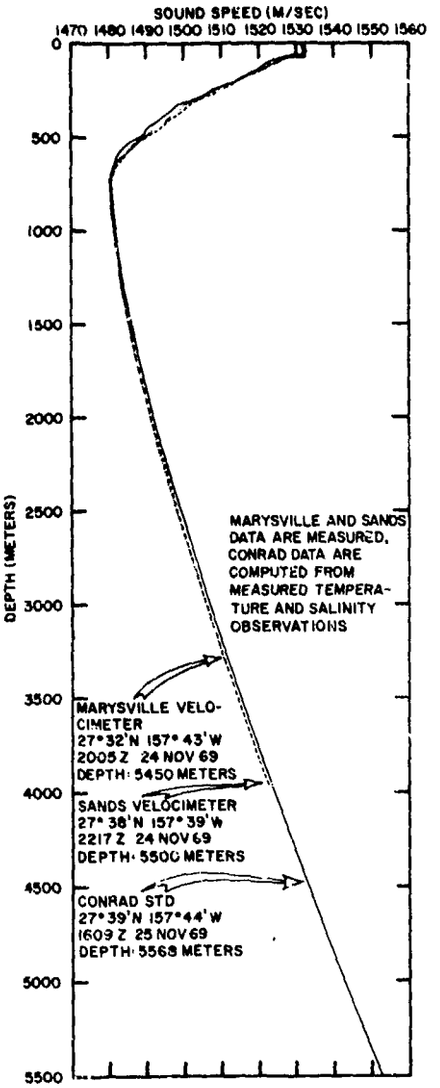

Fig. 45 — Comparison Between Two Measured and One Computed Sound Velocity Profile

Figure 45 and Table 2 show very close agreement between the two sound velocimeter systems used during the experiment. The observed differences appear mainly in the thermocline region, and probably can be accounted for by the changes taking place in the medium over a period of several hours. However, inspection

TABLE 2
Comparison Between CONRAD (Computed), MARYSVILLE (Measured), and SANDS (Measured) Sound Velocity Data

Depth (m)	CONRAD 1609Z, 25 Nov 69 27°39'N, 157°44'W	MARYSVILLE 2005Z, 24 Nov 69 27°32'N, 157°43'W	SANDS 2217Z, 24 Nov 69 27°38'N, 157°39'W	Differences in Sound Velocity (m/sec)		
	Sound Velocity (m/sec)	Sound Velocity (m/sec)	Sound Velocity (m/sec)	CONRAD-MARYSVILLE	CONRAD-SANDS	MARYSVILLE-SANDS
0	1532.0	1532.0	1532.0	0.0	0.0	0.0
50	1532.8	1532.2	1532.0	0.6	0.8	0.2
100	1522.8	1525.0	1524.5	−2.2	−1.7	0.5
200	1514.2	1514.2	1514.0	0.0	0.2	0.2
300	1503.0	1503.0	1503.6	0.0	−0.6	−0.6
400	1493.9	1496.1	1497.0	−2.2	−3.1	−0.9
500	1488.5	1489.8	1489.6	−1.3	−1.1	0.2
600	1482.6	1483.9	1484.3	−1.3	−1.7	−0.4
700	1481.0	1481.0	1481.3	0.0	−0.3	−0.3
800	1480.8	1480.8	1481.0	0.0	−0.2	−0.2
900	1481.5	1480.9	1481.1	0.6	0.4	−0.2
1000	1482.0	1481.7	1481.8	0.3	0.2	−0.1
1200	1483.5	1483.2	1483.3	0.3	0.2	−0.1
1500	1486.3	1485.7	1485.8	0.6	0.5	−0.1
2000	1491.8	1491.3	1491.2	0.5	0.6	0.1
3000	1506.7	1505.7	1505.9	1.0	0.8	−0.2
4000	1523.7	–	1523.0	–	0.7	–
5000	1543.9	–	–	–	–	–

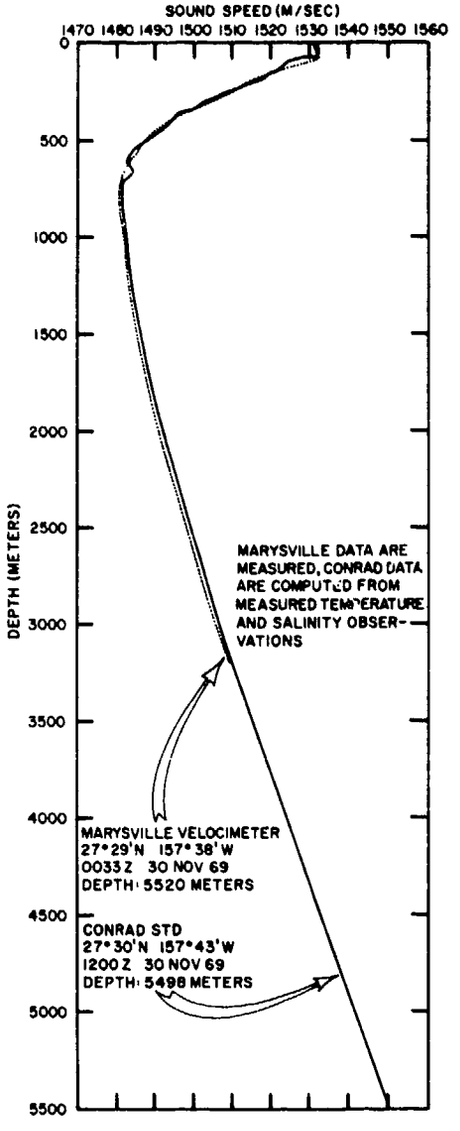

Fig. 46 — Comparison Between a Measured and a Computed Sound Velocity Profile

of both figures reveals a consistent discrepancy between directly measured and computed values for depths below the sound channel axis. Values determined from Wilson's equation in this region are all 0.5 m/sec or more higher than those measured directly. It also appears that this systematic difference is independent of depth. During PARKA I, the pressure sensors in some of the sound velocimeter systems used did not produce accurate depth measurements (Whalen and others, 1971). These differences, however, tended to increase proportionately with depth. In addition, although PARKA I computed sound velocities were also somewhat higher than the measured values, no real comparison was attempted, for several reasons. In PARKA I, most of the sound velocity computations were made with archival salinities, due to a lack of any deep PARKA salinity data (Wolff and Lackie, 1971). This use of archival (or assumed) salinity data occasionally caused differences of 0.1 to 0.2 m/sec in sound velocity, when compared with sound velocities computed from measured salinities. A "rounding off" error in the FNWC computation program also caused minor discrepancies between profiles. Any attempt at comparing computed and measured values was also overshadowed by the uncertainity caused by the inaccurate depth measurements referenced above (Whalen and others, 1971). Due to these uncertainties, the small differences noted between measured and computed sound velocities in PARKA I were not considered to be significant.

The discrepancies discovered in PARKA II-A are consistent, and suggest constant offset. Although some of the problems (such as the rounding off error) may continue to influence the PARKA II-A data, a different explanation may be required. Recently, Carnvale and others (1968) made a detailed laboratory comparison of sound speeds using various methods of measurement. Although pressure and salinity effects were not considered, it was found that in the 0°C to 25°C temperature range, values obtained from Wilson's equation were consistently higher than those measured directly by 0.2 to 0.3 m/sec. This may, at least partially, account for the observed discrepancy. Although this observed bias is not apparent above the sound channel axis, it may be overshadowed by

TABLE 3
Comparison Between CONRAD (Computed) and MARYSVILLE (Measured) Sound Velocity Data

Depth (m)	CONRAD 1200Z, 30 Nov 69 27°30'N, 157°43'W	MARYSVILLE 0033Z, 30 Nov 69 27°29'N, 157°38'W	Differences in Sound Velocity (m/sec)
	Sound Velocity (m/sec)	Sound Velocity (m/sec)	CONRAD-MARYSVILLE
0	1531.5	1530.0	1.5
50	1532.3	1531.9	0.4
100	1523.5	1527.1	−3.6
200	1514.7	1514.0	0.7
300	1502.9	1504.4	−1.5
400	1493.7	1493.0	0.7
500	1487.5	1487.7	−0.2
600	1482.9	1483.7	−0.8
700	1482.3	1481.3	1.0
800	1481.6	1480.9	0.7
900	1482.0	1481.2	0.8
1000	1482.6	1482.0	0.6
1200	1483.8	1483.2	0.6
1500	1486.5	1486.0	0.5
2000	1492.2	1491.0	1.2
3000	1506.8	1506.0	0.8
4000	1524.1	–	–
5000	1541.0	–	–

medium variability there. It should be stressed, however, that our comparisons have a small data base. Future comparisons of this type should be based on several simultaneous stations at the same location, using as many different measuring systems as possible.

Agreement between the various environmental sensor systems employed in PARKA II-A is considered generally excellent. Discrepancies noted between measured sound velocities and those computed from measured temperature and salinity data may be due to minor inaccuracies in Wilson's equation used in the computations. These discrepancies, however, will probably have a negligible effect on the usefulness of the data in predicting sound propagation.

REFERENCES

Carnvale, A., Bowen, P., Basileo, M., and Sprenke, J., 1968, "Absolute sound velocity measurement in distilled water": Jour. Acoust. Soc. Am., v. 44, n. 4, p. 1098-1102.

Christensen, N. and Lee, O. S., 1965, "Sound channels in the boundary region between Eastern North Pacific Central Water and Transition Water": Second U.S. Navy Symposium on Military Oceanography, Proceedings, v. 2, p. 203-225. (CONFIDENTIAL report, Unclassified title)

Hansen, P. G., 1969, "A sea going UNIVAC 1218 interfaced with NUWC's thermistor chain": Applications of Sea Going Computers, 1969, Symposium Transactions, Washington, Marine Technology Society, p. 105-114.

Hesselberg, T. and Sverdrup, H. U., 1915, "Stability conditions of sea water at vertical displacement": Bergen Museum Yearbook 1914-15, n. 15, p. 1-16. (Translation by U.S. Navy Hydrographic Office, 1962)

Jacobs, W. C., 1951, "The energy exchange between sea and atmosphere and some of its consequences": Scripps Inst. Oceanog. Bull., v. 6, n. 2, p. 22-122.

Lackie, K. W., 1971, "Review" (of PARKA I environmental operations), Appendix B1 to the PARKA I Experiment: Maury Center for Ocean Science Rept. 003, v. 2, 165 p. (CONFIDENTIAL report, Unclassified title)

LaFond, E. C., and LaFond, K. G., 1971, "Thermal structure through the California front": Naval Undersea Research and Development Center, Tech. Pub. 226, in press.

Latham, R. C., 1970, "Environmental oceanographic observations in support of PARKA II-A operations": Hawaii Inst. of Geophys., Interim Tech. Rept. n. 4.

Latham, R. C., Budd, R., and Zachariadis, R. G., 1969, "Report of work accomplished in support of PARKA II operations": Hawaii Inst. of Geophys., Interim Tech. Rept. n. 3.

Maury Center for Ocean Science, 1969a, "PARKA II, ONR scientific plan 2-69": Washington, Maury Center for Ocean Science Plan 01. (CONFIDENTIAL report, Unclassified title)

Maury Center for Ocean Science, 1969b, "The PARKA I Experiment": Washington, Maury Center for Ocean Science Rept. 003, v. 1, 82 p. (SECRET report, Unclassified title)

McGary, J. W., and Stroup, E. D., 1956, "Mid-Pacific oceanography, Part VIII, middle latitude waters, Jan-Mar 1954": U.S. Fish and Wildlife Serv., Spec. Scient. Rept.—Fisheries, n. 180.

NORPAC Committee, 1960, "Oceanic observations of the Pacific: 1955, The NORPAC Atlas": Berkeley and Tokyo, Univ. of California Press and Univ. of Tokyo Press.

Patzert, W. C., 1969, "Eddies in Hawaiian waters": Hawaii Inst. of Geophys., Rept. 69-8.

Pickard, G. L., 1963, "Descriptive physical oceanography": Oxford, Pergamon Press, 200 p.

Reid, J. L., 1965, "Intermediate waters of the Pacific Ocean": Baltimore, Johns Hopkins Univ. Press, 85 p.

Roden, G. I., 1964, "Shallow temperature inversions in the Pacific Ocean": Jour. Geophys. Research, v. 69, n. 14, p. 2899-2914.

Roden, G. I., 1970, "Aspects of the Mid-Pacific Transition Zone": Jour. Geophys. Research, v. 75, n. 6, p. 1097-1109.

Rudnick, P., and Hasse, R. W., 1971, "Extreme Pacific waves, December 1969": Jour. Geophys. Research, v. 76, n. 3, p. 742-744.

Seckel, G. R., 1962, "Atlas of the oceanographic climate of the Hawaiian Islands region": U.S. Fish and Wildlife Serv., Fishery Bull., n. 193.

Seckel, G. R., 1969, "Vertical sections of temperature and salinity in the trade wind zone of the central North Pacific, February 1964 to June 1965": U.S. Fish and Wildlife Serv., Circ. n. 323, 43 p.

Smith, E. L., 1967, "Migration and temperature structure of eddies on the leeward side of the Hawaiian Islands": Fourth U.S. Navy Symposium on Military Oceanography, Proceedings, v. 1, p. 396-414.

Smith, E. L., 1969, "Sensor depths and digital data correction methods for a towed thermistor chain": Naval Undersea Research and Development Center, Tech. Note 313, 17 p.

Smith, E. L., 1971a, "NURDC oceanographic operations" (in PARKA I), Appendix B7 to the PARKA Experiment: Maury Center for Ocean Science, Rept. 003, v. 2, 165 p. (CONFIDENTIAL report, Unclassified title)

Smith, E. L., 1971b, "Aircraft expendable bathythermograph observations" (in PARKA I), Appendix B8 to The PARKA I Experiment: Maury Center for Ocean Science Rept. 003, v. 2, 165 p. (CONFIDENTIAL report, Unclassified title)

Sverdrup, H. U., Johnson, M. W., and Fleming, R. H., 1942, "The oceans": New York, Prentice Hall, p. 605-761.

Uda, M., 1963, "Oceanography of the Subarctic": Jour. Fisheries Research Board Canada, v. 20, n. 1, p. 119-179

U.S. Naval Oceanographic Office, 1962, "Tables of sound speed in sea water": Washington, Spec. Pub. 58, 47 p.

Whalen, T. L., and Northrop, J., 1971, "WHOI oceanographic operations" (in PARKA I), Appendix B11 to The PARKA I Experiment: Maury Center for Ocean Science, Rept. 003, v. 2, 165 p. (CONFIDENTIAL report, Unclassified title)

Whalen, T. L. Northrop, J. and Lackie, K. W., 1971, "Data quality" (of PARKA I oceanographic data), Appendix B3 to The PARKA Experiment: Maury Center for Ocean Science, Rept. 003, v. 2, 165 p. (CONFIDENTIAL report, Unclassified title)

Wilson, W. D., 1960, "Speed of sound in sea water as a function of temperature, pressure and salinity": Jour. Acoust. Soc. Am., v. 32, p. 641. Revised and extended in v. 32, p. 1357, 1960, and v. 34, p. 866, 1962.

Wolff, P. M., and Lackie, K. W., 1971, "Salinity" (in PARKA I), Appendix B9 to The PARKA I Experiment: Maury Center for Ocean Science, Rept. 003, v. 2, 165 p. (CONFIDENTIAL report, Unclassified title)

Wyrtki, K., 1967, "The spectrum of ocean turbulence over distances between 40 and 1000 kilometers": Deutsche Hydrograph. Zeitschr., Jahrg. 20, Heft. 4, p. 176-185.

DEPARTMENT OF THE NAVY
OFFICE OF NAVAL RESEARCH
800 NORTH QUINCY STREET
ARLINGTON, VA 22217-5660

IN REPLY REFER TO
5510/1
Ser 93/160
10 Mar 99

From: Chief of Naval Research
To: Commander, Naval Meteorology and Oceanography Command
1020 Balch Boulevard
Stennis Space Center MS 39529-5005

Subj: DECLASSIFICATION OF PARKA I AND PARKA II REPORTS

Ref: (a) CNMOC ltr 3140 Ser 5/110 of 12 Aug 97

Encl: (1) Listing of Known Classified PARKA Reports

1. In response to reference (a), the Chief of Naval Operations (N874) has reviewed a number of Pacific Acoustic Research Kaneohe-Alaska (PARKA) Experiment documents and has determined that all PARKA I and PARKA II reports may be declassified and marked as follows:

   Classification changed to UNCLASSIFIED by authority of Chief of Naval Research letter Ser 93/160, 10 Mar 99.

   DISTRIBUTION STATEMENT A: Approved for public release. Distribution is unlimited.

2. Enclosure (1) is a listing of known classified PARKA reports. The marking on those documents should be changed as noted in paragraph 1 above. When other PARKA I and PARKA II reports are identified, their markings should be changed and a copy of the title page and a notation of how many pages the document contained should be provided to Chief of Naval Research (ONR 93), 800 N. Quincy Street, Arlington, VA 22217-5660. This will enable me to maintain a master list of downgraded PARKA reports.

3. Questions may be directed to the undersigned on (703) 696-4619, DSN 426-4619.

Peggy Lambert

PEGGY LAMBERT
By direction

Copy to:
NUWC Newport Technical Library (Code 5441)
NRL Washington (Mary Templeman, Code 5227)
NRL SSC (Roger Swanton, Code 7031)
DTIC (Bill Bush, DTIC-OCQ)

Continuation of LRAPP Final Report, February 1972, Contract N00014-71-C-0088, Bell Telephone Labs, Unknown # of pages
(NUSC NL Accession # 057708)

PARKA II-A, The Oceanographic Measurements, February 1972, MC Report 006, Volume 2, Maury Center for Ocean Science (ONR), 89 pages
(NUSC NL Accession # 059194) (NRL SSC Accession # 85007063) AD-596342

Project Pacific Sea Spider - Technology Used in Developing A Deep-Ocean Ultrastable Platform, 12 April 1974, ONR-ACR-196, 55 pages
√(DTIC # 529 945)

LRAPP Program Review at the New London Laboratory, Naval Underwater Systems Center, 24 April 1975, NUSC-TD-4943, Unknown # of pages
(NUSC NL Accession # 004943)

An Analysis of PARKA IIA Data Using the AESD Parabolic Equation Model, December 1975, AESD Technical Note TN-75-09, Acoustic Environmental Support Detachment (ONR), 53 pages
(NRL SSC Accession # 85004613)

Bottom Loss Measurements in the Eastern Pacific Ocean, 26 January 1977, NADC-76320-20, 66 pages
√(DTIC # C009 224)

PARKA I Oceanographic Data Compendium, November 1978, NORDA-TN-25, 579 pages
√(DTIC # B115 967)

Sonar Surveillance Through A North Pacific Ocean Front, June 1981, NOSC-TR-682, 18 pages
√(DTIC # C026 529)

The Acoustic Model Evaluation Committee (AMEC) Reports, Volume 1, Model Evaluation Methodology and Implementation, September 1982, NORDA-33-VOL-1, 46 pages
√(DTIC # C034 016)

The Acoustic Model Evaluation Committee (AMEC) Reports, Volume 1A, Summary of Range Independent Environment Acoustic Propagation Data Sets, September 1982, NORDA-34-VOL-1A, 482 pages
√(DTIC # C034 017)

The Acoustic Model Evaluation Committee (AMEC) Reports, Volume 2, The Evaluation of the Fact PL9D Transmission Loss Model, Book 1, September 1982, NORDA-35-VOL-2-BK-1, 179 pages
√(DTIC # C034 018)

The Acoustic Model Evaluation Committee (AMEC) Reports, Volume 2, The Evaluation of the Fact PL9D Transmission Loss Model, Book 2, Appendices A-D, September 1982, NORDA-35-VOL-2-BK-2, 318 pages
√(DTIC # C034 019)

DEPARTMENT OF THE NAVY
OFFICE OF NAVAL RESEARCH
875 NORTH RANDOLPH STREET
SUITE 1425
ARLINGTON VA 22203-1995

IN REPLY REFER TO:

5510/1
Ser 321OA/011/06
31 Jan 06

MEMORANDUM FOR DISTRIBUTION LIST

Subj: DECLASSIFICATION OF LONG RANGE ACOUSTIC PROPAGATION PROJECT (LRAPP) DOCUMENTS

Ref: (a) SECNAVINST 5510.36

Encl: (1) List of DECLASSIFIED LRAPP Documents

1. In accordance with reference (a), a declassification review has been conducted on a number of classified LRAPP documents.

2. The LRAPP documents listed in enclosure (1) have been downgraded to UNCLASSIFIED and have been approved for public release. These documents should be remarked as follows:

   Classification changed to UNCLASSIFIED by authority of the Chief of Naval Operations (N772) letter N772A/6U875630, 20 January 2006.

   DISTRIBUTION STATEMENT A: Approved for Public Release; Distribution is unlimited.

3. Questions may be directed to the undersigned on (703) 696-4619, DSN 426-4619.

BRIAN LINK
By direction

Subj: DECLASSIFICATION OF LONG RANGE ACOUSTIC PROPAGATION PROJECT (LRAPP) DOCUMENTS

DISTRIBUTION LIST:

NAVOCEANO (Code N121LC – Jaime Ratliff)
NRL Washington (Code 5596.3 – Mary Templeman)
PEO LMW Det San Diego (PMS 181)
DTIC-OCQ (Larry Downing)
ARL, U of Texas
Blue Sea Corporation (Dr.Roy Gaul)
ONR 32B (CAPT Paul Stewart)
ONR 321OA (Dr. Ellen Livingston)
APL, U of Washington
APL, Johns Hopkins University
ARL, Penn State University
MPL of Scripps Institution of Oceanography
WHOI
NAVSEA
NAVAIR
NUWC
SAIC

Declassified LRAPP Documents

Report Number	Personal Author	Title	Publication Source (Originator)	Pub. Date	Current Availability	Class.
IR 71-2	Fenner, D. F., et al.	SOUND VELOCITY AND BOTTOM CHARACTERISTICS FOR LRAPP ATLANTIC AREAS I, II, AND III (U)	Naval Oceanographic Office	710601	ADC008372; ND	U
T-71-NJ-4508-C	Larsen, H. L., et al.	LRAPP DATA COLLECTION (U)	Tracor, Inc.	710831	AD0517012; ND	U
Unavailable	Anderson, C. G., et al.	ADAPTIVE BEAMFORMING ANALYSIS FOR DIRECTIONALITY USING DATA FROM A VERTICAL ARRAY IN THE MEDITERRANEAN	Naval Undersea Research and Development Center	710901	AD0517696	U
MC PLAN 06	Unavailable	IOMEDEX LRAPP OPERATION ORDER (U)	Maury Center for Ocean Science	710924	ND	U
NRLFR7322	Lawson, W. M.	POSITION-DETERMINING SYSTEM FOR SEA-SPIDER HYDROPHONE ARRAYS	Naval Research Laboratory	711230	ND	U
N00014-71-C-0088	Unavailable	CONTINUATION OF LRAPP FINAL REPORT (U)	Bell Laboratories	720201	AD0520426; NS; ND	U
Unavailable	Unavailable	PARKA II-A EXPERIMENT. VOLUME 2	Maury Center for Ocean Science	720201	AD0596342	U
Unavailable	Unavailable	NOISE POWER MEASUREMENTS FROM THE LAMBDA TOWED ARRAY EXPERIMENT	Texas Instruments, Inc.	720401	ND	U
Unavailable	Anderson, P. R., et al.	LRAPP VERTICAL ARRAY PRELIMINARY DESIGN STUDY, PHASE I	Westinghouse Research Laboratories	720414	AD0900477	U
Unavailable	Unavailable	SUPPLEMENTARY DATA. NOISE POWER MEASUREMENTS FROM THE LAMBDA TOWED ARRAY EXPERIMENT	Texas Instruments, Inc.	720419	ND	U
MC Report 6, Volume 2	Unavailable	PARKA OCEANOGRAPHIC DATA COMPENDIUM-PARKA II-A	Maury Center for Ocean Science	720501	ND	U
MC Report 6, Volume 3	Unavailable	PARKA OCEANOGRAPHIC DATA COMPENDIUM-PARKA II-B	Maury Center for Ocean Science	720501	ND	U
Unavailable	Unavailable	NORLANT 72 PHASE 2 OPERATION PLAN	Naval Underwater Systems Center	720628	AD0521225	U
Unavailable	Unavailable	NORLANT 72 PHASE 2 SCIENTIFIC PLAN	Naval Underwater Systems Center	720628	AD0521226	U
Unavailable	Unavailable	NORLANT 72 PHASE 3 OPERATION PLAN	Naval Underwater Systems Center	720628	AD0521227	U
Unavailable	Unavailable	NORLANT 72 PHASE 3 SCIENTIFIC PLAN	Naval Underwater Systems Center	720628	AD0521228	U
MC PLAN 08	Unavailable	OPERATION PLAN. LRAPP TASSRAP EXERCISE (TEX)	Maury Center for Ocean Science	720701	ND	U
Unavailable	Miller, R. R., III	CURRENT REGIME OF THE MALTESE OCEANIC FRONTAL ZONE	Naval Underwater Systems Center	720906	AD0749706	U